Norwegian University
of Life Sciences

Master's Thesis 2022 60 ECTS
Faculty of Veterinary Medicine

Methods To Study Fusion Activation of Infectious Salmon Anaemia Virus

Metoder for å studere fusjonsaktivering i infeksiøst lakseanemi-virus

Frieda Betty Ploss
Biotechnology

Acknowledgements

This master's thesis was carried out in the period from August 2021 to May 2022 at the ILA-SAFE and BIO-DIRECT research projects of the Norwegian Veterinary Institute (NVI), Ås, Norway. The ILA-SAFE project is funded by the FHF - Norwegian Seafood Research Fund (project number FHF901674), and the BIO-DIRECT initiative is funded by the Norwegian Research Council (NFR) basic grant - strategic institute initiative (SIS). The thesis was a part of the master's degree in Biotechnology at the Norwegian University of Life Sciences (NMBU).

Foremost, I would like to express my deep gratitude to my supervisors Dr. Johanna Hol Fosse and Professor Maria Dahle at the NVI, and my NMBU supervisor, Professor Espen Rimstad, for your invaluable guidance, support and knowledge. Also, thanks to Dr. Øystein Wessel who has been a part of the supervisor-team. A special thanks to Dr. Hol Fosse for pushing me, for your patience and all your help in writing this thesis.

I also want to thank everyone at the NVI, especially Dr. Anita Solhaug, and laboratory engineers Inger Austrheim Heffernan, Lone Engerdahl, Ingebjørg Modahl, Karen Bækken Soleim, Subash Sapkota, Kathrine Andersen Moan, and Marit Måsøy Amundsen, for their expertise and guidance in the lab, and for providing information. My sincere thanks to Dr. Adriana Magalhaes Santos Andresen Andresen for answering endless questions and for the discussions we have had together. I want to extend a thanks to my fellow master's student, Iselin Maidili Arumairasa, for sharing lunch breaks, for the discussions, and occassional frustrations.

Last, but not least, a huge thanks to my family, especially Simon. I could not have done this without your support and encouragement.

Ski, May 2022

Frieda Betty Ploss

Abstract

Infectious salmon anaemia (ISA) is a serious viral disease caused by virulent ISA virus (ISAV). ISA is considered to be an important threat to Norwegian salmon farming. It is a widely held view that new virulent ISAV variants can arise from a reservoir of non-virulent ISAV-HPR0. The transition to virulence is associated with typical changes in the ISAV surface proteins that appears to enhance viral fusion. The mechanisms behind the enhanced fusion are not completely understood. More knowledge on fusion in non-virulent and virulent ISAV variants is necessary to understand the basis for ISAV virulence. Eventually, this could help us address central questions, like how ISAV HPR-del emerges and, if possible, how to limit the formation of new ISAV HPR-del variants. However, differences between non-virulent and virulent ISAV have been difficult to address experimentally because cultivation of ISAV-HPR0 has been challenging. The main aim of this thesis was to establish a tool box to study ISAV fusion, by using a CHSE cell line transfection-based model and erythrocytes to mimic the fusion process. CHSE cells were transfected with plasmids encoding HE and F proteins from closely related ISAV-HPR0 and HPR-del variants. Our hypothesis, based on previous studies, was that the non-virulent ISAV-HPR0 and the virulent HPR-del variants have similar receptor-binding and -destroying activities. Additionally, that the virulent HE/F variant combination has a higher activity of fusion compared to the non-virulent HE/F variant, in line with the current hypothesis that ISAV virulence is related to fusion activity. Functional analyses were performed on recombinantly expressed HE proteins to evaluate and compare receptor binding and -destroying activities. A lipid mixing assay was established to study and compare the fusion activity of recombinantly expressed HE and F proteins when priming and triggering was stimulated by trypsin and low pH.

The recombinantly expressed HPR0 and HPR-del HE showed similar receptor binding and destroying activities, in line with our hypothesis and a previous report [1]. Higher fusion activity was found for the HE and F proteins associated with the HPR-del virus variant than for those associated with the HPR0 virus variant. This was in line with our hypothesis and previous reports [2-4] that fusion activity relates to virulence. No fusion activation was seen in wells with single transfection of HE or F proteins. Additionally, single transfection of F protein did not reveal haemadsorption. Moreover, no fusion activation was observed in the absence of trypsin and low pH treatment for HPR-del HE/F, in contrast to a report by Fourrier et al. [3], that reports significant spontaneous fusion activity.

The work in this thesis has generated data and established methodology that form the basis for future fusion activity studies to understand the mechanisms involved in the ISAV fusion process and the impact of virulence-associated changes in ISAV surface proteins.

Sammendrag

Infeksiøs lakseanemi (ILA) er en alvorlig virussykdom forårsaket av virulent ILA-virus (ILAV). ILA anses å være en viktig trussel mot lakseoppdrett i Norge. Det er en utbredt oppfatning at nye virulente ILAV-varianter kan oppstå fra et reservoar av ikke-virulent ILAV-HPR0. Overgangen til virulens er assosiert med typiske endringer i ILAV-overflateproteiner som ser ut til å forbedre viral fusjon. Mekanismene bak fusjonsprosessen hos ILAV er ikke fullstendig kjent. Mer kunnskap om fusjon i ikke-virulente og virulente ILAV-varianter er nødvendig for å forstå grunnlaget for ILAV virulens. På sikt kan dette hjelpe oss med å ta opp sentrale spørsmål, som hvordan ILAV HPR-del oppstår og, hvis mulig, hvordan man begrenser dannelsen av nye ILAV HPR-del varianter. Imidlertid har forskjeller mellom ikke-virulent og virulent ILAV vært vanskelige å studere, fordi dyrking av ISAV-HPR0 har vært svært utfordrende. Hovedmålet med denne oppgaven var å etablere en verktøykasse for å studere ILAV-fusjon, ved å bruke en CHSE cellelinje transfeksjonsbasert modell og erytrocytter, for å etterligne fusjonsprosessen i ILAV. CHSE-celler ble transfektert med plasmider som koder for HE- og F-proteiner fra nært beslektede ILAV-HPR0- og HPR-del-varianter. Vår hypotese, basert på tidligere studier, var at den ikke-virulente ILAV-HPR0 og den virulente HPR-del-varianten har liknende reseptorbindende og -ødeleggende aktiviteter. I tillegg, at den virulente HE/F-varianten har en høyere fusjonsaktivitet sammenlignet med den ikke-virulente HE/F-varianten, i tråd med den nåværende hypotesen om at ILAV-virulens er relatert til fusjonsaktivitet. Funksjonelle analyser ble utført på rekombinant uttrykte HE-proteiner for å evaluere og sammenligne reseptorbindende og -ødeleggende aktiviteter. En lipid mixing assay ble etablert for å studere og sammenligne fusjonsaktiviteten i rekombinant uttrykte HE- og F-proteiner når priming og triggering ble stimulert av trypsin og lav pH.

De rekombinante HPR0- og HPR-del HE-proteinene viste liknende reseptorbindende og -ødeleggende aktiviteter, i tråd med vår hypotese og en tidligere studie [1]. Høyere fusjonsaktivitet ble funnet for HE- og F-proteiner assosiert med HPR-del-virusvarianten enn for de assosiert med HPR0-virusvarianten. Dette var i tråd med vår hypotese og tidligere rapporter [2-4] om at fusjonsaktivitet er relatert til virulens. Ingen fusjonsaktivitet ble observert i brønner med enkelt-transfeksjon av HE- eller F-proteiner. I tillegg ble det ikke observert hemadsorpsjon i brønner med enkelt-transfeksjon av F-protein. Dessuten ble ingen fusjonsaktivitet observert i fravær av trypsin og lav pH-behandling for HPR-del HE/F, i motsetning til en rapport fra Fourrier et al. [3], som rapporterer spontan fusjonsaktivitet. Arbeidet i denne oppgaven har generert data og etablert metodikk som danner grunnlaget for fremtidige studier for å forstå mekanismene involvert i fusjonsprosessen hos ILAV, og hvilken effekt de endringene i ILAVs overflateproteiner har for virulens.

Table of contents

List of abbreviations

Abbreviation	Full description
AP	Alkaline phosphatase
ASK	Atlantic salmon kidney
BSA	Bovine serum albumin
cELISA	Cellular ELISA
CMS	Cardiomyopathy syndrome
cRNA	Copy RNA
CT	Cytoplasmic tail
EDTA	Ethylenediaminetetra acetic acid
EIH	Enzyme immunohistochemistry
ELISA	Enzyme-linked immunosorbent assay
F protein	Fusion protein
F_0	Precursor F protein
F_1	F protein subunit 1
F_2	F protein subunit 2
HA	Haemagglutinin
HAU	Haemagglutinating units
HCl	Hydrochloric acid
HE	Haemagglutinin-esterase
HEF	Haemagglutinin-esterase-fusion
HPAI	Highly pathogenic avian influenza
HPR	Highly polymorphic region
HPR-del	Highly polymorphic region deletion
HRP	Horseradish peroxidase
HSMI	Heart and skeletal muscle inflammation
IF	Immunofluorescence
IPN	Infectious pancreatic necrosis
ISA	Infectious salmon anaemia
ISAV	Infectious salmon anaemia virus
kb	Kilobase
LPAIV	Low-pathogenic avian influenza A virus
M	Matrix protein
mRNA	Messenger RNA

NA	Neuraminidase
NP	Nucleoprotein
NS	Non-structural protein
OIE	The World Organisation for Animal Health
PA	Polymerase acidic protein
PB1	Polymerase basic 1 protein
PB2	Polymerase basic 2 protein
PBS	Phosphate-buffered saline
PBST	PBS with 0.1 % Tween detergent
PBS-TBN	PBS with 0.1 % BSA, 0.02 % Tween, and 0.05 % sodium azide
PD	Pancreas disease
p-NP	*p*-nitrophenol
p-NPA	*p*-nitrophenyl acetate
PE	Phycoerythrin
R18	Octadecyl rhodamine B chloride
RBC	Red blood cell
RBD	Receptor-binding domain
RDE	Receptor-destroying enzyme domain
RNA	Ribonucleic acid
RNP	Ribonucleoprotein
SP	Signal peptide
TM	Transmembrane domain
TMB	Tetramethylbenzidine
VHS	Viral haemorrhagic septicaemia
vRNA	Viral RNA
Å	Ångstrøm, $1*10^{-10}$ m

Glossary

3R principles	Replacement, reduction and refinement. The aim of the 3R principle is to completely replace animal experiments as soon as scientifically achievable
Adherent cells	Cell line that grow as a monolayer on artificial substrate
Anaemia	Red blood cell deficiency
Antagonist	An antagonist binds to the receptor and inhibits its biological activity by preventing the endogenous ligand from binding
Ascites	Free abdominal fluid
Cap snatching	The 5'cap end of host mRNA is snatched and used as a primer to start the synthesis of antigenomic (+) RNA/viral mRNA
Cell culture	Cells that have been isolated from living tissue and their subsequent growth under controlled conditions outside their natural environment
Cell tropism	The ability of a given virus to infect a particular cell type
CHSE	Chinook salmon embryo cells, CHSE-214, obtained from *Onchorhynchus tshawytsca* (king salmon)
Confluence	The degree of coverage of the culture dish or flask by adherent cells
Copy RNA	Positive-sense antigenome of negative-sense viral RNA
Epithelial-like cells	Adherent cells that are polygonal in shape with regular dimensions and grow in patches
Exophtalmia	Protruding eyes
Fluorescence	The emitted light from a fuorochrome molecule that absorbs light at one wavelength and emits light at a longer wavelength and with a lower photon energy than the absorbed light
Fusion protein	A protein that induces fusion of viral and host membranes.
Fusion peptide	A short hydrophobic amino acid sequence near or at the N-terminal of the F protein's F_2-subunit, which embeds itself into the endosomal membrane upon low pH to initiate fusion of membranes.
Haemorrhage	Bleeding
Oedema	Extravascular fluid
Salmon	Atlantic salmon (*Salmo salar*) if not otherwise specified in the text

1 Introduction

1.1 Atlantic salmon farming in Norway

Modern Atlantic salmon *(Salmo salar* L.) farming initiated in Norway in the 1970s [5, 6] and has developed into a major export industry [7]. Norway farms about 50 % of the world's production of Atlantic salmon. The national salmon production was 1.28 million tons in 2018, of which 1.06 million tons were exported. Since 2009, the economic value of the salmon industry has tripled and in 2019 it was 72.5 billion Norwegian kroner [7]. However, there are large losses due to mortality related to infectious diseases, parasites, damages secondary to handling and treatment, and escaped farmed salmon [8]. In 2021, a total of 61.1 million Norwegian farmed salmon were lost during the marine production phase, and of these 15.5 % were related to mortality on-site [9]. The mortality has increased by 14.3 % compared to 2018, while production has increased with 282 302 tons (22 %) in the same period. Stress, particularly related to delousing, contribute to reduced fish welfare and increased mortality. Viral diseases are important threats to the Atlantic salmon farming. They cause disease, poor growth, and mortality, and it has been difficult to obtain good protection by vaccination. Furthermore, detection of viral diseases that are included in the national list of notificable diseases according to Norwegian Food Safety Authority imply restrictions of movement and trade and may even require sanitation of entire farms. Common viral diseases in the Norwegian Atlantic salmon farming industry are: pancreas disease (PD), infectious pancreatic necrosis (IPN), heart and skeletal muscle inflammation (HSMI), cardiomyopathy syndrome (CMS), salmon pox, and infectious salmon anaemia (ISA).

1.1.1 Viral diseases in Norwegian farmed salmon

Three viral diseases have dominated the Norwegian salmon farming industry in the recent years: CMS, HSMI, and PD. In 2020, there were 158 registered outbreaks of PD, 154 of CMS, and 161 of HSMI, as shown in Table 1. Neither HSMI or CMS are notifiable diseases, which adds some uncertainty to the assessment of number of outbreaks. In 2021, the number of PD outbreaks was reduced to 100. The number of ISA outbreaks is much smaller, but the increase in ISA outbreaks over the last two years is subject to great concern [9, 10].

Table 1. Number of salmon farming localities diagnosed with viral disease in the period 2011-2021. The period 2011-2019 shows data submitted to the Norwegian Veterinary Institute. For 2020-2021, data marked with an asterix (*) includes numbers from private laboratories, explaining the apparent rise from previous years [9].

	2011	2012	2013	2014	2015	2016	2017	2018	2019	2020	2021
CMS	74	89	100	107	105	90	100	101	82	154*	155*
HSMI	162	142	134	181	135	101	93	104	79	161*	188*
PD	89	137	99	142	137	138	176	163	152	158	100
IPN	154	119	56	48	30	27	23	19	23	22*	20*
ISA	1	2	10	10	15	12	14	13	10	23	25

ISA is considered to be an important threat to the sustainability of salmon farming in Norway. Detection of ISA virus (ISAV) is notifiable to The World Organisation for Animal Health (OIE). The disease ISA is specific for Atlantic salmon. ISA epidemics in the early 2000s nearly destroyed the Chilean Atlantic salmon farming industry and resulted in complete sanitation of all marine farming sites in the Faroe Islands. Accordingly, ISA is of international significance and may induce restrictions on Norway's ability to export salmon and eggs. There were 25 registered outbreaks of ISA in Norway in 2021, which is the highest number since 1992, when 55 cases were recorded [9-11]. Figure 1 illustrates the annual number of ISA outbreaks from the first registered outbreak in 1984 [9].

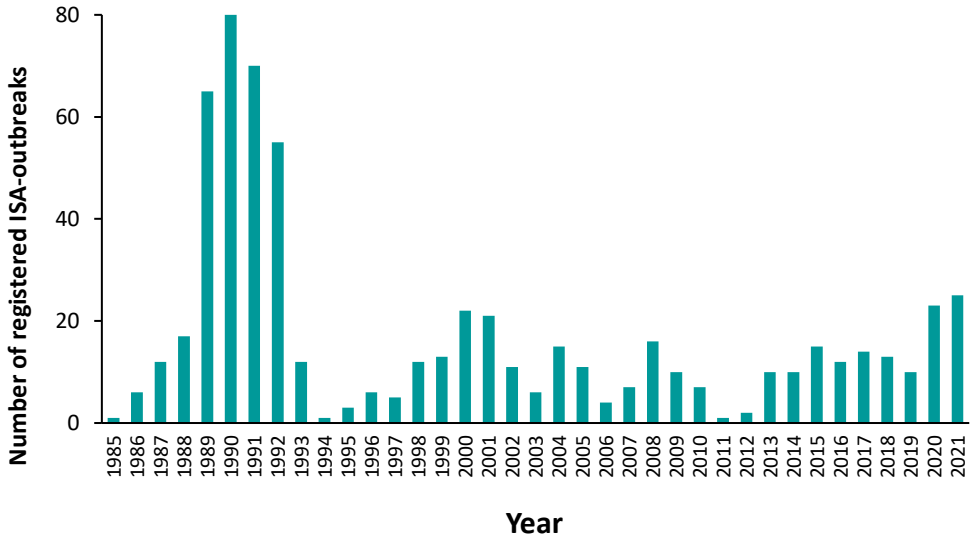

Figure 1. Annual number of ISA-outbreaks in Norway 1984-2021.

While ISA is a major cause of concern, it is not currently a top cause of mortality or reduced growth. Here, CMS is ranked as the number one cause of mortality in farmed salmon, followed by delousing, respiratory disease, and HSMI [9]. PD is ranked as number eight in terms of mortality, but number one in regards to reduction in growth. Several factors contribute to reduced fish health and welfare in farmed salmon, and probably also facilitate efficient spreading of infectious agents: high density of fish in a net pen, stress, and high number of individual hosts. Important infectious agents and the diseases they cause are listed in Table 2.

Table 2. Some important infectious agents in Norwegian farmed Atlantic salmon.

Agent	**Type**	**Disease**
Salmon alphavirus (salmon pancreas disease virus)	Virus	Pancreas disease
Infectious salmon anaemia virus	Virus	Infectious salmon anaemia
Infectious pancreatic necrosis virus	Virus	Infectious pancreatic necrosis
Piscine orthoreovirus	Virus	Heart and skeletal muscle inflammation in Atlantic salmon and HSMI-like disease in rainbow trout
Piscine myocarditis virus	Virus	Cardiomyopathy syndrome
Salmonid gill pox virus	Virus	Salmon pox (respiratory disease)
Flavobacterium psychrophilum	Bacterium	Flavobacteriosis
Aeromonas salmonicida subsp. *salmonicida*	Bacterium	Furunculosis
Moritella viscosa and *Tenacibaculum* spp.	Bacterium	Ulcer
Pasteurella spp.	Bacterium	Pasteurellosis
Lepeophtheirus salmonis (salmon louse)	Parasite	Anaemia and injuries
Caligus elongatus (sea louse)	Parasite	Injuries to skin
Parvicapsula pseudobranchiola	Parasite	Parvicapsulosis

1.2 Infectious salmon anaemia virus

Infectious salmon anaemia is a serious viral disease caused by virulent ISAV. It was first recognised as a new disease entity in 1984, in a salmon farm on the south-west coast of Norway [12]. Epidemic outbreaks of ISA followed over the next years, peaking around 1990, when ISA was diagnosed in 80 Norwegian salmon farms. One should remember that the number of farms and national production volume at that time was much smaller than today, i.e. the prevalence of ISA was very high. This resulted in strict mandatory biosecurity measures issued by the fish health authorities. Outbreaks of ISA have later been registered in Canada, Scotland, the Faroe Islands, Shetland, Chile, and the USA [13-15]. ISAV targets and replicates in endothelial cells lining blood vessels in all organs, and can also be associated with red blood cells (RBCs) and macrophages [16]. Clinically, salmon infected with ISAV may be lethargic and stay close to the wall of the net pen. Macroscopic findings of ISA are, anaemia, oedema, ascites, exophtalmia, and generalised petechial haemorrhages. The loss of RBCs cause anaemia seen as pale gills. Disposal of virus-associated RBCs, haemorrhages, and congestion give enlarged and dark spleen and liver. Later in the disease course, the liver often becomes yellow. Circulatory disturbances and bleedings are the assumed cause of death. On a farm-site, ISA may develop slowly with a daily mortality rate of only 0.05-0.1 % [13, 17, 18]. Figure 2a illustrates a healthy Atlantic salmon, whilst Figure 2b illustrates a salmon displaying typical clinical signs of ISA.

Figure 2. a) Control fish from an ISAV infection experiment showing no ISA signs. b) Salmon with ISA. Slightly pale gills, enlarged and dark liver and spleen, ascites, haemorrhages in eye, and petechial haemorrhages. *Photo: F. B. Ploss.*

1.2.1 ISAV classification and structure

ISAV has a negative-sense, single-stranded RNA genome and taxonomically belongs to the genus *Isavirus*, family *Orthomyxoviridae* [19]. The *Orthomyxoviridae* includes the Influenza A, B, C and D viruses, Quaranfil quaranjavirus and Thogoto thogotovirus [20]. ISAV is a pleomorphic, enveloped virus particle. The virions are between 90-130 nm in diameter, and the viral RNA-genome is segmented into eight linear segments, ranging between 0.8-2.2 kb each [19]. The total genome size is approximately 13.5 kb. Figure 3 is an illustration of the ISA virus.

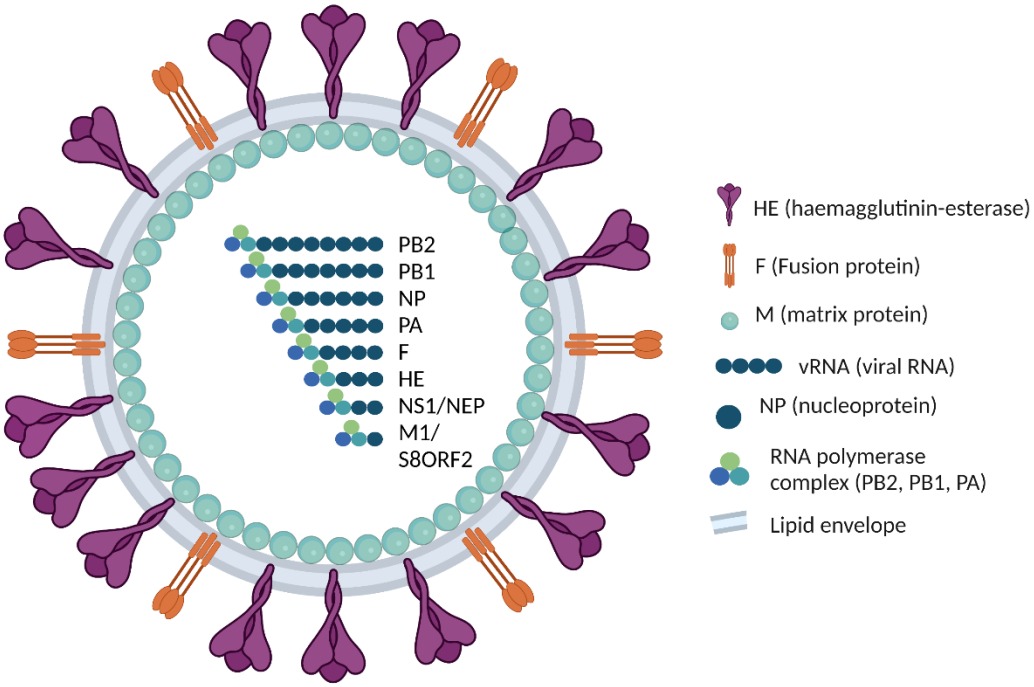

Figure 3. Schematic presentation of the ISAV particle. *Created with BioRender.com.*

The genomic segments are coated by the nucleoprotein (NP). A heterotrimeric RNA polymerase complex, which consists of polymerase basic 1 (PB1), polymerase basic 2 (PB2), and polymerase acidic proteins (PA), is bound to the end of each segment. Segments 1-6 encode one protein each, whereas segments 7 and 8 encode two proteins each, the former by alternative splicing [16, 19]. Table 3 gives an overview of the ISAV genome and the proteins encoded by the eight genomic segments.

Table 3. The ISAV genomic segments and functions [18, 21, 22].

Segment	Encoded proteins	Functional properties
1	Polymerase basic 2 (PB2)	Subunit of RNA polymerase complex
2	Polymerase basic 1 (PB1)	Subunit of RNA polymerase complex
3	Nucleoprotein (NP)	Encapsidates vRNA
4	Polymerase acidic (PA)	Subunit of RNA polymerase complex
5	Fusion protein (F)	Surface protein that induces fusion of viral and host cell membrane
6	Haemagglutinin-esterase (HE)	Surface protein that binds to 4-*O*-acetylated sialic acid residue (the ISAV receptor) on the cell surface. In addition to receptor binding, the HE has an esterase function, which cleaves the acetyl group to destroy the receptor binding in order to release virions.
7ORF1	Non-structural protein (NS)	Protein with innate immune response antagonist properties
7ORF2	Nuclear export protein (NEP)	Involved in export from nucleus
8ORF1	Matrix protein (M)	Structural protein that coats the inside of the membrane
8ORF2	S8ORF2	RNA-binding structural protein that antagonise the innate antiviral response

1.2.2 ISAV phenotypic variants

Non-virulent variants of ISAV (ISAV-HPR0) are characterised by a full-length highly polymorphic region (HPR) of the haemagglutinin-esterase (HE) surface glycoprotein, which corresponds to the near-membrane domain of the HE protein [23, 24]. In contrast, the great majority of ISAV variants that have been associated with disease have deletions in the HPR (HPR-del). Another characteristic of virulent ISAV HPR-del variants are specific mutations in the gene encoding the fusion protein: either a glutamine (Q_{266}) to leucine (L_{266}) substitution, or an insertion near and upstream of the cleavage site K_{276} [3, 23, 25]. F protein cleavage at K_{276} is essential for infection, because it primes the fusion peptide and allows for a subsequent conformational activation that mediates viral entry into the host cell. The phenotype-associated alterations around the F protein's cleavage site could be a key factor in altering the cell tropism, as described later in subchapter 1.2.6.

The ISAV-HPR0 variant mainly infects the mucosal epithelium of the gills, fins, and skin and is associated with transient subclinical infection [17, 24, 26]. Virulent variants targets and replicates in endothelial cells lining blood vessels in all organs. This has led to the hypothesis that virulent variants of ISAV repeatedly evolve from a reservoir of non-virulent ISAV-HPR0. Studies by Lyngstad et al. [27] and Christiansen et al. [23] support this hypothesis. The driving forces behind the deletions of the HE HPR and the F protein mutations and insertions are unknown, but a phenomenon found in influenza A

neuraminidase (NA), where deletions in the stem region has been linked to the adaption of host range [25].

1.2.3 Regulation of fusion in enveloped viruses

Attachment to the host cell is not sufficient to obtain viral infection of the cell. The virus must also deliver its genomic material to the cytoplasm in order to utilise the cell's replication machinery. For enveloped viruses, this includes a step with fusion of viral and host cell membranes, i.e. the plasma membrane or the endosomal membrane [28, 29]. Most enveloped viruses enter cells through endosomes. The membranes have a lipid bilayer, and fusion of membranes is a two-step process [29]. First step is fusion of the outer leaflets, an intermediate stage called hemifusion. The second step is fusion of the inner leafleats and leads to the formation of a fusion pore or aqueous channel between the two membranes. This fusion pore allows for mixing of contents of viral capsid and cytoplasmic. The fusion process is mediated by a viral fusion, "F" protein. The F proteins have been grouped into three classes based on four fusion triggering mechanisms, and structural criteria. For type I and type II F proteins, two steps are required for activation: *Priming*, which involves a protease that cleaves the F protein (for type I) or a companion protein (for type II). Priming leads to the F protein converting from a fusion-incompetent state to a fusion-competent state. Priming can take place at a cell surface, in an endosome, or in the Golgi apparatus, depending on the F protein and the infected cell. *Triggering* involves a series of structural changes of the cleaved fusion protein that exposes the fusion peptide, or the fusion loop, to the membrane. For viruses that enter via endosomes, triggering is often induced by environmental factors, such as low pH. When triggered, the fusion peptide, or fusion loop embeds itself into the host membrane, thus initiating membrane fusion [28]. Figure 4 illustrates the fusion process of type I F proteins.

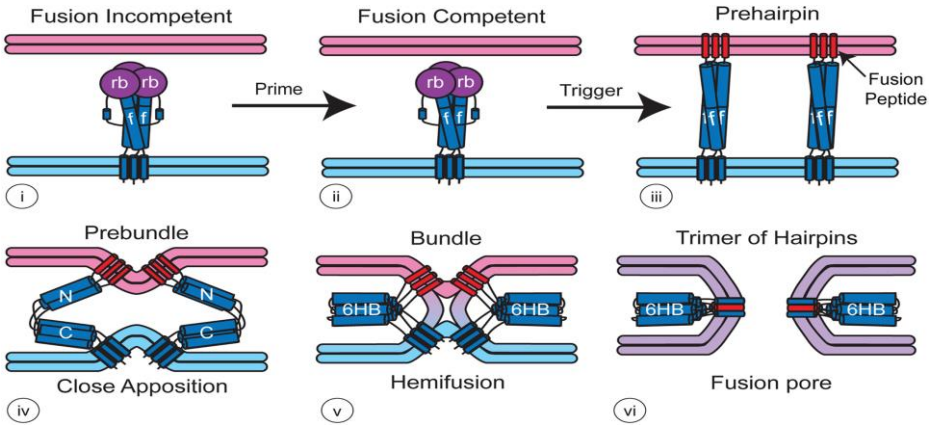

Figure 4. Schematic diagram of the function of viral type I F proteins. i) Prior to priming (cleavage), the F protein is a precursor polyprotein and is fusion incompetent. ii) After cleavage, the fusion peptide is exposed, and the F protein is fusion competent. iii) Triggering, such as low pH for some viruses, moves the receptor-binding subunit (rb) in purple to the side to insert the fusion peptide into the membrane, thus forming a structural prehairpin. iv) The prehairpin folds back on itself, pulling the viral- and host cell membrane closer to eachother. v)The N- and C-α-helical heptad repeats form a 6-helix-bundle (6HB), and the outer bilayer of the lipid membranes fuse (hemifusion). vi) Complete fusion of membranes leads to formation of a fusion pore between the two membranes [28]. *Reprinted by permission from John Wiley and Sons: Traffic, G. R. Whittaker, J. M. White, Fusion of Enveloped Viruses in Endosomes, Figure 2. Copyright (2016).*

There are four known fusion triggering mechanisms: by receptor-binding, by low pH, by receptor-binding followed by low pH, and by receptor-binding followed by proteolytic cleavage [28]. Different type I F proteins can be triggered by any of the four mechanisms, whereas exposure to low pH triggers all characterised type II fusion proteins. Different type III F proteins can be triggered by receptor-binding, by exposure to low pH, or by a combination of the two: receptor-binding followed by low pH [28].

1.2.4 Key proteins HE and F mediate viral attachment and entry

In ISAV, the HE- and the F protein mediate viral attachment and fusion. They are involved in receptor-binding, receptor-destroying and fusion activity that together mediate entry into and exit from the host cell. The combined changes to the HE HPR and the F protein that characterise virulent ISAV appears to enhance the viral fusion process [2, 3, 23]. Several studies show that the amino acid changes in the transition from non-virulent HPR0 to virulent HPR-del variants do not alter the receptor-binding- or -destroying activities, but rather change the threshold for fusion activation and thereby the virus' ability to enter cells [1, 4]. Since the requirements for successful fusion activation changes, the virus may change its cell tropism from mucosal epithelial cells to endothelial cells, and thereby cause disease.

In transfected cells, HE and F proteins appear to co-localise [2], forming a pre-entry complex of unknown ratio. ISAV is the only orthomyxovirus that encodes a F protein without receptor-binding or receptor-destroying activities, a property shared with many paramyxoviruses [16, 17]. For

orthomyxoviruses, like influenza A and B viruses, the fusion and receptor-binding activities reside in the haemagglutinin (HA) protein, whereas the receptor-destroying activity resides in the NA protein [25]. Influenza C virus has only one surface protein, the haemagglutinin-esterase-fusion (HEF) protein, which is multifunctional and responsible for receptor-binding, receptor-destroying activity, as well as the fusion process [30]. The mechanisms of the ISAV fusion process and how changes to the HE HPR and F protein eventually enhance the fusion process are not completely understood. More knowledge on these mechanisms will give a better understanding of how ISAV HPR-del emerges and eventually how to limit the formation of new ISAV HPR-del variants, if possible. However, this has been difficult to study because cultivation of ISAV-HPR0 has been very difficult.

The two envelope glycoproteins; the F and the HE protein, are encoded by segment 5 and 6, respectively. They are embedded in the viral envelope where the matrix (M) protein structurally lines the lipid envelope inside [21, 31]. The HE protein is a trimer where the complex is stabilised by a hydrophobic interface and by 12 hydrogen bonds between the monomers [32]. The trimeric HE protein forms a «broccoli floret» shape of approximately 130 x 70 x 70 Å, as shown in Figure 5. Each monomer contains three functional domains: the stem domain, the receptor-binding domain (RBD), and the esterase domain, which is the receptor-destroying enzyme domain (RDE). ISAV attachment to the host cell occurs when the RBD located on the HE globular head, binds to 4-*O*-acetylated sialic acid residues on the cell surface [2, 32]. Upon receptor-binding, HE and F proteins are believed to dissociate, and the virion enters the host cell by endocytosis [32].

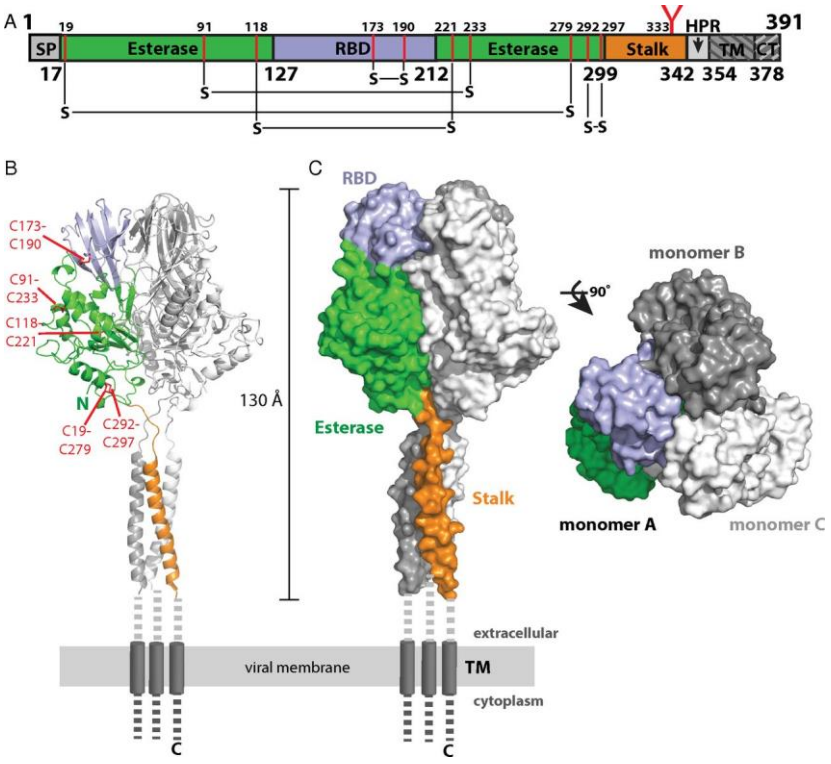

Figure 5. Schematic illustration of the domain structure of ISAV HE. A) signal peptide (SP), receptor-binding domain (RBD), red Y is the predicted N-linked glycosylation site at N333, highly polymorphic region (HPR), transmembrane domain (TM), cytoplasmic tail (CT). B) Ribbon diagram of the ISAV HE with domains in one monomer. The coloured domains correspond to A). C) Representations of ISAV HE molecular surface [32]. *Reprinted by permission from Proceedings of the National Academy of Sciences: J.D. Cook, A. Sultana, J.E. Lee, Structure of the infectious salmon anemia virus complex illustrates a unique binding strategy for attachment, Figure 1.*

The F protein is also trimeric and has been classified as a type I fusion protein [3, 15, 31]. It is present in the viral membrane as a precursor (F_0), which primes when cleaved into F_1 and F_2 subunits by cellular proteases. The cleavage site was identified as K_{276} by Fourrier et al. [3]. The cleaved subunits are bound together by disulfide-bridges. Figure 6 is an illustration of the F protein. Once cleaved, the F protein is trapped in a metastable state by a kinetic barrier and is dependent on low pH , to activate the protein to refold into a stable conformation [3, 31]. Type I F proteins have a fusion peptide, a short hydrophobic sequence near or at the N-terminal of the F_2-subunit, which embeds itself into the endosomal membrane upon low pH. Exposure to low pH induces the F protein to protrude forwards, thus inserting the fusion peptide in the endosomal membrane. The ISAV fusion peptide has been identified at C_{277} to Y_{292} [31]. Another characteristic of the type I F protein is a heptad-repeat of leucine or isoleucine residues that fold into an α-helical coiled-coil, also called a leucine zipper. The three monomers with the leucine zippers form a central three-stranded coiled-coil, in which the C-terminal of each monomer folds over. This *hairpin* structure forms after the insertion of the fusion peptide into the host membrane. The hairpin structure draws the viral and host cell membranes together and mediates fusion [15, 28, 29, 31]. ISAV is a cold adapted pathogen, thus fusion occurs at 12-15 °C [32].

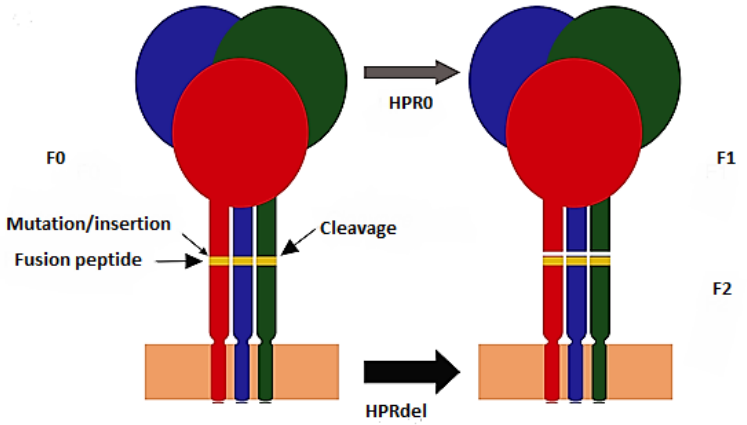

Figure 6. Schematic illustration of F protein cleavage from F_0 to F_1 and F_2. The cleavage site, mutation/insertion sites and the fusion peptide in yellow are indicated. The F protein is inactive in it's F_0 state and is activated upon cleavage that exposes the fusion peptide. Thicker and bigger arrow at the bottom refers to easier cleavage of F protein if co-expressed with ISAV HE HPRdel *[21]. Reprinted by permission from John Wiley and Sons: Journal of Applied Microbiology, E. Rimstad, T. Markussen, Infectious salmon anaemia virus – molecular biology and pathogenesis of the infection, Figure 4b. Copyright (2020).*

1.2.5 Replication cycle

ISAV appears to have a similar replication cycle to influenza viruses, illustrated in Figure 7. ISAV replicates in the nucleus because it utilises the host cell splicing machinery, as well as a phenomenon referred to as cap snatching: the 5'cap end of host mRNA is snatched and used as a primer to start the synthesis of antigenomic (+) RNA/viral mRNA, [16, 21, 33]. Segment 1-6 encodes one protein each, whereas segment 7 and 8 each encodes two proteins, due to mRNA splicing in segment 7, and overlapping reading frames in segment 8.

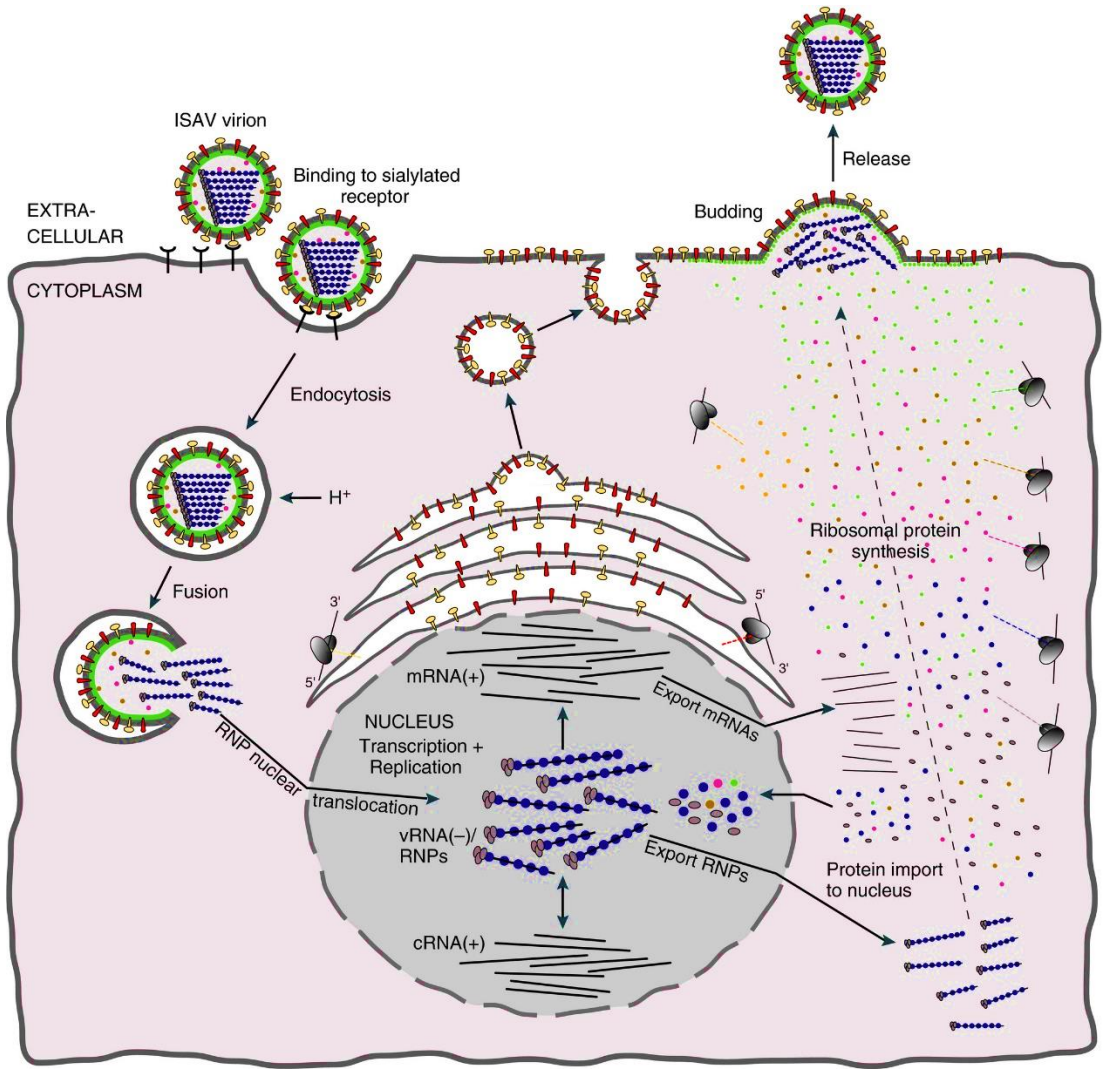

Figure 7. Schematic illustration of the replication cycle of ISAV. host cell receptor (4-O-acetylated sialic acid), HE (haemagglutinin-esterase), F (fusion protein), NP (nucleoprotein), RNA polymerase complex (PB2, PB1, PA), M (matrix protein), NS (non-structural protein), NEP (nuclear export protein), S8ORF2 protein, RNP (ribonucleoprotein) [21]. *Reprinted by permission from John Wiley and Sons: Journal of Applied Microbiology, E. Rimstad, T. Markussen, Infectious salmon anaemia virus – molecular biology and pathogenesis of the infection, Figure 3. Copyright (2020).*

Upon fusion, the viral ribonucleoproteins (RNP) are released into the cytoplasm. The viral proteins of the RNP have nuclear localisation signals (NLS) and the RNP is transported into the nucleus. Here, the negative sense vRNA is transcribed by the viral RNA polymerase complex (that was a part of the RNP) into viral mRNA, and cap snatching from cellular mRNA takes place. The mRNA of segment 7 is spliced, and the mRNAs are transported to the cytoplasm and translated. The mRNA that encodes the viral membrane proteins are translated on ribosomes associated with the endoplasmatic reticulum (ER) and glycosylated in the Golgi apparatus, before they are transported and inserted into the plasma membrane. The other mRNAs are translated on free ribosomes in the cytoplasm. Newly translated proteins of the RNP are transported back into the nucleus by the help of the NLS. When they accumulate they induce a switch from the synthesis of mRNAs to synthesis of full-length

(+) antigenome, lacking cap and referred to as copy RNA (cRNA). The nucleoproteins bind to nascent (+) antigenome and inhibits premature termination of RNA synthesis by enabling the RNA polymerase to add several adenine residues by backsliding repeatedly on the RNA template on a short stretch of uracil residues. This phenomenon is called poly(A) stuttering and allows for a full-length (+) antigenome synthesis, which in turn will be transcribed into new copies of vRNA in the form of nucleocapsids. The M- and nuclear export proteins (NEP) are transported into the nucleus where M proteins bind to newly synthesised vRNA, which stops further viral mRNA synthesis. NEP mediates export of the nucleocapsids associated with M to the cytoplasm, where they are transported to the plasma membrane for assembly of new viral particles, which subsequently exit the cell by budding. The RDE of the HE protein is assumed to cleave the cell receptor allowing the release of viral particles [16, 21, 34].

1.2.6 Host proteases in virus tropism

Gill and skin mucus forms a protective overlay covering the epithelium of the fish, and is considered to be the first barrier of defense against pathogens [35, 36]. Mucus is a viscous and semipermeable, complex hydrated secretion, and has components that are involved in respiration, nutrition, osmoregulation, locomotion, as well as immune functions [37, 38]. The mucus layer is impermeable to most microorganisms and pathogens, where they are trapped and removed by water current, before they can reach the epithelial surfaces [35, 39]. Additionally, the mucus layer is constantly secreted and replaced, thereby limiting colonization of microorganisms and pathogens [35, 40].

Proteases play an important role in fish mucus. Proteases can kill bacteria by catalysing cleavage of their proteins, or they can remove the pathogens by modifying the mucus texture to increase the shedding of mucus. Additionally, proteases can activate and stimulate components of the innate immune system in fish mucus, including antibacterial peptides and immunoglobulins [35, 41].

Mutations in the cleavage site of viruses that contain class I fusion proteins can alter their proteolytic activation and modify the cell and tissue tropism of the virus. This can again alter their host range and pathogenesis. HPR0 variants target epithelial cells, whereas the virulent HPR-del variants have changed tropism and target endothelial cells. The mutations around the HPR-del F protein cleavage site could be comparable to the genomic alterations in avian influenza A haemagglutinin (HA) of subtypes H5 and H7 that are associated with increased virulence [42]. Moreover, a recent study used reverse genetics to link ISAV segment 5 and 6 to cell tropism by showing that substituting HPR0 segment 5 and 6 with segment 5 and 6 from a virulent ISAV isolate completely rescued virus replication in cultured cells to a level comparable to virulent ISAV [43].

Considering how other viruses enter cells may help us understand ISAV fusion. In influenza A, fusion is mediated by the HA surface glycoprotein, which activation requires prior cleavage (priming) of the precursor HA_0. In low-pathogenic avian influenza A virus (LPAIV), HA_0 is cleaved by trypsin-like extracellular proteases localised in respiratory and intestinal organs. The low-pathogenic type causes mild infections of the respiratory and intestinal tracts of the host. The acquirement of basic amino acids through mutations near the HA_0 cleavage site causes a change in virulence and leads to serious systemic infection in poultry. The cleavage-site becomes accessible to ubiquitous proteases, such as furin-like cellular endoproteases. This means that the HA_0 can be cleaved as it is processed and matured through the Golgi apparatus, and the virion is therefore infectious already when it buds from the cell. The result is that highly pathogenic avian influenza (HPAI) is not restricted to organs or tissues containing extracellular trypsin, and can spread to all organs of the infected host and cause severe disease [25, 44-46].

Coronaviruses have a wide host range and can infect many species of birds and mammals, as well as humans. Their ability to jump beween species is partly due to the several strategies they utilise to infect cells [47-49]. Coronaviruses have a surface glycoprotein called the spikeprotein. The spike protein mediate viral attachment and entry by having both receptor binding and membrane fusion functions [49, 50]. Proteolytic activation of the spike protein is a critical factor for membrane fusion, and coronaviruses have evolved several strategies for this [49]. Many host proteases such as trypsin, furin, cell surface transmembrane protease/serine proteases, endosomal cathepsins, and more, have been shown to catalyse cleavage of the spike protein. Several proteolytic cleavage sites on the spike protein has been found [50]. Cleavage at the different sites can either take place during virus entry or during the biosynthesis of the spike protein, thus these spatio-temporal cleavage events are important factors in tissue and cell tropism, host range and pathogenicity [49]. These cleavage events are dependant on the coronavirus and the host cell infected. Strains from the same coronavirus can use different entry strategies, i.e. the Omicron spikeprotein favours entry via endocytosis in contrast to Delta and other variants of Sars-CoV-2 [51].

1.3 Findings from previous studies

Previous studies have compared and combined HE and F protein sequences from naturally occurring ISAVs that are only distantly related. Because of this, the HE and F sequences used also have other differences in the amino acid sequence than the ones that correlates with the transition to virulence. The effects of these additional changes are unknown but should not be ignored. Some of the studies have also induced artificial mutations in the HPR0 sequence [2, 3]. A summary of published fusion assay studies that compare ISAV HPR0 and HPR-del is listed in Table 19, Appendix 3. Because the interaction between the HE and F proteins are unknown, it is not certain that all virulent HE variants work equally well with all virulent F variants. As a result, some findings may be difficult to interpret.

Key findings from previous studies:

- McBeath et al. showed that HPR0 and HPR-del HE have similar receptor binding and receptor destroying activities [1]. However, the authors observed differences between the HE variants that were not due to the HPR-deletion but that they suggest could be related to seven amino acid differences in other parts of the HE protein. This has resulted in several studies [4, 32] citing the paper as evidence for HPR0 having a stronger esterase activity than HPR-del.
- In contrast, a recent study by Cárdenas et al. [43] showed that HPR0 binds Atlantic salmon kidney (ASK) cells more efficiently than HPR-del. Again, this indicates that not all differences between the HE proteins are due to HPR-deletion.
- When combining HPR0/HPRdel HE with different virulent F proteins, Fourrier et al. [2] observed virus-specific differences in fusion activity that is explained by other differences than the prototypic changes, again suggesting that variation in other parts of the protein should not be ignored.

There are knowledge gaps concerning F protein cleavage: The F protein can be cleaved by trypsin [3, 31], but which protease(s) that actually cleaves during an infection is yet to be determined. Furthermore, the effect of the mutations in the HE HPR and F protein on the protease-specificity and conformational stability remains unknown. To understand the complex interplay between HE and F proteins that results in viral entry, we need to make our model system as simple as possible. In this study, the use of recombinant ISAV HE and F proteins based on naturally occurring viruses from the field and without other amino acid changes than those correlated with the transition to virulence limits the complexity of the system.

A strength in this study is that the sequences used are from closely related viruses detected on farms. The fact that they were detected in material from the fish means that they can maintain themselves in a fish population and have a certain level of fitness. While the relationship between the non-virulent and virulent variant has not been confirmed by whole genome sequencing, we know that the amino acid sequence differences between the variants are limited to those correlated with the transition to virulence. This means that it will be easier to ensure that the changes we observe are due to these correlated mutations only.

1.4 Aims of the thesis

This study aimed to understand the biological relevance of the changes in HE and F when non-virulent ISAV-HPR0 develops into virulent ISAV-HPR-del, and to study the mechanisms involved in the ISAV fusion process. More specifically, the study set out to establish fusion assays inspired by a previous study [3], and use these assays to evaluate the fusion activity of HE and F proteins from closely related ISAV-HPR0 and HPR-del variants.

Based on previous studies [1], our hypothesis was that the non-virulent ISAV-HPR0 and the virulent HPR-del variants have similar receptor-binding and receptor-destroying activities. Additionally, that the virulent HE/F variant combination has a higher activity of fusion compared to a non-virulent HE/F variant, in line with the current hypothesis that ISAV virulence is related to fusion activity [2-4].

Sub-goals:

- Express closely related HPR0 and HPR-del variants of HE and F glycoproteins, with origin from recent outbreaks in Norway, in CHSE cells.
- Compare receptor binding and receptor destroying activity of HPR0 and HPR-del HE proteins.
- Establish lipid mixing assays for evaluation of hemifusion activity.
- Use the assay to compare the fusion activity of virulent and non-virulent HE/F protein combinations when priming and triggering is stimulated by trypsin and low pH.

1.5 Institutional context

The work in this thesis is part of two larger research projects, ILA-SAFE and BIO-DIRECT. The main objective of the ILA-SAFE project is to gain more knowledge about the transition from non-virulent to virulent ISAV, and to develop best-practice measures for hatcheries to reduce the risk of change to, and the spread of virulent ISAV. The goal of the work package this thesis is a part of, is to identify virus – host interactions that influence the transition from non-virulent to virulent ISAV. More specifically, this thesis contributes to developing methods to measure ISAV fusion activation.

The main objective of the BIO-DIRECT cross-disciplinary initiative at the Norwegian Veterinary Institute is to develop future-oriented veterinary research and diagnostics through identification of new biomarkers, multiplexed detection assays, and cell-based bioassays. The BIO-DIRECT initiative will build an internal technology platform that includes methods for biomarker discovery and analysis tools. The goal of the work package this thesis is a part of, is to establish and optimise methodology for Bio-Plex assays, and other multiplexed biomarker assays. More specifically, this thesis aimed to establish a bead-based protease activity assay to identify proteases that can cleave and activate ISAV in mucus and other substances.

2 Materials and Methods

This chapter gives an overview of materials and methods used in this study. An overview of the main experimental steps performed in this thesis is presented in Figure 8.

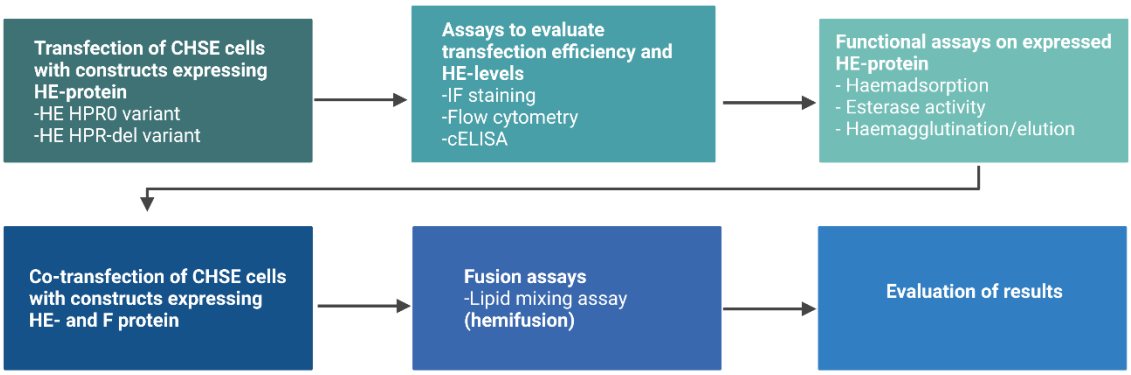

Figure 8. Flow chart of the main experimental steps in this study. *Created with BioRender.com.*

The HPR0 HE and F-sequences (strain NO/Finnmark/NVI-07-7/2021) used in this thesis originated from salmon gill samples from a Norwegian smolt farm during routine surveillance for ISAV. The HPR-del sequences are from an ISAV isolate (NO/Finnmark/NVI-70-1250/2020) propagated from dish organ samples from a Norwegian sea farm, which received salmon from the smolt farm and experienced an ISA outbreak nine months after the HPR0 detection in the smolt farm (Figure 9). The HE and F-sequences of the HPR-del isolate from the sea farm are identical to those of the HPR0 from the smolt farm, except for the characteristic amino acid changes that correlates with the transition from non-virulent HPR0 to virulent HPR-del. The epidemiological link has led to the hypothesis that the HPR-del isolate from the sea farm originated from the smolt farm. However, the relationship has not yet been confirmed by whole genome sequencing.

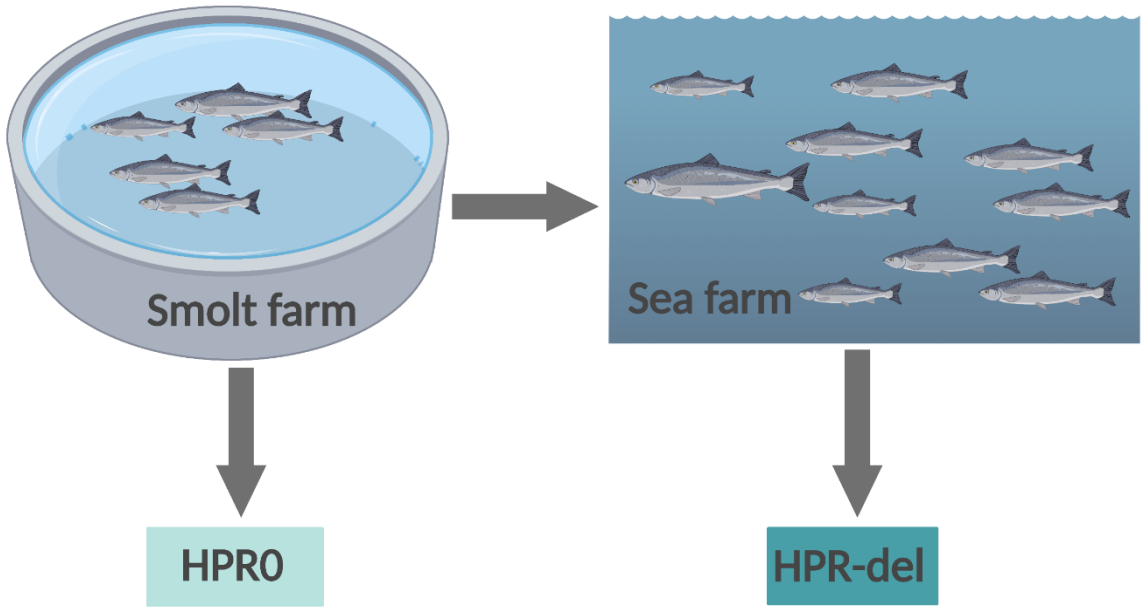

Figure 9. Non-virulent ISAV-HPR0 was detected on salmon from a smolt farm during routine surveillance for ISAV. The smolt farm delivered salmon to a sea farm, which later experienced an outbreak of virulent HPR-del. The HE and F-sequences of the variants were identical, except for characteristic amino acid changes that correlates with the transition from HPR0 to HPR-del. *Created with BioRender.com.*

The mutations in the amino acid sequences for HPR0 and HPR-del HE and F proteins used in this study are shown in Figure 10.

HPR0 HE protein	323-HKEMISKLQRNITDVKIRVDAIPPQLNQTF NTNQVEQPATS VLSNIFISMGVAGFG-378
HPR-del HE protein	323-HKEMISKLQRNITDVKIRVDAIPPQLNQTF---------- GVAGFG-378
HPR0 F protein	256-QHGWSKYNFNQRAFPGEEFIKCCGFTLGIGGAWFQAYLNG-295
HPR-del F protein	256-QHGWSKYNFNLRAFPGEEFIKCCGFTLGIGGAWFQAYLNG-295

Figure 10. The mutations in HE and F proteins used in this study. The red box frames the full-length and deleted HPR region of the HE-sequences. The F protein have a Q266L mutation (in blue). The cleavage site is K_{276} (in red), and the fusion peptide is at C_{277}-Y_{292} (in green).

2.1 Cell line

The experiments in this thesis were performed *in vitro*, with the use of cell cultures. An advantage with cell culture studies is that they can be studied in a controlled environment, as opposed to whole organisms [52]. Cell culture can replace experimental animals, in line with the 3R principles. Also, strict control of experimental conditions and many available tools makes it easier to study biological processes. However, because cells in culture are not in their natural environment and complex intercellular processes are not accounted for, these models rarely predict the effects on the whole organism [53, 54]. Therefore, it is important to choose the right cell line model to address the particular research question. In many cases, it is important to choose a cell line from the same species, target

organ and cell type, or choose one that is as close as practically possible in order to represent the *in vivo* situation.

The cell line should also be easy to work with, have an appropriate growth rate, and have observable responses for the focus of interest. Some cell lines grow as monolayers, also called adherent culture, whereas some cell lines are floating freely in the culture medium, called suspension cultures [55]. A disadvantage of adherent cell cultures, is that they require enzymatic or mechanical dissociation from the substrate. Some cell lines are easy to detach, while others require long enzymatic incubation time. Suspension cultures do not require dissociation, and are therefore easier to passage.

2.1.1 CHSE cells

Chinook salmon embryo (CHSE-214, here called CHSE) cells were originally obtained from *Onchorhynchus tshawytsca*, a Pacific salmon species also called king salmon. CHSE cells are extensively used in research of viral diseases in fish, because the cell line is susceptible to a number of fish viruses. CHSE is an adherent cell line and grows in a monolayer, has a robust growth, and have an epithelial-like morphology [56] as shown in Figure 11. Additionally, CHSE cells have a higher transfection efficiency than Atlantic salmon cell lines, such as ASK cells [57].

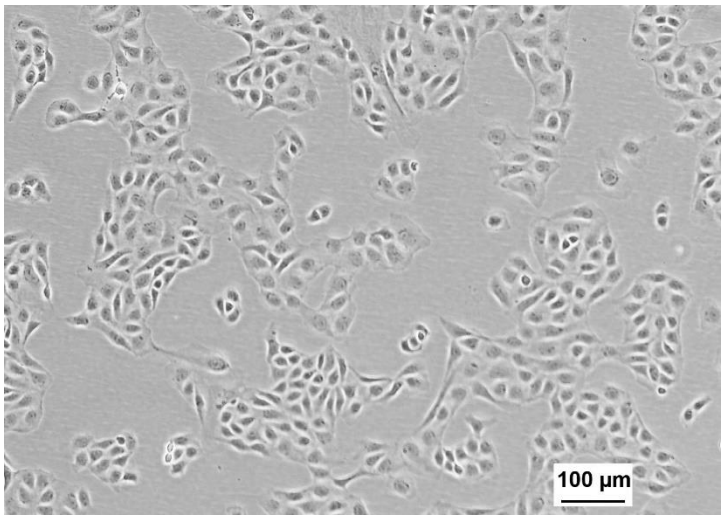

Figure 11. CHSE cells are epithelial-like and grow in patches attached on surface. Cells in the photo show a confluence of approximately 50-60 %. Cells were photographed with a Nikon DS-Fi3 Digital camera at 10X magnification on a Nikon Eclipse Ts2-FL inverted microscope.

In this thesis, the goal was to obtain a model that mimics the ISAV fusion process. CHSE cells are susceptible to some virulent ISAV variants, but it is worth noting that the CHSE cells themselves were not target cells for ISAV in this study, but utilised as a model system. The CHSE cells were transfected

with plasmids encoding HE and F proteins, and RBCs were used to mimic target cells, as illustrated in Figure 12.

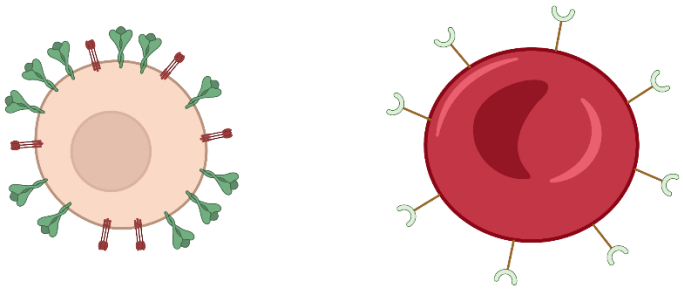

Figure 12. Cell model mimicking the ISAV fusion process: CHSE cell transfected with plasmids encoding HE and F proteins, and RBCs with sialic acids presented on their surface mimic target cells. *Created with BioRender.com.*

2.1.2 Subculturing CHSE cells

Adherent cells are anchorage-dependent, which means they must be attached to a surface to grow. They need to be subcultured or passaged in fresh growth medium to reach full confluency. CHSE cells must be trypsinised and detached before they are split into new cell flasks. Trypsin is a proteolytic enzyme, which catalyses the hydrolysis of peptide bonds in proteins that adhere the cells to the surface [58]. Depending on the cell line and concentration of trypsin added, the trypsination step can take from a few minutes up to several minutes. However, the cell surface receptors can be damaged if the incubation time with trypsin is too long. The trypsin used for detaching CHSE cells contain a chelating agent, ethylenediaminetetraacetic acid (EDTA), which binds inhibitory cations. Trypsin is inactivated by serum from the culture medium, and it is essential to remove the medium by washing the cell monolayer with phosphate-buffered saline (PBS) without Ca^{2+} or Mg^{2+} prior to trypsination. When the cells are detached, fresh growth medium with serum is added to neutralise the trypsin, and the cells are split into new cell flasks for further growth [59].

2.2 Transfection

The term transfection is used to describe the method where nucleic acids can be introduced into eukaryotic cells [60, 61]. Transfection is widely used to express recombinant proteins by a using transfection substrate, such as mRNA or plasmid vector. In a natural target cell, the recombinant protein is likely synthesised with appropriate folding and post-translational modifications, and can be used for functional studies [60].

If the transfected nucleic acid is active in the cell for short period of time, it is called transient transfection. The introduced genetic material is not integrated into the genome and eventually stops expressing protein. If the nucleic acid exists long-term in the cell due to genomic integration of the transfected gene material, it is called stable transfection. Transient transfection was used in this study. During cell division, the gene material gets diluted, or can be degraded by cell nucleases. However, in the short period of the introduced genetic material's existence, the cells express high protein levels due to high copy number of the genetic material or very efficient promoter; a process called over-expression. Transiently transfected cells are usually studied between 24 to 96 hours after transfection. The optimal time for studying transfected cells depends on factors such as cell type, expression characteristics of introduced nucleic acid, temperature, and research goals [62].

Many different chemical, biological, and physical methods can be used for transfection [62]. The different methods have advantages and disadvantages, and suit different cell types, due to differences in transfection efficiency, cell toxicity, and gene expression levels. Chemical methods include lipofection, calcium phosphate transfection, and DEAE-dextran transfection [61]. These methods are based on using positively charged molecules to deliver the negatively charged nucleic acid through the negatively charged cell membrane. Viral transduction is a biological transfection method where a virus is used to carry the genetic material into cells. Importantly, viral transduction depends on the viral vector being able to enter the target cell type.

2.2.1 Electroporation

Electroporation is a physical transfection method where the foreign gene material is introduced to cells due to temporary pores created in the cell membrane by applying an electrical charge. Cells must be in suspension with the plasmid vector in an electroporation buffer. Pulses of high-voltage electricity are applied to create a change in potential across the cell membrane, which creates the temporary pores [61]. Electroporation was used in this study to transfect CHSE cells with plasmids encoding HE and/or F proteins.

2.2.2 Transfection procedure

Plasmid vectors used in the transfection work were pcDNA 3.1 +/HPR0 HE, pcDNA 3.1 +/HPR-del HE, and/or pcDNA 3.1 +/HPR0 F and pcDNA 3.1 +/HPR-del F (Genecust, Boynes, France). The GenBank accession numbers for the nucleotide sequences for segment 5 and segment 6 of the Norwegian strains are listed in Table 4.

Table 4. GenBank accession numbers for the sequences of segment 5 and segment 6 for the Norwegian ISAV strains used in this study [63].

Variant	Strain	Segment	Collection date	Nucleotide sequence	Protein sequence
HPR0	NO/Finnmark/NVI-07-7/2021	5	19.01.2021	MW711822	UGL76657.1
		6		MW711826	UGL76661.1
HPR-del	NO/Finnmark/NVI-70-1250/2020	5	09.10.2020	MW292221	UGL76647.1
		6		MW292225	UGL76651.1

CHSE cells were cultured in Leibovitz L15 medium supplemented with 5 % foetal bovine serum, 4 mM l-glutamine, and antibiotics; 500 IU Penicillin, 500 µg Streptomycin, and 1.25 µg AmphotericinB (Lonza, Basel, Switzerland). Cell cultures were incubated at 20 °C for 1-4 days until they reached 90-100 % confluency.

Cell monolayers were trypsinised (Lonza, Basel, Switzerland), and washed with PBS. Transfection was performed using the Neon Transfection System (Invitrogen, Waltham, MA, USA). The electroporation conditions were set to three pulses at 1600 V and 10 ms width. After 24 hours of incubation, media from wells were replaced with L15 media supplemented with antibiotics (Lonza, Basel, Switzerland). Further details on different conditions for each assay are described below.

Cells used in immunofluorescent staining

CHSE cells were transfected using the Neon 10 µL kit (Invitrogen) with approximately 10^5 cells to 2 µg DNA per reaction. Quadruplicate reactions were made, and cells were dispensed into wells on a 24-well plate, each well containing 1 mL of L15 media without antibiotics (10^5 cells/well). Non-transfected CHSE cells were plated as negative controls in quadruplicate parallells.

Cells used in flow cytometry

CHSE cells were transfected using the Neon 10 µL kit (Invitrogen) with approximately 10^5 cells to 1.6 µg DNA per reaction. Duplicate reactions were made, and cells were plated on a 24-well plate, each well containing 1 mL of L15 media without antibiotics (10^5 cells/well). Non-transfected CHSE cells were plated as negative controls in duplicate parallells.

In a second experiment, CHSE cells were transfected with only plasmid pcDNA3.1+/HPR0 HE using the Neon 100 µL kit (Invitrogen) with approximately 10^6 cells to 10 µg DNA per reaction. Cells were plated

on a 12-well plate, each well containing 2 mL of L15 media without antibiotics (300 000 cells/well). Non-transfected CHSE cells were plated as negative controls in duplicate parallells.

Cells used in haemadsorption, esterase activity, and cELISA assays

CHSE cells were transfected using the Neon 10 µL kit (Invitrogen) with approximately 10^5 cells to 1.6 µg DNA per reaction. Triplicate reactions were made. Reactions were added to 390 µL of L15 media (Lonza) without antibiotics and dispensed into four wells on different 96-well culture plates (25 000 cells/well); for haemadsorption and esterase activity assays, and two 96 well 1 x 8 strip plates for cELISA. Non-transfected CHSE cells were plated as negative controls. These monolayers were incubated for 24-48 hours at 20 °C.

Cells used in haemagglutination/elution assay

CHSE cells were transfected using the Neon 100 µL kit (Invitrogen) with approximately 10^6 cells to 10 µg DNA per reaction. Reactions were performed in triplicate, and transfected cells were pooled in a 6-well plate containing L15 media (Lonza) without antibiotics (3 mL/well) and incubated for 48 hours at 20 °C. Non-transfected CHSE cells were plated as negative control.

Cells used in lipid mixing and haemadsorption assay

CHSE cells were transfected using the Neon 10 µL kit (Invitrogen) with approximately 10^5 cells to a total of 2 µg DNA per reaction (0.5 µg of HE and 1.5 µg of F protein). Triplicate reactions were made. Cells were plated on two 96-well plates ($2.5*10^4$cells/well). Each well had been pre-coated with 0.2 % gelatin (in PBS). 100 µL of transfected cell solution was dispensed per well of a 96-well plate (Corning, St.Lois, MO, USA). A total of 2 parallell wells were prepared for each combination of ISAV HE and F protein. Non-transfected CHSE cells were plated as negative controls. These monolayers were incubated for 48 hours at 20 °C and used in two assays: lipid mixing assay and haemadsorption assay. After 24 hours, media from wells were replaced with L15 media supplemented with antibiotics (Lonza).

2.3 Immunofluorescent staining

Immunofluorescence (IF) is widely used to detect specific proteins and molecules in cells. The IF method is based on detection of a fluorophore coupled to an antibody [64, 65]. With IF, the cellular and subcellular location of the protein(s) of interest can be visualised in a fluorescent microscope. IF makes it possible to assess protein expression and post-translational modifications, depending on the specificity of the primary antibody. Different methods are used to amplify the fluorescent signal; fluorophores can be coupled directly to primary antibodies, or more commonly, fluorescently labelled

secondary antibodies are used for indirect detection of unlabelled primary antibodies [64, 66]. The latter is a more sensitive detection method, because several secondary antibodies can recognise and bind to each primary antibody. Fluorophores can also be used in tertiary amplification systems, such as the biotin/avidin system, where a biotin-labelled secondary antibody is bound by several fluorophore-conjugated avidin-molecules. IF was used in this study to evaluate if the transfected CHSE cells expressed HE proteins and get an impression of expression levels.

Procedure

Cells were transfected as described in subchapter 2.2.2. The media was aspirated from wells 48 hours post-transfection, and the cells were fixed with PFA 4 % (w/v) for 10 minutes at room temperature. Cells were washed twice with PBS and 100 µL PBS was added to each well. Primary antibody, 3H6F8 (mouse IgG1, anti-ISAV HE) was diluted (1:50 in PBS) and added to two parallell wells, and primary antibody with 0.1 % saponin was added to two other parallell wells (100 µL/well), followed by 60 minutes incubation on a shaker in the dark. Saponin is used to permeabilise the cell membrane after PFA fixation in order to IF stain for HE protein intracellularly as well. Cells were washed three times with PBS and secondary antibody, goat anti-mouse IgG Alexa 488-conjugated (Life Technologies, Waltham, MA, USA) was diluted (1:200 in PBS) and added to wells (100 µL/well) followed by 45 minutes incubation in the dark. Negative controls (non-transfected cells) were stained with and without saponin, and two wells were kept unstained. Cells were washed three times with PBS, 500 µL PBS was added to wells, and cells were analysed on a Zeiss Axio Observer A1 inverted microscope (Carl Zeiss MicroImaging GmbH, Göttingen, Germany).

2.3.1 Flow cytometry

Flow cytometry is used to measure and characterise cells in suspension. Cell surface or intracellular molecules can be immunostained with antibodies coupled to fluorochromes, and analysed to provide both qualitative and quantitative data on a single cell level [67]. The cells are injected into a stream of fluid narrowed by hydrodynamic focusing, which forces the cells into a single line [65, 67, 68]. As they pass individually through a laser, the laser-beamed cells create light scattering, which is detected by different photodiodes and converted to an electrical signal. The forward scatter of light in the laser path is a function of the cell size. Side scattering is often related to the morphological complexity of a cell, i.e. internal structures or granularity [68]. A schematic presentation of flow cytometry is illustrated in Figure 13.

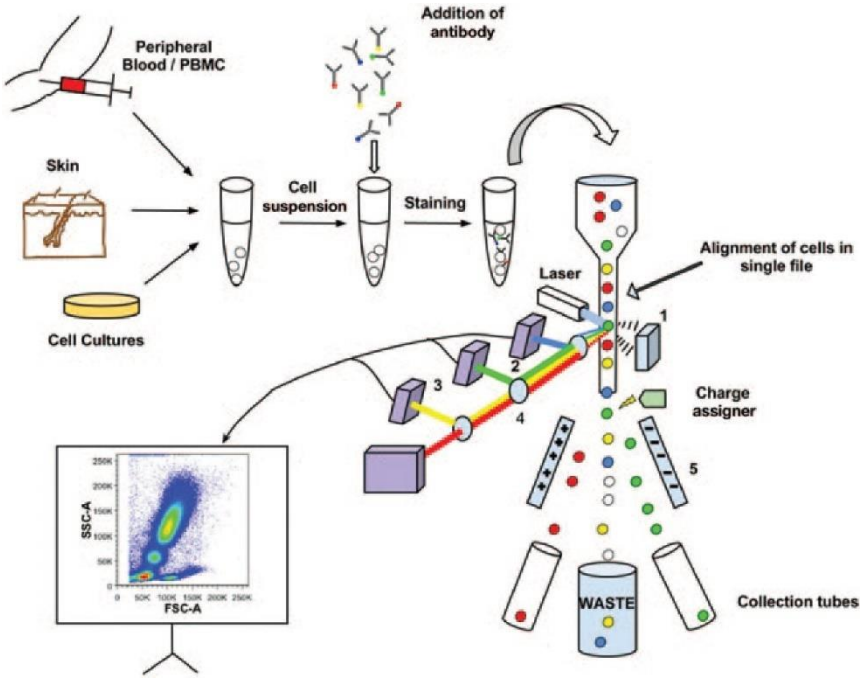

Figure 13. Schematic illustration of flow cytometry [69]. Cells in suspension are immunostained and separated into a single line before they pass a laser beam. If the cells have the antibody-fluorochrome attached, they will absorb the laser energy and create light scattering, which is detected by different photodiodes and converted into an electrical signal. *Reprinted by permission from Elsevier: Journal of Investigative Dermatology, R. R. Jahan-Tigh, C. Ryan, G. Obermoser, K. Schwarzenberger, Flow cytometry, Figure 1. Copyright (2012).*

In this study, to determine the transfection efficiency, flow cytometry was used as a complement to IF to provide a more quantitative measure of transfection efficiency.

Procedure

Cells were transfected as described in subchapter 2.2.2. Media from wells was aspirated 48 hours post-transfection, and plates were washed twice with PBS before cells were trypsinised and resuspended in L15 media. Cell suspension was transferred to 1.5 mL eppendorf tubes, centrifuged at 400 x g for 5 minutes, and cell pellets resuspended in 100 µL PBS. Primary antibody, 3H6F8 (mouse IgG1, anti-ISAV HE) was diluted (1:50 in PBS with 3 % BSA) and added to tubes (100 µL/tube) followed by 60 minutes incubation in the dark. Cells were washed three times with PBS and centrifigation at 500 x g for 5 minutes at 10 °C. Cell pellets were resuspended in 100 µL PBS. Secondary antibody, goat anti-mouse IgG Alexa 488-conjugated (Life Technologies, Waltham, MA, USA) was diluted (1:200 in PBS with 3 % BSA) and added to tubes (100 µL/tube) followed by 45 minutes incubation in the dark. One negative control (non-transfected cells) was stained, whereas the other was kept unstained. Cells were washed three times with PBS and analysed on an ACEA Novocyte® flow cytometer (Acea Biosciences Inc, San Diego, CA, USA) in experiment 1, and on a BD Accuri™ C6 flow cytometer (BD Biosciences, Franklin Lake, NJ, USA) in experiment 2.

2.4 Enzyme-linked immunosorbent assay

Enzyme-linked immunosorbent assay (ELISA) is a method to detect and quantify proteins with the use of antibodies that are coupled to an enzyme, such as horseradish peroxidase (HRP) or alkaline phosphatase (AP) [70-72]. If the target protein is present, the antibody:enzyme-complex will recognise and bind it and not be removed by washing. When a chromogenic substrate is applied, the enzyme will catalyse the reaction with the substrate to yield a coloured product, and the absorbance can be measured. There are different variations of ELISA, including the ones shown in Figures 14-17. The direct ELISA has antigen immobilised to the bottom of wells of the plate. The antigen is detected by an antibody, which is directly coupled to an enzyme (Figure 14).

Figure 14. Illustration of direct ELISA. Immobilised antigen at the bottom of the wells is detected by an antibody coupled directly to an enzyme [72].

The indirect ELISA also have immobilised antigen in the wells of the ELISA plate, but instead of using an enzyme-linked antibody to detect the antigen, the indirect ELISA utilises two antibodies, called primary and secondary antibodies. The primary antibody is unlabelled and recognises the immobilised antigen. The secondary antibody is enzyme-linked and recognises and detects the primary antibody (Figure 15).

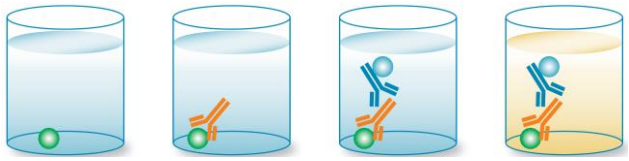

Figure 15. Illustration of indirect ELISA. Immobilised antigen at the bottom of the wells is recognised by an unlabelled primary antibody, which is in turn detected by a secondary enzyme-linked antibody [72].

In the sandwich-ELISA, a capture antibody, which is an antibody recognising a specific antigen, is first adsorbed to the wells on an ELISA plate. The samples are applied to the wells, and if the samples contain antigen, it will bind to the capture antibody. A second, different enzyme-linked antibody will detect the antigen [70, 71] (Figure 16).

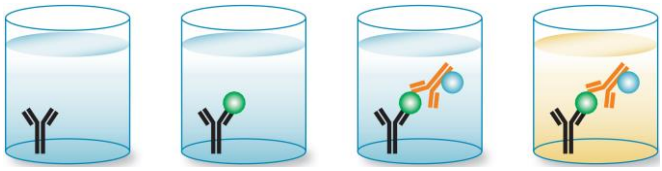

Figure 16. Illustration of sandwich-ELISA. The capture antibody is coated to the bottom of the wells. The samples are applied, and antigen in the samples (if present) binds to the capture antibody. A secondary, enzyme-linked antibody will detect the antigen [72].

2.4.1 Cellular ELISA (cELISA)

cELISA is a technique used for the semi-quantification of cell surface antigen expression [73]. This technique is executed directly on cell culture plates, and was established on the basis of enzyme immunohistochemistry (EIH), a method to identify and localise antigens in histological preparations, and ELISA. cELISA have two variations: direct- and indirect cELISA, which can be applied to both adherent and non adherent cells. In this study, indirect cELISA was used to detect and measure the HE protein expressed on the surface of transfected CHSE cells, as shown in Figure 17.

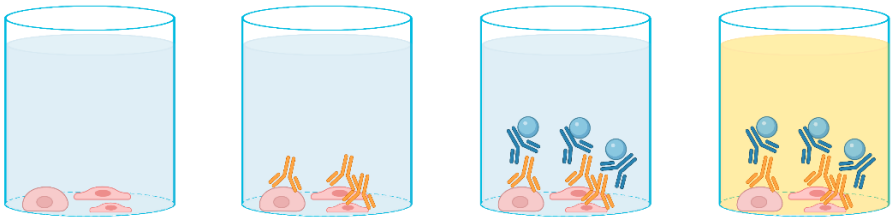

Figure 17. Illustration of indirect cELISA on transfected CHSE cells expressing ISAV HE protein on the cell surface. Cells with HE protein on the surface is coated to the bottom of the wells. HE protein is recognised by an unlabelled primary antibody, which in turn is recognised by a secondary enzyme-linked antibody. *Created with BioRender.com.*

Procedure

Cells were transfected as described in subchapter 2.2.2. After 24 hours incubation time, one of the strips with CHSE/HE cells were fixed with acetone 80 % (w/v) and frozen at -80 °C. CHSE/HE cells in wells on the second strip were fixed after 48 hours and cELISA was performed on both strips at the same time. Cells were washed once with 250 µL PBS per well. Primary antibody, mouse IgG_1, anti-ISAV HE (3H6F8) [74] was diluted with clear milk block (Thermo Scientific, Waltham, MA, USA) solution (1:10 in PBS) to a 1:100 concentration (CMB) and added to wells (50 µL/well) followed by 60 minutes incubation at 37 °C. The plate was washed three times with PBST, and the plate tapped dry on paper. Secondary antibody, goat anti-mouse HRP-conjugated (Invitrogen, Waltham, MA, USA) was diluted in CMB to a concentration of 1:5000 and 100 µL was added per well. Incubation time was 45 minutes at 37 °C. The plate was washed five times with PBST (250 µL/well). TMB-substrate (Thermo Scientific) was added (100 µL/well) and incubated 2 minutes in the dark. The enzyme reaction was stopped by adding

H_2SO_4 (0.18 M), and the optical density was read at 450 nm on a Tecan Sunrise plate reader (Tecan, Männedorf, Switzerland). The experiments were repeated five times, and results from one representative experiment is presented in Figure 24.

2.5 Functional assays for the expressed HE protein

2.5.1 Haemadsorption assay

The haemadsorption assay was used to test if the expressed HE proteins in the transfected cells had functional RBDs, and to compare the receptor binding activity of the virulent and non-virulent HE constructs. Salmon RBCs present 4-*O*-acetylated sialic acid receptors on their surface that can be targeted by the RBD of the HE glycoprotein [75-77]. The principle behind the assay is to incubate RBCs from salmon with transfected cells, and after several washing steps, check visually under the microcope for RBC binding and release. The cells are subsequently lysed with dH_2O, and tetramethylbenzidine (TMB), which is a chromogenic substrate for RBC endogenous pseudoperoxidase, is added. To stop the TMB-peroxidase reaction, sulfuric acid is added, and the amount of RBCs can be measured as optical density at 450 nm on a plate reader.

Procedure

A 1 % RBC solution was prepared from density-purified RBCs from Atlantic salmon. HE-transfected CHSE cells were used 48 hours post transfection (transfection described in subchapter 2.2.2). Monolayers were washed once with PBS, and 100 µL RBC solution was added to each well. Incubation time was 15 minutes on shaker at 15 °C. Each well was washed three times with PBS and observed microscopically. A standard calibration curve was made on a separate plate by adding 50 µL PBS to each well except the first well in a row. A volume of 100 µL RBC solution was added to the first well, and diluted in a twofold series. The standard calibration curve was transferred to a row on the plate with HE-transfected CHSE cells. PBS was aspirated from wells with CHSE/HE cells, and 150 µL dH_2O was added to lyse the cells. 100 µL dH_2O was added to each well in the standard curve. After 20 minutes incubation time, 50 µL lysate from each well was transferred to new rows on the same plate, and 100 µL TMB (Thermo Scientific, Waltham, MA, USA) was added, followed by 2 minutes incubation time at room temperature in the dark. To stop the enzyme reaction, H_2SO_4 (0.18 M) was added and the optical density was read at 450 nm on a Tecan Sunrise plate reader (Tecan, Männedorf, Switzerland). The number of adherent RBCs was calculated from the standard curve. The experiments were repeated five times, and standard curve from one representative experiment is presented in Figure 26. The haemadsorption data was used in combination with cELISA and esterase activity data to compare HPR0

and HPR-del. The haemadsorption assay was also used on co-transfected cells for the lipid mixing assay.

2.5.2 Esterase activity assay

To evaluate if the expressed HE proteins in the transfected cells had functional RDE domains, i.e. esterase cleavage of the sialic acid receptors, the haemadsorption assay can also be used. Different incubation times can be tested to see if the expressed HE proteins elute RBCs by visual check under the microscope and quantitatively measured as described above [1].

An esterase activity assay can also be used to evaluate if the expressed HE proteins have functional RDE domains. An ester substrate, *p*-nitrophenyl acetate is added (*p*-NPA), and the chromogenic product, *p*-nitrophenol (p-NP) can be measured spectrophotometrically as the increase of absorbance at 405 nm [78, 79]. An illustration of the *p*-NPA reaction is shown in Figure 18.

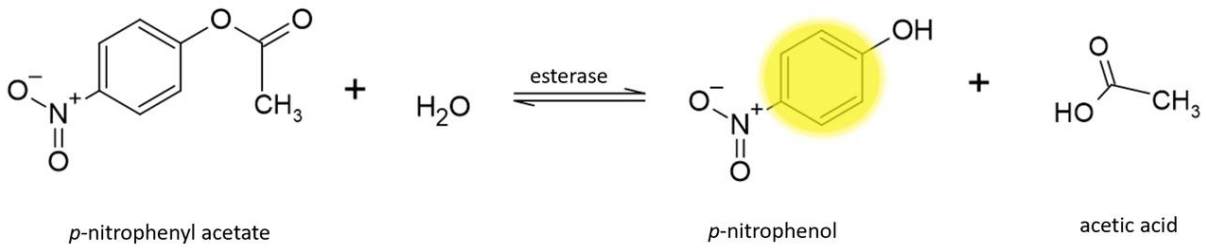

Figure 18. Hydrolysis reaction of *p*-NPA to *p*-NP. The chromogenic aromat (in yellow) can be measured spectrophotometrically.

Procedure

Cells were transfected as described in subchapter 2.2.2. The plate was washed once with PBS (100 µL/well) and 100 µL substrate solution, *p*-NPA (1 mM) (Sigma-Aldrich, St.Louis, MO, USA) was added. The level of autohydrolysis of *p*-NPA substrate in PBS was quantified and subtracted from sample values. These blanks were made by adding substrate-solution to wells with only PBS. Non-transfected CHSE-cells served as negative controls. The esterase activity was measured at 405 nm every 5 minutes over one hour on a SpectraMax® i3x Multi-mode microplate reader (Molecular Devices, San Jose, CA, USA). The experiment was repeated five times, and the esterase activity data was used in combination with the haemadsorption data to measure differences between HPR0 and HPR-del.

2.5.3 Haemagglutination assay

Another method to test binding and elution from HE-transfected CHSE cells antigen is to perform a haemagglutination assay. Membrane fractions of HE-transfected CHSE cells are diluted in a twofold series in a microtiter-plate. RBC suspension (1 %) is added to the wells, and the haemagglution titer is read after one hour. The agglutinated RBCs will form a diffuse lattice, whilst the unbound RBCs will fall to the bottom of the well and appear as a little sharp button that runs downwards when the plate is tilted [66, 71], as shown in Figure 19. The haemagglutination titer is the highest dilution of membrane fractions that slows down the running of the RBC button, and defined to contain one haemagglutinating unit (HAU). From this, the haemagglutination titer of the membrane preparation can be calculated. After a certain time, receptor-destroying enzyme activity will release the haemagglutination and cause elution, which is seen as reappearance of a RBC button.

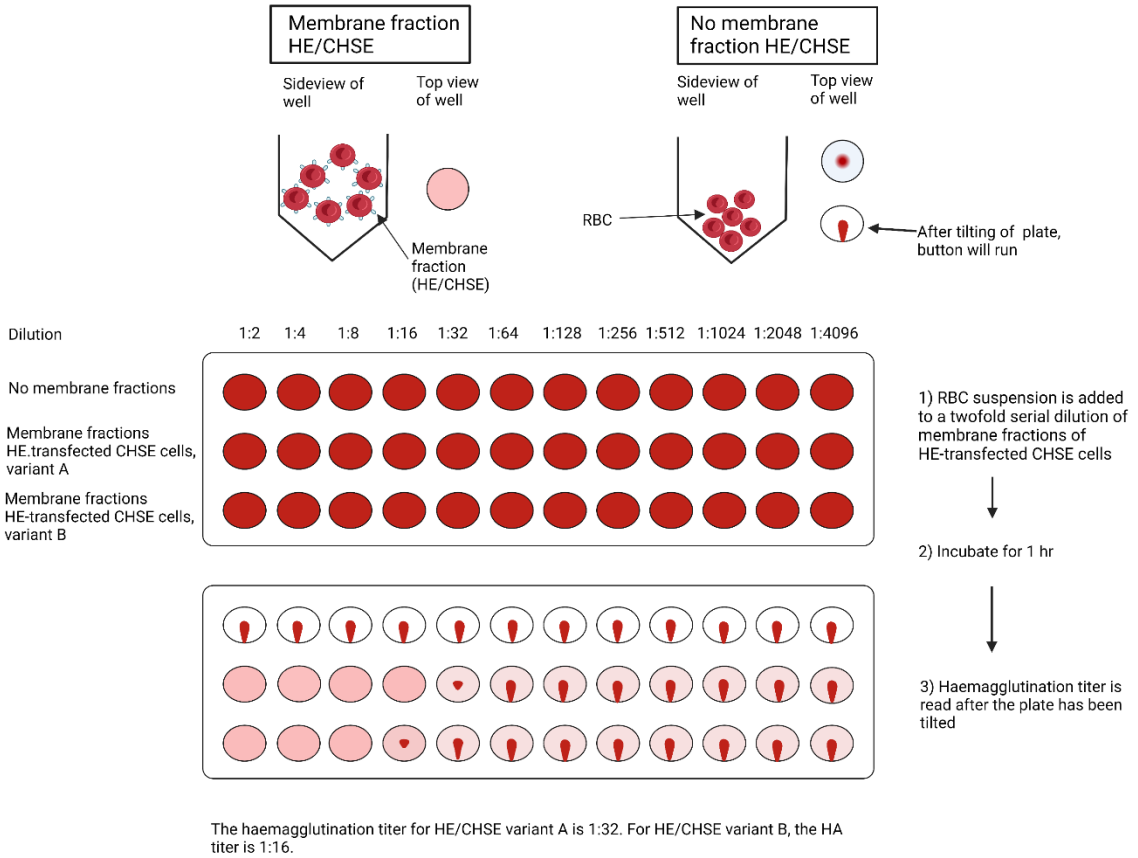

Figure 19. Example of the haemagglutination test used in this study. See details in text/figure. *Created with BioRender.com.*

Procedure

Cells were transfected as described in subchapter 2.2.2 and used 48 hours post-transfection. Antigen (membrane fractions) from transfected cells were prepared by rinsing three times with cold PBS before detaching the cell monolayers with a cell scraper. Cells were transferred to eppendorf tubes, centrifuged at 500 x g for 5 minutes and cell pellets washed three times with PBS. Cell pellets were resuspended in 50 µL PBS, and cells were lysed by freezing at -80 °C and thawed three times. The supernatant was cleared by centrifuging at 10 000 rpm for 10 minutes.

Haemagglutination titrations were performed in a 96-well plate by mixing 50 µL of antigen suspension diluted in a twofold series in PBS with 50 µL of 1 % salmon RBC suspension. The haemagglution titer is read after one hour incubation at room temperature. Receptor-destroying enzyme activity (elution) was assessed after 20- 21 hours. The experiments were repeated four times, and data is presented in Table 13, Appendix 1. Images from one haemagglutination assay are presented in Figures 29-30, and the images from the remaining assays are presented in Figures 41-46, Appendix 1.

2.6 Fusion assay

2.6.1 Lipid mixing assay

Lipid mixing assay is a technique used to study hemifusion. It is a fluorometric assay based on labelling erythrocytes with octadecyl rhodamine B chloride (R18) [80-82]. R18 is a self-quenching lipid dimer probe, and when fusion occurs, the probe is redistributed in the fused membranes. The redistribution leads to de-quenching of the probe and an increase in fluorescence, which can be measured (excitation/emission maxima 560/590 nm). Figure 20 shows a schematic overview of a lipid mixing assay.

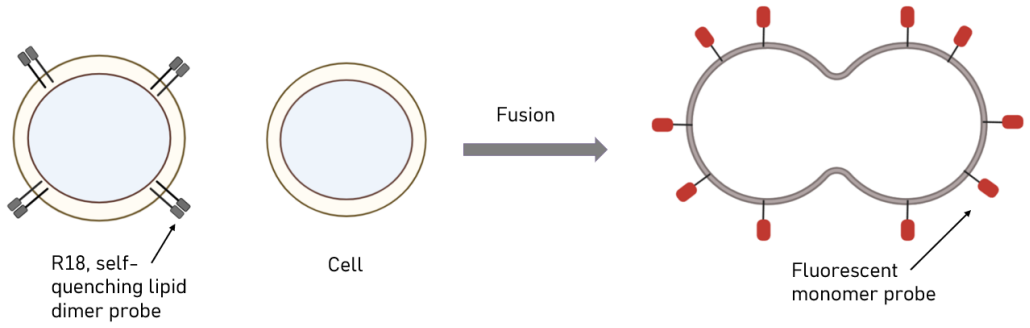

Figure 20. Schematic overview of a lipid-mixing assay based on R18 fluorescence self-quenching. R18 is a self-quenching lipid dimer probe, and when fusion with unlabelled membrane occurs, the probe is redistributed in the fused membranes. The redistribution results in de-quenching of the probe and an increase in fluorescence, which can be measured (excitation/emission maxima 560/590 nm) [82]. The fluorescence increase is represented by the colour change from black to red. *Created with BioRender.com.*

Alternatively, if the concentration of R18 of the erythrocyte-membrane after R18-labelling is low, the lipid probes may not be properly quenched and will only show some fluorescence. When fusion occurs with the unlabelled cell membranes, the fluorescence is nonetheless transferred to the cell membranes, as shown in Figure 21, and fusion can be assessed.

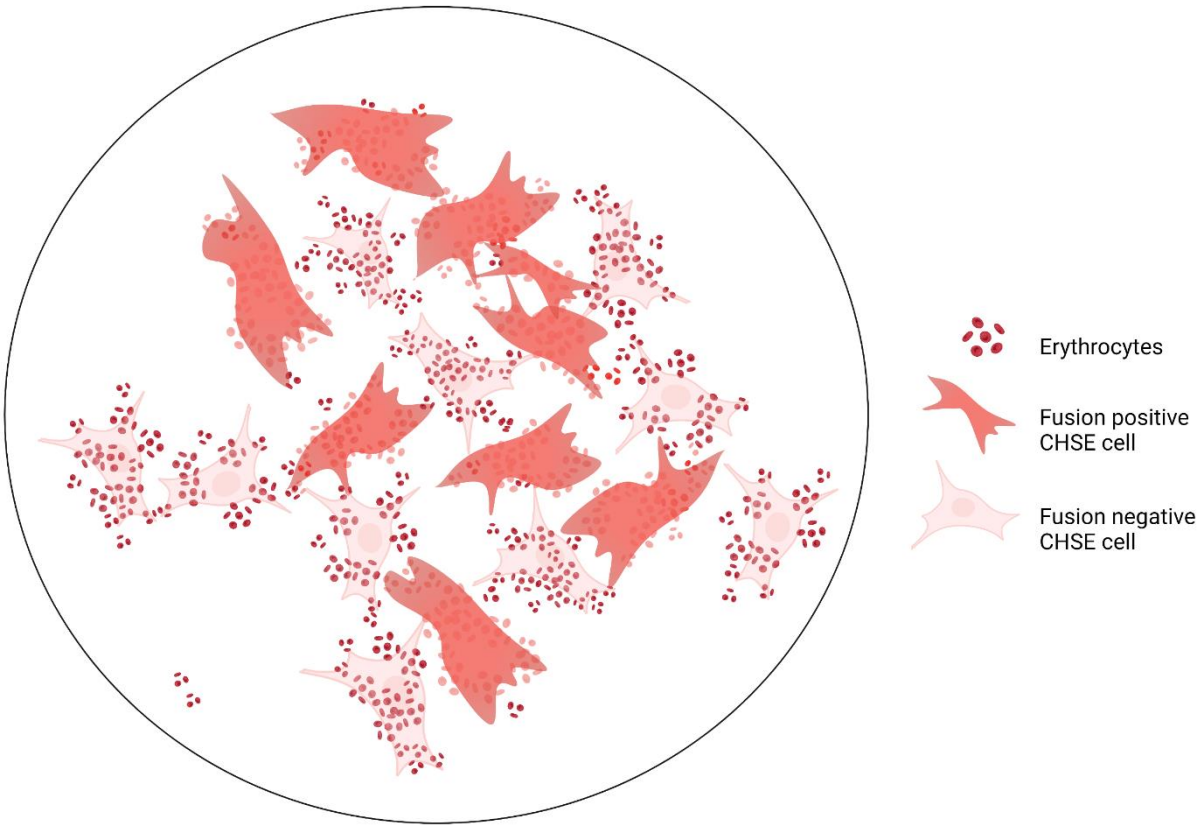

Figure 21. Illustration of how a well looked in the microscope in the fusion assay. Clusters of small red dots represent R18/RBCs. The light pink coloured cells represent fusion negative CHSE cells. The darker coloured cells represent fusion positive CHSE cells where fluorescence has been transferred from the R18-labelled RBCs to the CHSE cell membrane. *Created with BioRender.com.*

Protocol

R18-labelling of RBC membranes

48 hours post-transfection (tranfection described in subchapter 2.2.2), salmon RBCs were fluorescently labelled with R18 (Invitrogen, Waltham, MA, USA): 15 µL of a 1 mg/mL R18 solution (in EtOH) was added to 10 mL of a 1 % RBC suspension (in PBS) and incubated for 15 minutes at room temperature. To absorb the unbound R18 lipid probe, 30 mL of L15-media supplemented with 5 % FBS and l-glutamine (Lonza, Basel, Switzerland) was added and incubated further for 20 minutes at room temperature. The R18/RBC suspension was sedimented and washed 6 times by centrifugation at

500 x g for 5 minutes with 50 mL PBS. After each resuspension, the R18/RBC suspension was transferred to a new Falcon tube. R18/RBCs were resuspended in 10 mL PBS.

Haemadsorption

Cell monolayers were incubated with 0.1 % R18/RBC suspension for 15 minutes at room temperature in the dark (100 µL/well) and washed twice with L15-media without supplements (Lonza) to remove unbound RBCs.

Cleavage and activation of F protein

50 µL of a 2.5 mg/mL trypsin solution (Sigma-Aldrich, St.Louis, MO, USA) (in L15-media without supplements) was added per well and incubated for 15 minutes at room temperature. To stop trypsination and trigger fusion, L15-media with 5 % FBS at pH 4.5 was added and incubated for 30 minutes. Cells were fixed with 4 % PFA (100 µL/well) after a wash with L15-media without supplements at neutral pH.

Cells were photographed with an Zeiss Axiocam 503 mono camera at 20X magnification under red fluorescence channel (555 nm) on a Zeiss Axio Observer A1 inverted microscope (Carl Zeiss MicroImaging GmbH, Göttingen, Germany), and 10 fields of view were photographed in preset areas that did not overlap. Cells were analysed on ImageJ, and fusion activity was measured as the ratio of fusion-positive cells (where fluorescence was transferred from bound R18/RBCs to co-transfected CHSE cells) to the total number of co-transfected CHSE cells bound to RBCs. Additionally, fusion activity was measured as the ratio of fusion-positive cells to the OD values from the haemadsorption assay performed from the same transfection.

2.7 Data analysis

Normalisation of functional biological data is a way to make certain that the interpretation of results are accurate and consistent, and to make it easier to statistically compare samples, for example between experiments [83]. By normalising data, the differences between the samples are more likely to be due to biological differences, rather than unintended variation between experiments. The data must be normalised to a shared parameter for a correct comparison. To remove variations between experiments, data from the functional assays for the expressed HE protein, i.e. haemadsorption, esterase activity, and cELISA were normalised to the mean value of HPR0 in the same experiment. In the fusion assay, data was normalised to the haemadsorption data, and the counted number of RBC-bound CHSE cells. D'Agostino and Pearson normality test was performed on to assess if the data were

normally distributed. Because not all were normally distributed, statistical significance was determined with the non-parametric two-tailed Mann Whitney U-test. Data was analysed in GraphPad Prism, version 9.3.0 (463).

3 Results

3.1 HE is expressed and transported to the cell surface

IF staining was performed 48 hours post-transfection to see if the transfected cells expressed HE proteins, and if these were located on the cell surface. IF provided a qualitative estimate of the transfection efficiency. The transfected CHSE cells expressed HE, and at least a proportion of the HE was located on the cell surface (Figure 22).

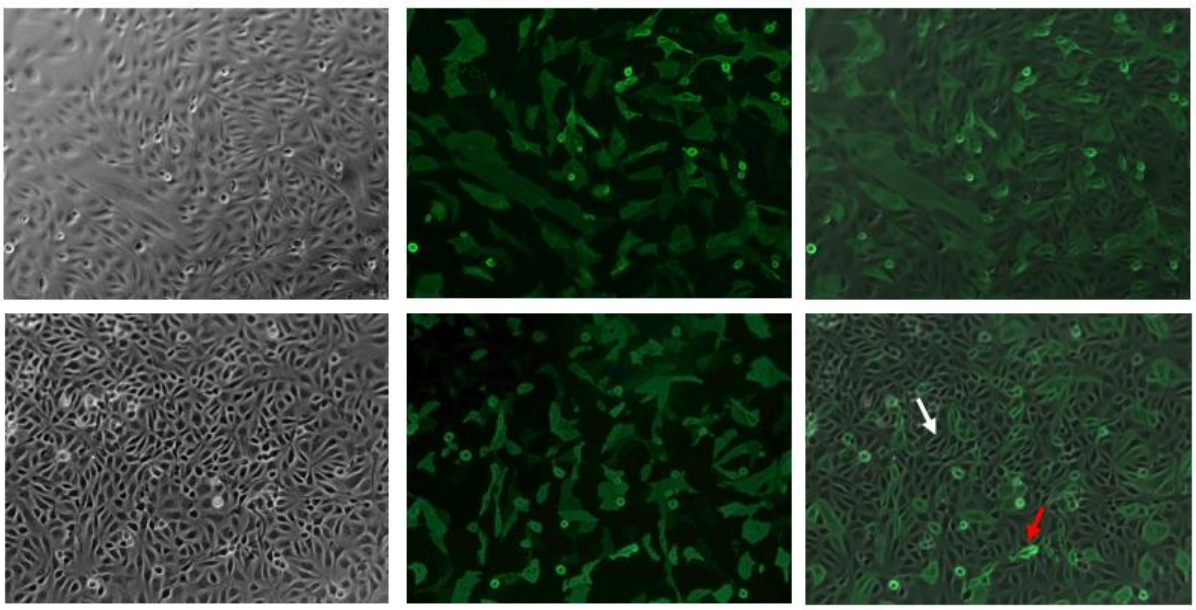

Figure 22. Microscope images of transfected CHSE cells. Each row represents the same captured image, taken with different channels: Brightfield channel to the left, fluorescence in the middle, and a merged photo to the right. The white arrow points to a negative CHSE cell, and the red arrow points to a positive CHSE cell. The top row panel shows cells treated with saponin to allow detection of intracellular HE, as well as HE on the cell surface. Bottom row panel shows IF stained cells without saponin treatment detecting HE on the cell surface only. Cells were photographed with a Zeiss Axiocam 503 mono digital camera at 20X magnification on an Axio Observer A1 inverted microscope.

Non-transfected CHSE cells were plated as negative controls and showed no fluorescence (not shown). Fluorescence was observed both intracellularly and on the cell surface. Permeabilisation by saponin did not cause a visible change in fluorescence signal between the permeabilised and non-permeabilised cells. This shows that recombinant HE can be detected by the antibody, and that detection was not dependent on permeabilisation, suggesting that most of the HE proteins were folded correctly and transported to the cell surface.

IF staining was also done on CHSE cells transfected with plasmids encoding F by others (lab engineer, Subash Sapkota, and my supervisor, Dr. Hol Fosse). Results showed that the cells expressed F proteins and that these were transported to the cell surface (not shown in this thesis).

Flow cytometry was performed to determine the transfection efficiency. The results show a transfection efficiency of approximately 30 %. Results from one experiment (using the ACEA Novocyte® flow cytometer) is presented in Figures 36-38, Appendix 1.

3.2 The levels of HE increase from 24 hours to 48 hours after transfection

cELISA was performed on cell monolayers that expressed HE protein (transfection, see subchapter 2.2.2) at two different time points to compare the expression of HE protein at 24 hours and 48 hours after transfection. One experiment is presented in Figure 23. Graphs from three other experiments are presented in Figure 39, Appendix 1.

Figure 23. The graph represents the HE expression measured from the same transfection (seeded into two wells) at 24 hours and 48 hours post transfection. Indirect cELISA method was used. HE expression is higher 48 hours post transfection. Triplicate reactions were performed in this experiment.

The HE expression was higher 48 hours post-transfection, thus this time point was chosen to perform the other assays. Because it was difficult to generate a standard curve for HE, for this assay, it was not possible to determine the linear range.

3.3 Recombinantly expressed HE proteins show receptor binding and destroying activities

To compare receptor binding and destroying activities, functional assays were performed on cells from twelve individual transfections, as illustrated in Figure 24.

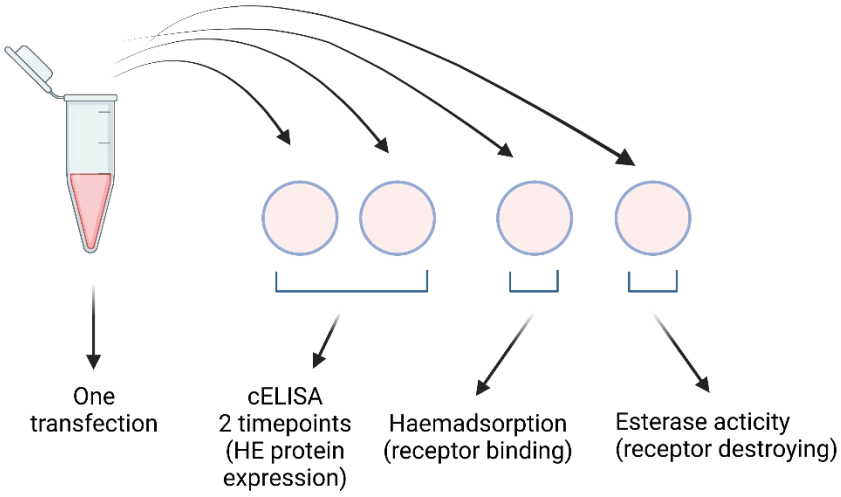

Figure 24. Experimental design to determine receptor binding and destroying activities for the recombinantly expressed HE protein. Cells from each transfection were plated in four wells and used in three different assays: cELISA, haemadsorption, and esterase activity, to allow comparisons within transfections. Two wells were used for the cELISA (for comparison of HE expression at two different timeponts). A total of 12 transfections were performed in four independent experiments. *Created with BioRender.*

3.3.1 Bound RBCs can be quantified by measuring pseudoperoxidase activity by TMB

The haemadsorption assay was used to evaluate if the recombinantly expressed HE proteins had functional RBDs, and to assess if there is a significant difference between the HE constructs. First, different methods to quantify the number of bound RBCs were evaluated. A common method to measure RBC levels is to perform a haemoglobin assay where the haemoglobin levels are measured spectrophotometrically after the cells have been lysed. This was tested, but was not very sensitive (Figure 40, Appendix 1). It was therefore tested if the amount of bound RBCs could be evaluated by measuring endogenous pseudoperoxidase activity by TMB [84]. The pseudoperoxidase quantification was found to be more sensitive than direct spectrophotometric measurement of haemoglobin, providing a linear measure of RBCs in the range needed for the haemadsorption assay. The standard curve of one representative experiment is presented in Figure 25.

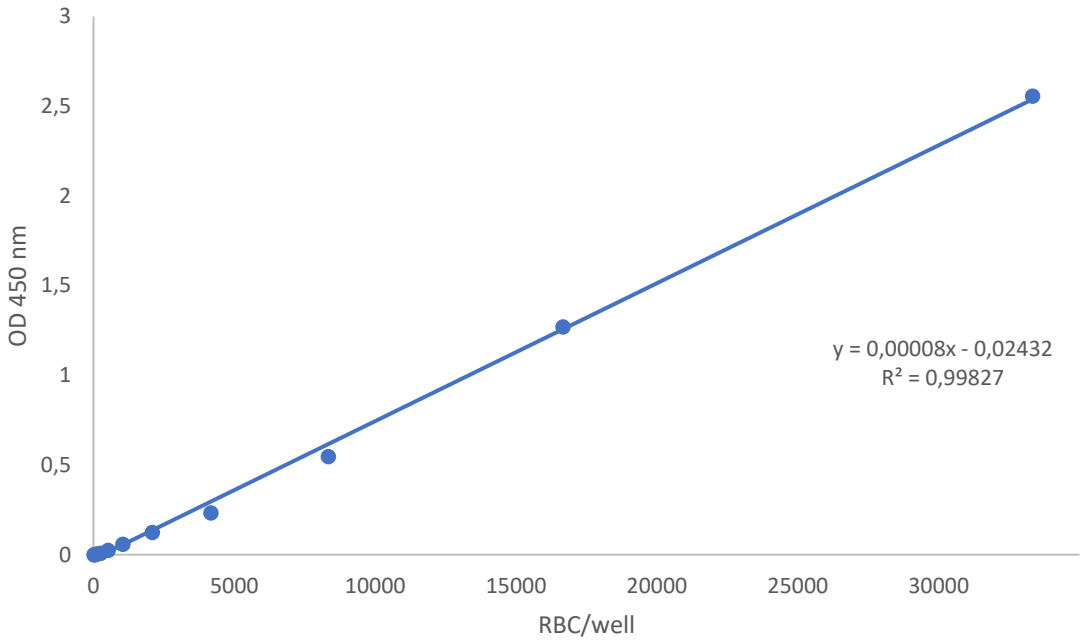

Figure 25. Standard curve from one representative experiment. The OD value at 450 nm is plotted as a function of the amount of RBCs per well.

The linear equation in the presented standard curve is y = 0.00008x – 0.02432, where y is the measured OD value, and x is the amount of RBCs per well. The amount of RBCs per well was determined from the standard curve equation.

3.3.2 HPR0 and HPR-del show similar receptor binding activities

The raw data from the haemadsorption assay and from the cELISA, and receptor binding results related to HE expression are shown in Figure 26.

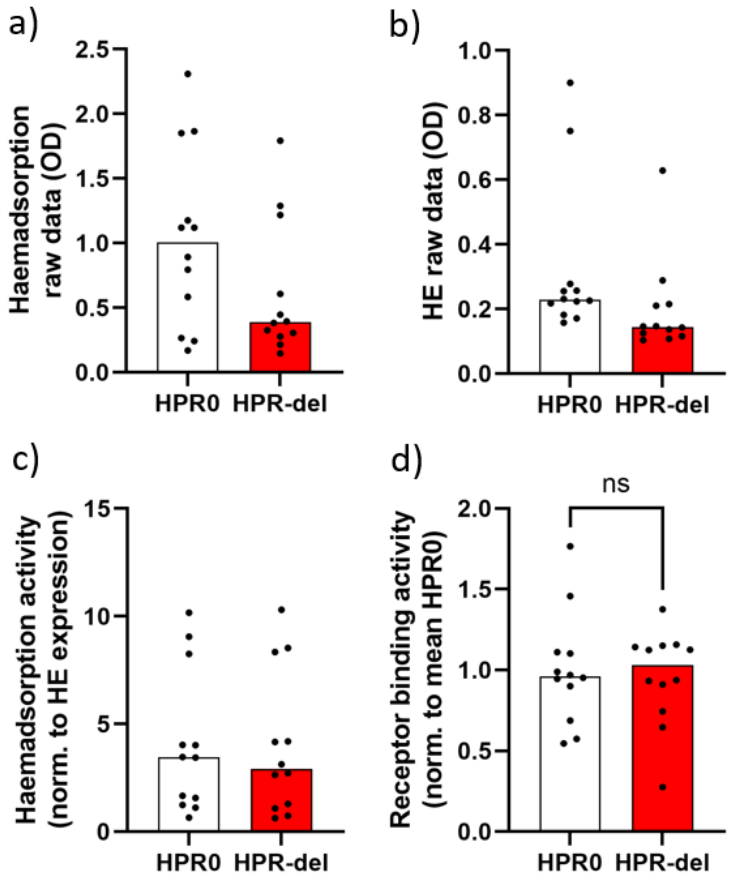

Figure 26. Results from the haemadsorption assay (and cELISA). Each dot in the graphs represents a single transfection. The horisontal line represents the median of each group. Three individual transfections were performed in each experiment, and data from four independent experiments are plotted. a) Raw data of endogenous pseudoperoxidase activity measured by TMB. Data plotted is listed in Table 5, Appendix 1. b) Raw data of HE levels measured by cELISA. Data plotted is listed in Table 6, Appendix 1. a,b) Cells transfected with HPR0 had higher haemadsorption and expressed higher levels of HE than cells transfected with HPR-del. c) Normalised receptor binding activity (haemadsorption data was normalised to the HE expression). Data plotted is listed in Table 7, Appendix 1. d) Normalised receptor binding activity (HA:HE ratio shown in c) expressed as the fraction of the mean value for HPR0 in that experiment. There was no significant difference in receptor binding between HPR0 and HPR-del. Data plotted is listed in Table 8, Appendix 1, n=12. Statistical significance was determined by Mann Whitney U-test.

The recombinantly expressed HE proteins bound RBCs demonstrating that the RBDs of the expressed HE proteins were functional (Figur 26a). Cells transfected with HPR0 showed higher haemadsorption, that could be explained by a higher HE expression in these experiments (Figure 26a,b). To allow comparison between HPR0 and HPR-del, the haemadsorption data was normalised to the HE-expression (Figure 26c). To reduce the variation between experiments, the normalised receptor binding activity (haemadsorption/HE-expression ratio) was expressed as the fraction of the mean HPR0-value in that experiment (Figure 26d). The results show that there was no significant difference

in receptor binding activity between HPR0 and HPR-del. Statistical significance was determined by the non-parametric Mann Whitney U-test. A limitation to this is that it is possible that the HE expression data is not in a linear range, due to the lack of a standard curve for HE in the cELISA assay.

3.3.3 Non-transfected CHSE cells have endogeneous esterase activity

Esterase activity assay was performed to evaluate if the expressed HE proteins had functional RDE domains. A substrate, *p*-NPA was added and the esterase activity was measured as the yield of the chromogenic product, *p*-NP. The results showed esterase activity of the expressed HE proteins, but also showed that the non-transfected CHSE cells had marked background esterase activity (Figure 27).

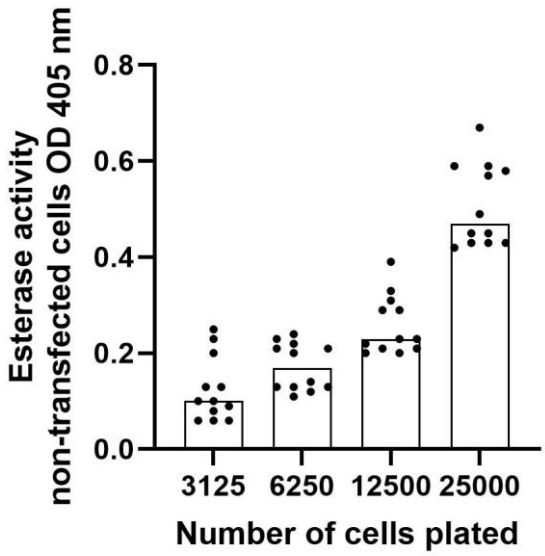

Figure 27. The esterase activity (measured as the yield of chromogenic *p*-NP) in the negative controls (non-transfected cells) increased with cell density. Each dot represents one replicate. The horisontal line represents median of each group. Triplicate transfections were performed in each experiment, and data from four independent experiments are plotted (Table 9, Appendix 1).

The results showed that the esterase activity in the negative controls increased with the cell density. It was challenging to correct for this background, because the cell density of the transfected cells varied widely, as a result of differences in the cell response to electroporation.

3.3.4 HPR0 and HPR-del HE show similar receptor binding and receptor destroying activities

The raw data from the esterase acivity assays, and the results related to haemadsorption are shown in Figure 28a-c).

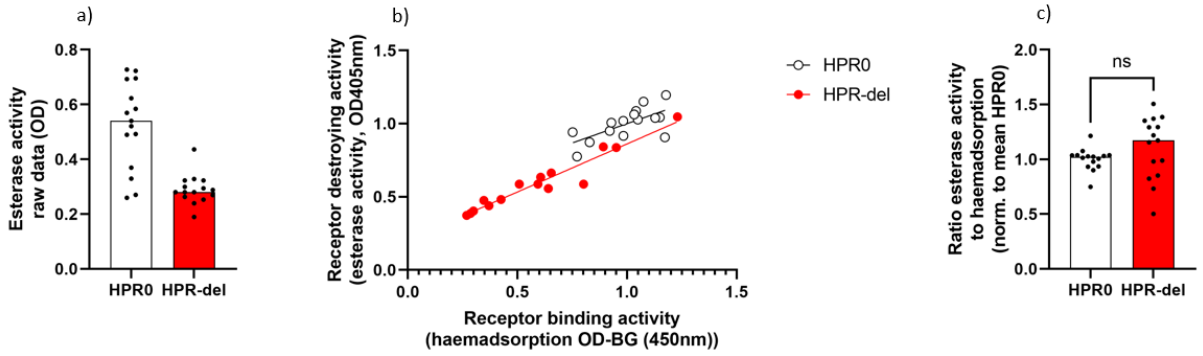

Figure 28. Results from the esterase activity assays. The substrate p-NPA was added, and the esterase activity was measured as the yield of *p*-NP. a) Raw data of esterase activity. Data plotted is listed in Table 10, Appendix 1. b) Correlation between receptor binding and receptor destroying activities. Data plotted is listed in Table 11, Appendix 1. c) Normalised receptor destroying activity (esterase activity:haemadsorption activity ratio) expressed as the fraction of the mean value for HPR0 in that experiment. There was not a significant difference in receptor binding or -destroying activities of the expressed HE between HPR0 and HPR-del. Also, the relative receptor binding and destroying activity is similar for both groups, indicating functional balance. Data plotted is listed in Table 12, Appendix 1. Mann Whitney U-test was performed to determine statistical significance. For all graphs: Each dot represents one transfection. Triplicate transfections per experiment was performed. Data from five experiments are plotted. The horisontal line represents median of each group.

The recombinantly expressed HE proteins have esterase activity, and the RDE domains of the expressed HE proteins were functional (Figure 28a). The esterase activity data was also plotted as a function of the haemadsorption data (Figure 28b). There is a correlation between receptor binding and receptor destroying activities for the HE variants. The graph shows that they increase in parallell. This implies that they depend on the expression of HE protein, despite the background activity in non-transfected cells. Visual inspections of the graphs in Figure 28 a,b) gave the impression of a higher esterase activity in the HPR0 transfected cells. To investigate this further, and to assess the functional balance between these activities, the esterase activity was normalised to the haemadsorption data, and expressed as the fraction of the mean value for HPR0 in that experiment, to correct for variation between experiments (Figure 28c).

There was not a significant difference in esterase activity normalised to haemadsorption activity between HPR0 and HPR-del. The results support our hypothesis that HPR0 and HPR-del HE variants have similar receptor-binding and receptor-destroying activities. The relative receptor binding and destroying activity is similar for both groups, indicating functional balance. Mann Whitney U-test was

performed to determine the statistical significance. A limitation to this is that the high background esterase activity from the negative controls.

3.3.5 HPR0 and HPR-del show similar elution from salmon RBCs.

To further evaluate the balance between receptor binding and -destroying activities, haemagglutination assays were performed to test elution of HE-transfected CHSE cells from salmon RBCs. RBC suspension was added to a twofold serial dilution of membrane fractions of HE-transfected CHSE cells. After one hour incubation time, the plate was tilted, and haemagglutination titer could be read. The plates were assessed for elution after a time period of 20-21 hours. The haemagglutination titer and -elution from one experiment are shown in Figures 29-30. Images from the other haemagglutination assays are presented in Figures 41-46, Appendix 1.

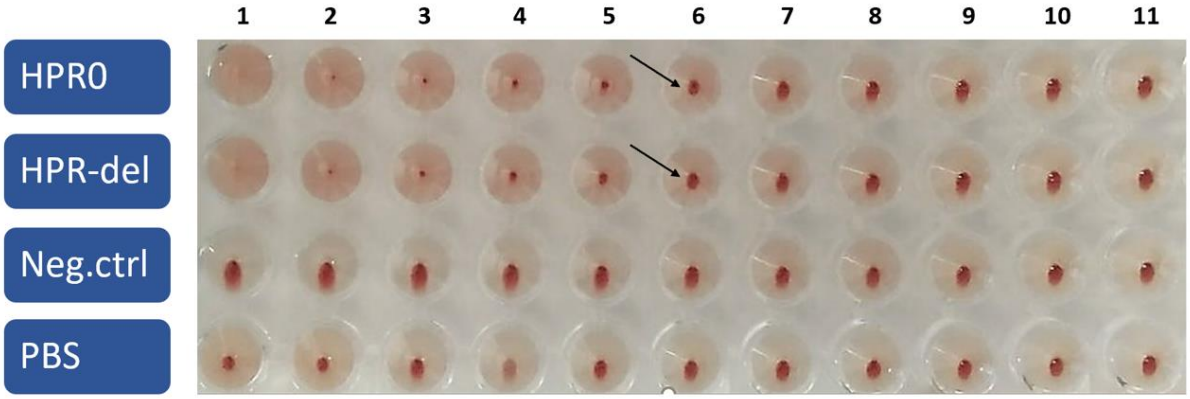

Figure 29. RBC suspension was added to a twofold serial dilution (1:2-1:4096) of membrane fractions of HE-transfected CHSE cells. After one hour incubation time, the plate was tilted. The top arrow indicates that for HPR0, well 6 slowed down the running of the RBC button and contains 1 HAU. Lower arrow shows that the haemagglutination titer was the same for HPR-del.

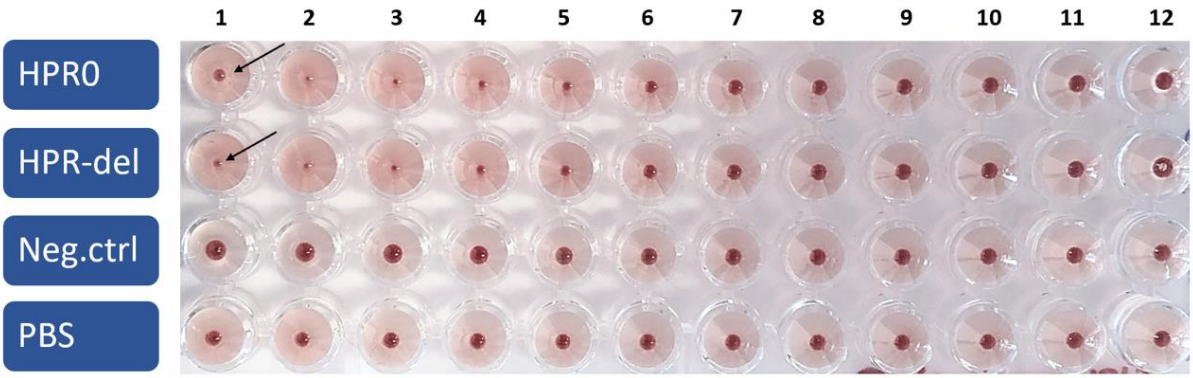

Figure 30. The plate was checked for elution after 20 hours. Arrows indicate that the reapperance of a RBC button in the first wells have occurred.

HAU required for elution was calculated from HAU per well. 32 HAU was required for elution for both HPR0 and HPR-del in the experiment above (Figure 30). Findings indicated no difference between HPR0

and HPR-del in two of the experiments. However, in two other experiments, slightly higher HAU was required for elution in HPR0. Data is listed in Table 13, Appendix 1. Statistical significance was determined by Mann Whitney U-test and showed no significant difference between HPR0 and HPR-del.

3.4 Fusion assays

3.4.1 The same CHSE cells express HE and F proteins, and the recombinantly expressed F proteins are functional

A pilot run of the lipid mixing assay was set up as a first approach to assess if the co-transfection protocol works, in regards to if the same cells express both HE and F, and if the expressed F proteins are functional. Co-transfected CHSE cells were incubated with R18-labelled RBCs, then treated with trypsin and low pH for priming and triggering of F. The plate was photographed and analysed in ImageJ. Figure 31 illustrates the experimental design of the pilot run.

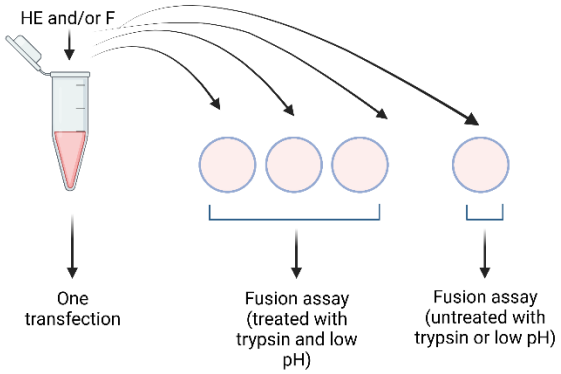

Figure 31. Experimental design to determine if the co-transfection protocol works and if the expressed F proteins are functional. Additionally, if the single HE or F transfected cells induce fusion alone, and if F single transfected cells alone bind RBCs. Cells from one transfection were plated into four wells, where one well was left untreated with trypsin and low pH to assess if there was fusion activity under unstimulated conditions. *Created with BioRender.*

The assay was performed on single- and co-transfected CHSE cells with plasmid pcDNA3.1+/HE and/or pcDNA3.1+/F (HPR0 and HPRdel variants). Only one replicate was performed. The single HE-transfected cells were performed as a negative control where only RBC-binding and no fusion was expected to be observed. The single F-transfected cells were performed to assess if F proteins bind RBCs, and if the F protein alone can induce fusion. Additionally, one well from each transfection was untreated with trypsin and low pH to assess if there was fusion activity under unstimulated conditions.

The plate was photographed (10 fields of view in set areas that did not overlap per well) and analysed on ImageJ. Results are shown in Figure 32 a-j).

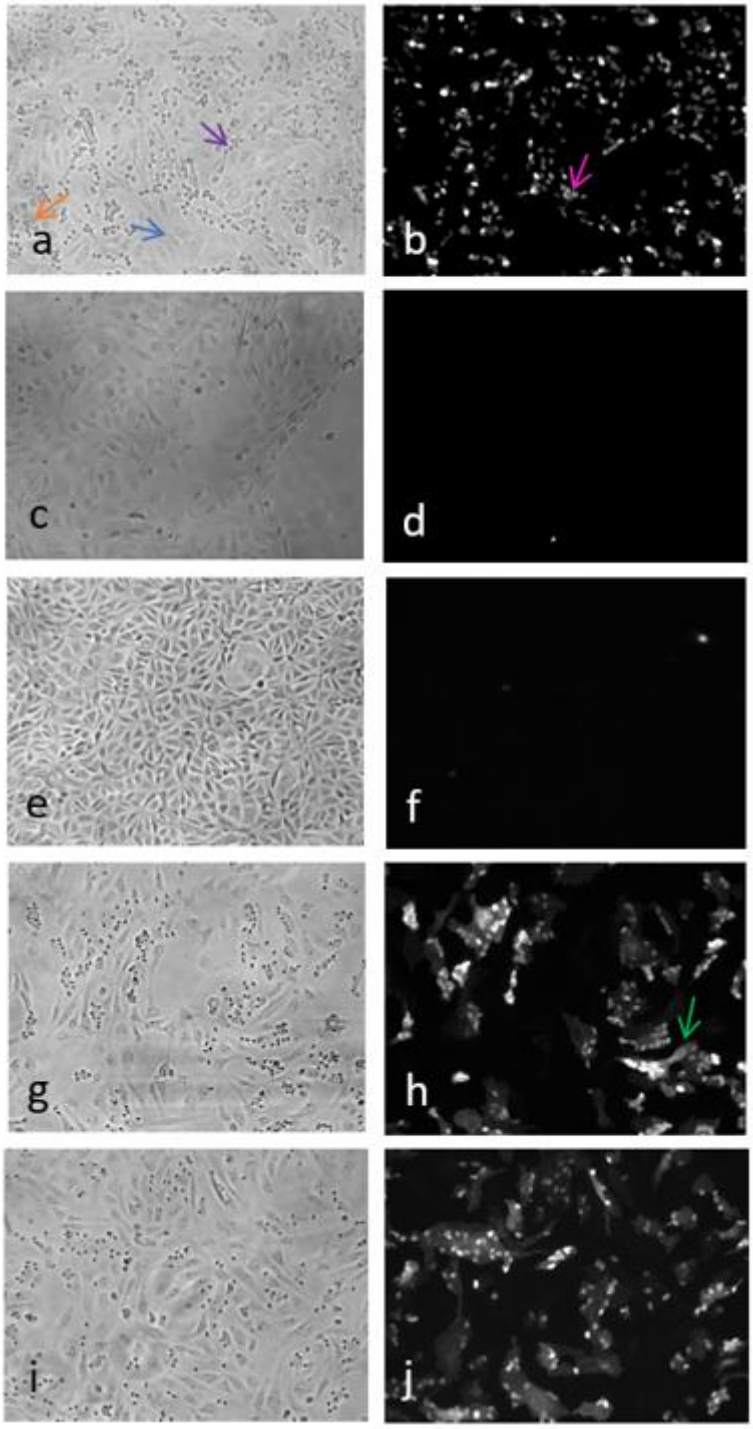

Figure 32. Microscope images of single-transfected cells/negative controls, and co-transfected cells. Each row represents the same captured image, taken in different channels: Brightfield channel to the left, and fluorescence channel to the right. The contrast is shown in black and white in the fluorescence photos, because contrast is easier to see in black and white, rather than in colour. The blue arrow is pointing to a CHSE cell. The orange arrow is pointing to a CHSE cell bound to RBCs. The purple and pink arrows are pointing to a cluster of R18/RBCs. The green arrow in h) points to a fusion positive CHSE cell. a,b) Single HE-transfected cells showed only RBC-binding, and no fusion. c,d) Single F-transfected cells showed no RBC-binding or fusion. e,f) Non-transfected cells/negative control showed no RBC binding or fusion. g,h) HPR0 HE/F-transfected cells showed fusion positive cells (where fluorescence is transferred from R18/RBCs to CHSE cells). i,j) HPR-del HE/F-transfected cells. Fusion positive cells were observed. Cells were photographed with a Zeiss Axiocam 503 mono digital camera at 20X magnification on an Axio Observer A1 inverted microscope, fluorescence channel 555 nm.

The results showed fusion in the co-transfected CHSE cells, which means that HE and F proteins were expressed in the same cells, and that the recombinantly expressed F proteins were functional (Figure 32 g-j). As expected, no fusion activation was seen in wells with single transfection of HE or F (Figure 32 a-d). No haemadsorption was observed in wells with single transfection of F (data not shown). Moreover, no fusion activation was observed in the absence of trypsin and low pH treatment (data not shown).

3.4.2 HPR-del HE/F has a higher fusion activity than HPR0 HE/F

The pilot showed that the lipid mixing assay worked, and the next step was to compare fusion activity between the HPR0 and HPR-del constructs, treated with trypsin and low pH, i.e. under stimulated conditions, as illustrated in Figure 33.

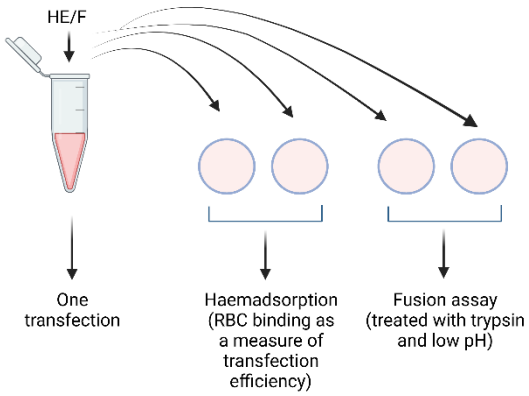

Figure 33. Experimental design to determine if there is a difference in fusion activation between HPR0 and HPR-del. Cells from one co-transfection were plated into four wells and used in two assays: fusion-, and haemadsorption (to adjust for transfection efficiency). *Created with BioRender.*

Triplicate transfections were performed of each HE/F construct, and data from the pilot was included as a single replicate. Results are shown in Figure 34 a-d).

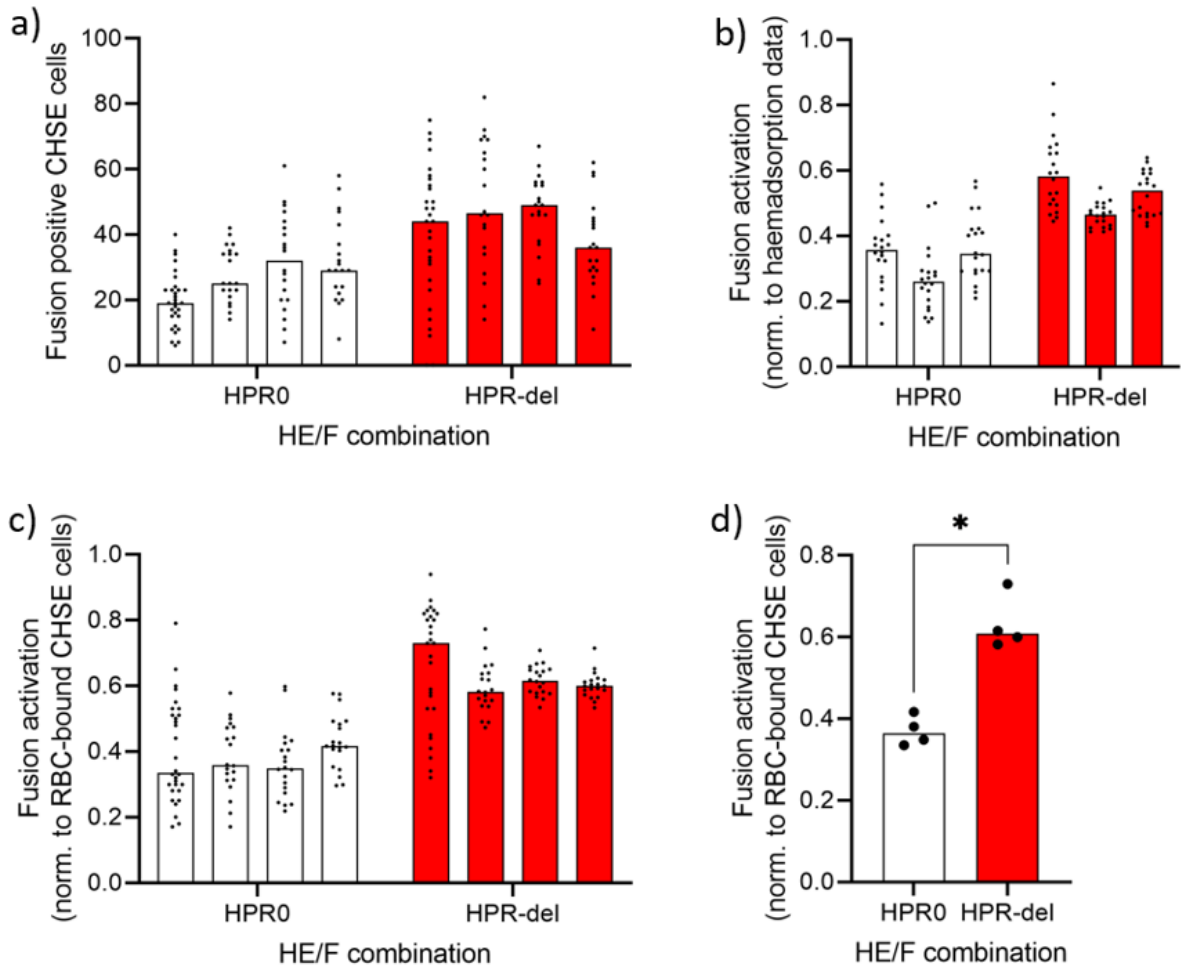

Figure 34. Results from the fusion assays. Co-transfected CHSE cells were incubated with R18-labelled RBCs, then treated with trypsin and low pH for priming and triggering of F. The plate was photographed and analysed on ImageJ. a) Fusion activity was observed for both HPR0 and HPR-del constructs. Each bar represents one transfection. Each dot represents the number of positive CHSE cells counted from one image from a well. 10 images were taken from each well, and two wells were counted from the same transfection. The horisontal line represents median of each group. Data plotted is listed in Table 14, Appendix 2. b) Normalising fusion positive cells to haemadsorption data (n=3) or c) RBC-binding (counted RBC-bound CHSE cells) (n=4) showed similar results. Data plotted is listed in Table 15-16, Appendix 2. d) The results showed a significant difference between HPR0 and HPR-del. Each dot represents the median from each transfection, and the horisontal line represents the median between them. Statistical significance was determined with Mann Whitney U-test (p=0.0286).

The recombinantly expressed HE/F proteins have fusion activity (Figure 34a). Haemadsorption assay was performed as described in subchapter 2.5.1 to quantify the amount of bound RBCs to co-transfected cells, to serve as a measure of transfection efficiency. Previous assays for the recombinantly expressed HE protein showed no difference in haemadsorption between HPR0 and HPR-del, and the haemadsorption data was in linear range. Fusion activity was therefore normalised to the haemadsorption data (Figure 34b) to adjust for differences in transfection efficiency, as well as to the number of counted RBC-bound CHSE cells to assess if there is a significant difference between the constructs (Figure 34c), showing similar results. HPR-del HE/F showed higher fusion activity than HPR0 HE/F (Figure 34d). Because the data (Table 16, Appendix 2) did not pass the D'Agostino and

Pearson normality test (Table 17, Appendix 2), a non-parametric Mann Whitney U-test was performed to assess the statistical significance (Table 18, Appendix 2).

The results showed that the HE and F proteins associated with the HPR-del virus variant have higher fusion activity than those associated with the HPR0 virus variant, which was in line with our hypothesis and previous reports that ISAV virulence is related to fusion activity.

4 Discussion and future perspectives

The main objective of the thesis was to study the mechanisms involved in the ISAV fusion process by using molecular techniques to investigate fusion activity. A fusion assay was established to evaluate the fusion activity of HE and F proteins from closely related ISAV-HPR0 and HPR-del variants. Receptor binding and -destroying activities between HPR0 and HPR-del HE were also compared. The methods used is discussed first, followed by a general discussion and finally, future perspectives.

4.1 Discussion of methods

4.1.1 Methods for transfection

Several methods for transfection can be used as described in subchapter 2.2. mRNA is an effective transfection substrate that induces rapid protein expression, because mRNA only needs to enter the cytoplasm, as opposed to using DNA that need to enter the nucleus. However, mRNA is more unstable compared to DNA, which can make it more challenging to work with, and lead to a lower protein production overall. Electroporation using the Neon system with plasmid DNA as substrate was chosen in this thesis, because this was used in a previous study by Fourrier et al. [2, 3], and was also optimised in a previous master's thesis [85].

4.1.2 Methods for evaluating transfection efficiency

In this study, flow cytometry was used as a complement to IF to provide a more quantitative measure of transfection efficiency. Flow cytometry provides a better quantitative measure of signal intensity and cell count than IF and microscopy, however, the disadvantage with flow cytometry is that during the preparation, cells are lost in the wash steps, requiring a higher number of cells per sample. The advantage of using IF and microscopy is that the cells can be stained when they are adherent in plates, without the need of detachment. This requires less cells than for flow cytometry, and the cells can be visualised in the microscope for qualitative and semi-quantitative analysis. However, there is a possibility to use a microplate reader with IF to measure signal intensity, and to quantify the number of cells, or to take images and analyse the wells on an image software, i.e Fiji ImageJ.

Some challenges limited the use of flow cytometry in this study. First, a significant proportion of cells were lost during the washing steps of the staining procedure, with only a few thousand cells left in some samples. Second, our trypsin-based detachment method for flow cytometry was not suitable for cells transfected with plasmids encoding the F proteins, because the F proteins have a trypsin cleavage site that removes the epitope recognised by the antibody available to us. Based on the results from IF

for the F and HE proteins and flow cytometry for the HE proteins, we determined to move ahead to the functional assays rather than optimising other detachment methods.

4.1.3 Quantitative measure of expressed HE

cELISA was performed on cell monolayers that express HE protein at two different time points to compare the expression of HE protein after 24 hours and 48 hours. The challenge was that we did not have a standard for recombinant HE protein to make a standard curve. Therefore, we could not perform a quantitative analysis of the HE-levels to assess if the HE-expression levels were in a linear range. However, cELISA could still be used to evaluate at what time point HE-levels were highest and to give an impression of the protein levels in subsequent analysis.

4.1.4 Methods for measuring receptor binding activity

A common method to measure RBC levels is to perform a haemoglobin assay where the haemoglobin levels are measured spectrophotometrically after the cells have been lysed. This was tested, but this assay was not sensitive enough to detect low numbers of RBCs. The addition of TMB-substrate for measuring endogenous pseudoperoxidase activity and measuring the absorbance (OD 450 nm) showed standard curves with better linearities than the haemoglobin assay, especially at lower RBC numbers, and was therefore a more sensitive assay (Figure 40, Appendix 1). There are also commercial kits for measuring haemoglobin available that are highly sensitive, but the method used was fast and easy, inexpensive, and good enough as the standard curves showed good linearities in the required range.

4.1.5 Methods for measuring receptor destroying activity

Several methods can be used to evaluate the receptor destroying activity in the recombinantly expressed HE proteins. The haemadsorption assay can be used, by testing different incubation times , then visually check under the microscope if the expressed HE proteins elute and quantitatively measure as described earlier. However, it was difficult to get the elution from transfected cells to work properly (data not shown), even using erythrocytes from rainbow trout, which have been described to elute from ISAV agglutination [1, 77].

An esterase activity assay was used in this thesis, where an ester substrate, *p*-nitrophenyl acetate was added, and the chromogenic product, *p*-nitrophenol was measured spectrophotometrically as the increase of absorbance at 405 nm. We observed that cell density in the negative controls/non-transfected cells play a role in the esterase activity. A lot of the transfected cells die, so

the cell numbers are not the same in all wells. The high background is an important limitation of this assay, which means that the enzyme-substrate reaction is not specific to ISAV RDE, but is also catalysed by endogenous enzymes in the CHSE cells. This was a challenge in this assay, because this meant that the high background could not be corrected for. It is worth looking into other esterase activity assays in future experiments. One option would be to test 4-methylumbelliferyl acetate, which is also efficiently cleaved by the ISAV RDE [78]. Another possibility is to choose a different negative control. Rather than using non-transfected CHSE cells as negative control, we could transfect cells with a plasmid/HE where the receptor destroying function is switched off. The ISAV RDE is a serine protease, hence, we could mutate the catalytic serine (Serine 32) to inactivate the enzyme [75].

Due to the high background activity from negative controls, a haemagglutination assay was performed in addition to the esterase activity assay to evaluate elution.

4.1.6 Normalising data from functional assays

The HE-expression levels from cELISA were also intended to be used for normalising data to, but a limitation of the HE-data is that we cannot be sure that the data are linear, due to the lack of a standard curve in the cELISA assay. Generation of a recombinant HE protein to make a standard curve can solve this in future work. Our next approach was to normalise data to the haemadsorption data. This gave better correlation, and we knew that the haemadsorption data was in a linear range. We then compared the haemadsorption/esterase ratio directly. This also translated well to the haemagglutination assay, and to the biological function.

4.1.7 Methods for evaluating fusion activity

Different methods can be used to evaluate fusion. The lipid mixing assay used in the thesis is a method to evaluate hemifusion, the fusion of the outer lipid bilayer, described in subchapter 2.6.1. The content mixing assay is a technique where the aqueous content mixing, and the final stage of fusion is assessed. That assay is based on erythrocyte ghost-facilitated gene delivery method normally used for *in vivo* plasmid DNA expression [86]. Plasmids expressing firefly luciferase reporter gene is loaded into the cytoplasm of erythrocytes by electroporation. The erythrocyte ghosts will function as gene delivery vesicles, and upon fusion, the plasmids are delivered to the target cells cytoplasm where the firefly luciferase reporter gene is expressed, which can be measured. The principle behind this assay is illustrated in Figure 35.

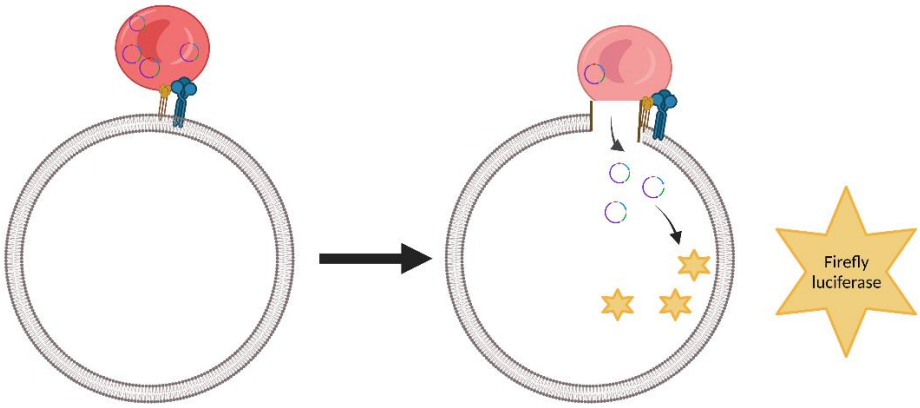

Figure 35. Schematic presentation of content mixing assay. Erythrocytes loaded with plasmids expressing firefly luciferase gene delivers the plasmids into cells upon fusion of erythrocyte ghost with cell membrane. The firefly reporter gene is expressed by the cell machinery and can be measured. *Created with Biorender.com.*

Fourrier et al [2] performed both lipid mixing and content mixing assays in a study where the results were comparable between the assays. It was natural to start with the lipid mixing assay in this thesis. It was an easy method to perform, but a downside was that manually counting cells (fusion positive CHSE cells and RBC-bound cells), in addition to microscopy and taking images, was time-consuming (several days on the microscope and 1-2 weeks counting cells). A content mixing assay would have given higher throughput, because it does not have the same amount of "after-work" with taking images and cell counting as in the lipid mixing assay. Additionally, any bias related to manually counting cells in the lipid mixing assay will be avoided.

4.2 General discussion

4.2.1 No difference in receptor binding and destroying activities between HPR0 and HPR-del

We did not detect a significant difference in the receptor binding and destroying activities between HPR0 and HPR-del. This was in line with our hypothesis that the non-virulent ISAV-HPR0 and the virulent HPR-del variants have similar receptor-binding and receptor-destroying activities. Our hypothesis was based on a previous study [1] where the authors compared RBC adsorption to and elution from CHSE cells transfected with HPR0 and HPR-del HE, including cells treated with esterase inhibitors. Initial results of that study suggested that cells transfected with HPR0 HE had a higher esterase activity than cells transfected with HPR-del HE. However, deletion of the HPR region did not affect elution. Because the amino acid sequence of the transfected HPR0 and HPR-del HE variants also differed in other regions of the HE molecule than the HPR, the authors proposed that the observed variation in elution depended on protein domains outside the HPR region.

The results from the functional analyses of recombinantly expressed HE and HE/F support our hypothesis and is in line with previous findings. It is worth mentioning that differences in HE expression in the first rounds of experiments might have influenced our results and made them more susceptible to noise (Figures 25 and 28). In the earlier assays, the expression of HPR-del was consistently lower than HPR0, but when we received a new batch of the HPR-del plasmid, this difference disappeared. This new batch of plasmid was used for all experiments assessing elution from a haemagglutination reaction and fusion (Figure 29 onwards).

4.2.2 Fusion activation

The results showed that the HE and F proteins associated with the HPR-del virus variant have higher fusion activity than those associated with the HPR0 virus variant. Our hypothesis was that the virulent HE/F variant combination has a higher activity of fusion compared to a non-virulent HE/F variant, in line with the current hypothesis that ISAV virulence is related to fusion activity [2-4]. Our results confirmed our hypothesis and previous reports.

No fusion activation was observed in wells with single transfection of HE or F. It was also interesting to evaluate if F alone bound RBCs. No haemadsorption was observed, in contrast to a recent study by Ojeda et al. that report that F bind ASK cells [4]. One explanation could be that ASK cells have different sialic acid residues on their cell surface than RBCs. Moreover, no fusion activation was observed for HPR-del HE/F in the absence of trypsin and low pH treatment, in contrast to a report by Fourrier et al., that reports significant spontaneous fusion activity [3]. It must be noted that only one replicate was used in this pilot assay where unstimulated conditions were tested. Further experiments are required before any conclusions can be made.

4.2.3 Are the fusion models suitable for understanding ISAV fusion?

In this thesis, the goal was to obtain a model that mimics the ISAV fusion process. CHSE cells were transfected with plasmids encoding HE and F proteins, and RBCs were used to mimic target cells. This model system has been used in previous studies [2-4], and we know it works. A strength of our study is that we have used sequences from closely related viruses detected on farms. These viruses were detected in material from fish, which means that they can maintain themselves in a fish population and have a certain level of fitness. The relationship between the non-virulent and virulent variant has not been confirmed by whole genome sequencing, but we know that the amino acid sequence differences between the variants in the segments encoding HE and F are limited to those correlated

with the transition to virulence. It is therefore reason to believe that the differences observed were due to these correlated mutations only.

In contrast to this, previous studies have used viruses that also have other amino acid changes in their HE and F sequences than the ones that correlates with the transition to virulence. A number of these additional changes are in the receptor binding domain and esterase regions and could have unknown effects. Also, some of these studies have induced artificial mutations in the HPR0 isolate [2, 3]. Because the interaction between the HE and F proteins are unknown, it is not certain that all virulent HE variants work equally well with all virulent F variants. As a result, some findings in these studies may be difficult to interpret.

The fusion model we used is based on the fusion of membranes between CHSE cells and RBCs, where the CHSE cells are transfected with plasmids encoding HE and F proteins to mimic ISAV. It is worth noting that there might be differences in the lipid membrane bilayers of the CHSE cells and ISAV that could have an effect, but this is unknown.

4.3 Future perspectives

The work in this master's thesis consisted of many complex assays, some of which had limitations worth improving in future studies. The cELISA assay lacked a standard curve, so we could not be sure that the HE-expression data was in a linear range. A recombinant HE protein to make a standard curve can solve this in future work. In addition, the esterase activity assay had limitations. The non-transfected CHSE cells that served as negative controls in the assay had high endogenous enzyme activity, and therefore could not be corrected for. Using a different negative control, such as a plasmid/HE with a mutated/inactive serine in future studies is recommended. Improving these limitations will help confirm and strengthen findings from this thesis.

4.3.1 What are the future possibilities, and what have we started/planned

The next step in the fusion assay is to investigate priming and triggering separately: treat with either trypsin or low pH. The fusion assay under these conditions has already been performed, but due to time constraints, the results are not ready for this thesis. It will be interesting to evaluate if HPR-del F induces fusion activation without prior priming with trypsin. If we see spontaneous fusion activation, that indicates that perhaps the F protein has been primed by cellular proteases, either before it was transported to the surface of the CHSE cells, on the surface of the CHSE cells, or on the RBC surface and is not dependent on exogenous trypsin to be cleaved in our assay. It will also be interesting to

evaluate if either construct combinations can trigger fusion activity when they only have been treated and primed with trypsin. The treatment with low pH mimics the fusion of viral and endosomal host membrane, so if we can see fusion activation without adding low pH, this could suggest that these ISAV-variant(s) perhaps do not enter cells via endocytosis alone, or that they perhaps have a another triggering mechanism. Another future objective is to compare heterotypic combinations of the HPR0 and HPR-del HE/F constructs.

The content mixing assay (described in subchapter 4.1.7) is also recommended in future studies. The content mixing assay is easier and more practical with regards to the extensive "after-work" required for the lipid mixing assay. Also, the content mixing assay is a fusion assay where the final stage of fusion is assessed, whereas the lipid mixing assay is where the intermediate stage of fusion (hemifusion) is assessed. There are examples in the literature where the results from hemifusion assays does not always reflect results from content mixing. Both fusion assays should be performed in parallell to compare if they will yield similar results, such as previously done in a study by Fourrier et al. [2].

As part of this thesis, a bead-based protease acticity assay was to be established to assess the ability of different proteases to cleave target peptides of F proteins from closely related ISAV-HPR0 (strain NO/Finnmark/NVI-07-7/2021) and ISAV HPR-del (NO/Finnmark/NVI-70-1250/2020). The target peptides includes the cleavage site, K_{276}, of the F protein, as well as the mutation site at position 266 that is characteristic for the transition from ISAV-HPR0 to HPR-del. There are knowledge gaps concerning F protein cleavage: The F protein can be cleaved by trypsin, but which protease(s) that actually cleaves during an infection is yet to be identified. Furthermore, the effect of the mutations in the HE HPR and F protein on the protease-specificity is unknown. This protease activity assay could provide new insight by identifying proteases that can cleave the target peptides. Preliminary experiments were performed, but due to time constraints, further work on this was put on hold and will be pursued in the future. Method description and results from the preliminary experiments are described in A4.1, Appendix 4. Once established, this assay is intended to be used for testing the protease activity in different samples in future studies (as part of the BIO-DIRECT project), including mucus, blood serum, plasma, and cell medium, to name a few.

Another great advantage for future work would be to develop a method to grow the ISAV-HPR0 variant in cell culture. This has proved to be difficult in previous studies, however, two very recent studies have reported successful HPR0-cultivation [43, 87].

4.3.2 How can increased understanding of viral fusion mechanisms help us understand and fight viral disease?

A key step in infection by enveloped viruses is the fusion of viral and host cell membranes that allows the virus to enter host cell cytoplasm. As discussed above, all available evidence suggest that the viral fusion process represents the step in the infectious cycle where ISAV HPR0 and HPR-del behave differently. If we can unravel and better understand the mechanisms of the ISAV fusion process, we may also be better equipped to address central questions like the transition from non-virulent to virulent ISAV, as well as how we can use this knowledge to find methods to reduce the transition to virulent ISAV, to fight ISA.

5 Conclusions

The aim of this thesis was to establish fusion assays and use these assays to evaluate fusion activity of HE and F proteins from closely related ISAV-HPR0 and HPR-del variants.

The results showed that the transfection method and cell model system used was successful, and that recombinantly expressed HE and F proteins were transported to the cell surface, and functional. Furthermore, HPR0 and HPR-del HE proteins showed similar receptor binding and destroying activities, in line with our hypothesis and a previous report [1]. By plotting esterase activity as a function of haemadsorption, the graphs showed that there is a correlation between receptor binding and receptor destroying activities for both HE variants, and, as expected, that they depend on the expression of HE protein.

The results showed that the HE and F proteins associated with the HPR-del virus variant have higher fusion activity than those associated with the HPR0 virus variant, which is in line with our hypothesis and previous reports [2-4] that fusion activity relates to virulence. As expected, no fusion activation was seen in wells with single transfection of HE or F proteins. Additionally, single transfection of F protein did not reveal haemadsorption. Moreover, no fusion activation was observed in the absence of trypsin and low pH treatment for HPR-del HE/F.

The work in this thesis has generated a foundation for future fusion activity studies as a step towards the understanding of the factors involved in the ISAV fusion process and the mechanisms underlying ISAV virulence.

6 References

[1] A. McBeath, M. Fourrier, E. Munro, K. Falk, and M. Snow, "Presence of a full-length highly polymorphic region (HPR) in the ISAV haemagglutinin-esterase does not affect the primary functions of receptor binding and esterase activity," *Arch Virol,* vol. 156, no. 12, pp. 2285-2289, 2011, doi: 10.1007/s00705-011-1106-9.

[2] M. Fourrier *et al.*, "Deletions in the highly polymorphic region (HPR) of infectious salmon anaemia virus HPR0 haemagglutinin-esterase enhance viral fusion and influence the interaction with the fusion protein," *J Gen Virol,* vol. 95, no. Pt 5, pp. 1015-1024, 2014, doi: 10.1099/vir.0.061648-0.

[3] M. Fourrier *et al.*, "Dual Mutation Events in the Haemagglutinin-Esterase and Fusion Protein from an Infectious Salmon Anaemia Virus HPR0 Genotype Promote Viral Fusion and Activation by an Ubiquitous Host Protease," *PLoS One,* vol. 10, no. 10, pp. e0142020-e0142020, 2015, doi: 10.1371/journal.pone.0142020.

[4] N. Ojeda, C. Cárdenas, and S. Marshall, "Interaction of the Amino-Terminal Domain of the ISAV Fusion Protein with a Cognate Cell Receptor," *Pathogens,* vol. 9, no. 6, p. 416, 2020, doi: 10.3390/pathogens9060416.

[5] N. S. Council. "Innovating a new industry: Aquaculture." Norwegian Seafood Council. https://seafoodfromnorway.us/Stories-from-Norway/the-gift-keeps-on-giving/innovating-a-new-industry---aquaculture/ (accessed 30.07.2021).

[6] FAO. "National Aquaculture Sector Overview Norway." Fisheries and Aquaculture Department, Food and Agriculture Organization of the United Nations. http://www.fao.org/fishery/countrysector/naso_norway/en (accessed 30.07.2021).

[7] T. A. Steinset. "Oppdrettslaks til heile verda." Statistisk Sentralbyrå. https://www.ssb.no/jord-skog-jakt-og-fiskeri/artikler-og-publikasjoner/oppdrettslaks-til-heile-verda (accessed 30.07.2021).

[8] T. Kristiansen. "Farmed fish are Norway's most important farm animals. Each year, over 350 million salmon and rainbow trout are put out in fish cages in the sea." Institute of Marine Research. https://www.hi.no/en/hi/temasider/aquaculture/fish-welfare (accessed 11.08.2021).

[9] I. Sommerset *et al.*, "The Health Situation in Norwegian Aquaqulture 2021," The Norwegian Veterinary Institute, 2022. [Online]. Available: https://www.vetinst.no/rapporter-og-publikasjoner/rapporter/2022/fiskehelserapporten-2021

[10] I. Sommerset, B. Bang Jensen, G. Bornø, A. Haukaas, and E. Brun, "The Health Situation in Norwegian Aquaqulture 2020," The Norwegian Veterinary Institute, 2021. [Online]. Available: https://www.vetinst.no/rapporter-og-publikasjoner/rapporter/2021/fiskehelserapporten-2020

[11] I. Sommerset, C. S. Walde, B. Bang Jensen, G. Bornø, A. Haukaas, and E. Brun, "The Health Situation in Norwegian Aquaqulture 2019," The Norwegian Veterinary Institute, 2020. [Online]. Available: https://www.vetinst.no/rapporter-og-publikasjoner/rapporter/2020/fiskehelserapporten-2019

[12] K. Thorud and H. O. Djupvik, "Infectious anaemia in Atlantic salmon (*Salmo salar* L.)." *Bull. Euc. Assoc. Fish Pathol.,* vol. 8, pp. 109-111, 1988.

[13] E. Rimstad, O. B. Dale, B. H. Dannevig, and K. Falk, "Infectious Salmon Anaemia," in *Fish diseases and disorders*, vol. 3: Viral, bacterial and fungal infections, P. T. K. Woo and D. W. Bruno Eds. Oxfordshire: CAB International, 2011, ch. 4, pp. 143-165.

[14] A. Nylund, J. Brattespe, H. Plarre, M. Kambestad, and M. Karlsen, "Wild and farmed salmon (*Salmo salar*) as reservoirs for infectious salmon anaemia virus, and the importance of horizontal- and vertical transmission," *PLoS One,* vol. 14, no. 4, pp. e0215478-e0215478, 2019, doi: 10.1371/journal.pone.0215478.

[15] J. D. Cook, H. Soto-Montoya, M. K. Korpela, and J. E. Lee, "Electrostatic Architecture of the Infectious Salmon Anemia Virus (ISAV) Core Fusion Protein Illustrates a Carboxyl-Carboxylate pH Sensor," *J Biol Chem,* vol. 290, no. 30, pp. 18495-18504, 2015, doi: 10.1074/jbc.M115.644781.
[16] F. S. B. Kibenge and M. J. T. Kibenge, "Orthomyxoviruses of Fish," in *Aquaculture Virology*, F. S. B. Kibenge and M. G. Godoy Eds.: Elsevier Inc, 2016, ch. 19, pp. 299-326.
[17] M. Aamelfot, O. B. Dale, and K. Falk, "Infectious salmon anaemia - pathogenesis and tropism," *J Fish Dis,* vol. 37, no. 4, pp. 291-307, 2014, doi: 10.1111/jfd.12225.
[18] OIE. "Infection with HPR-deleted or HPR0 infectious salmon anaemia virus." OIE World Organisation for Animal Health. https://www.oie.int/fileadmin/Home/eng/Health_standards/aahm/current/2.3.04_ISAV.pdf (accessed 01.09.2021).
[19] Viralzone. "*Isavirus*." SIB Swiss Institute of Bioinformatics. https://viralzone.expasy.org/95 (accessed 11.08.2021).
[20] Viralzone. "Orthomyxoviridae." SIB Swiss Institute of Bioinformatics. https://viralzone.expasy.org/223 (accessed 11.08.2021).
[21] E. Rimstad and T. Markussen, "Infectious salmon anaemia virus—molecular biology and pathogenesis of the infection," *J Appl Microbiol,* vol. 129, no. 1, pp. 85-97, 2020, doi: 10.1111/jam.14567.
[22] M. Fourrier, "Development of molecular virology techniques and functional analysis of the mechanisms leading to virulence acquisition in Infectious Salmon Anaemia Virus (ISAV)." Doctor of philosophy, Univerity of Aberdeen, Aberdeen, 2015.
[23] D. H. Christiansen *et al.*, "First field evidence of the evolution from a non-virulent HPR0 to a virulent HPR-deleted infectious salmon anaemia virus," *J Gen Virol,* vol. 98, no. 4, pp. 595-606, 2017, doi: 10.1099/jgv.0.000741.
[24] D. H. Christiansen, P. S. ØStergaard, M. Snow, O. B. Dale, and K. Falk, "A low-pathogenic variant of infectious salmon anemia virus (ISAV-HPRO) is highly prevalent and causes a non-clinical transient infection in farmed Atlantic salmon (Salmo salar L.) in the Faroe Islands," *J Gen Virol,* vol. 92, no. Pt 4, pp. 909-918, 2011, doi: 10.1099/vir.0.027094-0.
[25] T. Markussen *et al.*, "Evolutionary mechanisms involved in the virulence of infectious salmon anaemia virus (ISAV), a piscine orthomyxovirus," *Virology,* vol. 374, no. 2, pp. 515-527, 2008, doi: 10.1016/j.virol.2008.01.019.
[26] M. Aamelfot, D. H. Christiansen, O. B. Dale, A. McBeath, S. L. Benestad, and K. Falk, "Localised Infection of Atlantic Salmon Epithelial Cells by HPR0 Infectious Salmon Anaemia Virus," *PLoS One,* vol. 11, no. 3, pp. e0151723-e0151723, 2016, doi: 10.1371/journal.pone.0151723.
[27] T. M. Lyngstad *et al.*, "Low virulent infectious salmon anaemia virus (ISAV-HPR0) is prevalent and geographically structured in Norwegian salmon farming," *Dis Aquat Organ,* vol. 101, no. 3, pp. 197-206, 2012, doi: 10.3354/dao02520.
[28] J. M. White and G. R. Whittaker, "Fusion of Enveloped Viruses in Endosomes," *Traffic,* vol. 17, no. 6, pp. 593-614, 2016, doi: 10.1111/tra.12389.
[29] J. Flint, V. R. Racaniello, G. F. Rall, T. Hatziioannou, and A. M. Skalka, "Attachment and entry," in *Principles of virology*, vol. 1, A. Press Ed., 5th ed. Hoboken, NJ: John & Wiley Sons Inc, 2020, ch. 5, pp. 132-165.
[30] J. C. Dyason and M. von Itzstein, "Viral surface glycoproteins in carbohydrate recognition: Structure and modelling," ed, 2010, pp. 269-283.
[31] V. Aspehaug, A. B. Mikalsen, M. Snow, E. Biering, and S. Villoing, "Characterization of the Infectious Salmon Anemia Virus Fusion Protein," *J Virol,* vol. 79, no. 19, pp. 12544-12553, 2005, doi: 10.1128/JVI.79.19.12544-12553.2005.
[32] J. D. Cook, A. Sultana, and J. E. Lee, "Structure of the infectious salmon anemia virus receptor complex illustrates a unique binding strategy for attachment," *Proc Natl Acad Sci U S A,* vol. 114, no. 14, pp. E2929-E2936, 2017, doi: 10.1073/pnas.1617993114.

[33] T. Sandvik, E. Rimstad, and S. Mjaaland, "The viral RNA 3'- and 5'-end structure and mRNA transcription of infectious salmon anaemia virus resemble those of influenza viruses," *Arch Virol,* vol. 145, no. 8, pp. 1659-1669, 2000, doi: 10.1007/s007050070082.
[34] J. Flint, V. R. Racaniello, G. F. Rall, T. Hatziioannou, and A. M. Skalka, "Orthomyxoviruses," in *Principles of virology*, vol. 1, A. Press Ed., 5th ed. Hoboken, NJ: John & Wiley Sons Inc, 2020, pp. 536-537.
[35] M. Ángeles Esteban, "An Overview of the Immunological Defenses in Fish Skin," *ISRN immunology,* vol. 2012, pp. 1-29, 2012, doi: 10.5402/2012/853470.
[36] K. L. Shephard, "Functions for fish mucus," *Reviews in fish biology and fisheries,* vol. 4, no. 4, pp. 401-429, 1994, doi: 10.1007/BF00042888.
[37] S. Dash, S. K. Das, J. Samal, and H. N. Thatoi, "Epidermal mucus, a major determinant in fish health: a review," *Iran J Vet Res,* vol. 19, no. 2, pp. 72-81, 2018.
[38] I. Salinas, Y.-A. Zhang, and J. O. Sunyer, "Mucosal immunoglobulins and B cells of teleost fish," *Dev Comp Immunol,* vol. 35, no. 12, pp. 1346-1365, 2011, doi: 10.1016/j.dci.2011.11.009.
[39] R. A. Cone, "Barrier properties of mucus," *Adv Drug Deliv Rev,* vol. 61, no. 2, pp. 75-85, 2009, doi: 10.1016/j.addr.2008.09.008.
[40] S. K. Linden, P. Sutton, N. G. Karlsson, V. Korolik, and M. A. McGuckin, "Mucins in the mucosal barrier to infection," *Mucosal Immunol,* vol. 1, no. 3, pp. 183-197, 2008, doi: 10.1038/mi.2008.5.
[41] J. H. Cho, I. Y. Park, H. S. Kim, W. T. Lee, M. S. Kim, and S. C. Kim, "Cathepsin D produces antimicrobial peptide parasin I from histone H2A in the skin mucosa of fish," *FASEB J,* vol. 16, no. 3, pp. 429-431, 2002, doi: 10.1096/fj.01-0736fje.
[42] M. Richard, R. Fouchier, I. Monne, and T. Kuiken, "Mechanisms and risk factors for mutation from low to highly pathogenic avian influenza virus," *EFSA Supporting Publications,* vol. 14, no. 10, p. n/a, 2017, doi: 10.2903/sp.efsa.2017.EN-1287.
[43] M. Cárdenas *et al.*, "Infectious Salmon Anemia Virus Infectivity Is Determined by Multiple Segments with an Important Contribution from Segment 5," *Viruses,* vol. 14, no. 3, p. 631, 2022, doi: 10.3390/v14030631.
[44] F. X. Bosch, W. Garten, H. D. Klenk, and R. Rott, "Proteolytic cleavage of influenza virus hemagglutinins: primary structure of the connecting peptide between HA1 and HA2 determines proteolytic cleavability and pathogenicity of avian influenza viruses," *Virology,* vol. 113, no. 2, pp. 725-735, 1981, doi: 10.1016/0042-6822(81)90201-4.
[45] D. A. Senne *et al.*, "Survey of the hemagglutinin (HA) cleavage site sequence of H5 and H7 avian influenza viruses: amino acid sequence at the HA cleavage site as a marker of pathogenicity potential," *Avian Dis,* vol. 40, no. 2, pp. 425-437, 1996, doi: 10.2307/1592241.
[46] W. Garten and H.-D. Klenk, "Cleavage Activation of the Influenza Virus Hemagglutinin and Its Role in Pathogenesis," vol. 27, ed. Basel, Switzerland: Basel, Switzerland: S. Karger AG, 2008, pp. 156-167.
[47] S. Belouzard, J. K. Millet, B. N. Licitra, and G. R. Whittaker, "Mechanisms of coronavirus cell entry mediated by the viral spike protein," *Viruses,* vol. 4, no. 6, pp. 1011-1033, 2012, doi: 10.3390/v4061011.
[48] B. J. Bosch, W. Bartelink, and P. J. M. Rottier, "Cathepsin L Functionally Cleaves the Severe Acute Respiratory Syndrome Coronavirus Class I Fusion Protein Upstream of Rather than Adjacent to the Fusion Peptide," *J Virol,* vol. 82, no. 17, pp. 8887-8890, 2008, doi: 10.1128/JVI.00415-08.
[49] J. K. Millet and G. R. Whittaker, "Host cell proteases: Critical determinants of coronavirus tropism and pathogenesis," *Virus Res,* vol. 202, pp. 120-134, 2015, doi: 10.1016/j.virusres.2014.11.021.
[50] P. Masters and S. Perlman, "Coronaviridae," vol. 1, ed, 2013, pp. 825-858.

[51] X. Du *et al.*, "Omicron adopts a different strategy from Delta and other variants to adapt to host," *Signal Transduct Target Ther,* vol. 7, no. 1, pp. 45-45, 2022, doi: 10.1038/s41392-022-00903-5.
[52] M. Pallavi Suyog Uttekar. "Why Is In Vivo Better Than In Vitro?" MedicineNet, Inc. https://www.medicinenet.com/why_is_in_vivo_better_than_in_vitro/article.htm (accessed 15.09.2021).
[53] M. Nikolic, T. Sustersic, and N. Filipovic, "In vitro Models and On-Chip Systems: Biomaterial Interaction Studies With Tissues Generated Using Lung Epithelial and Liver Metabolic Cell Lines," (in English), *Frontiers in Bioengineering and Biotechnology,* Review vol. 6, no. 120, 2018-September-03 2018, doi: 10.3389/fbioe.2018.00120.
[54] O. Graudejus, R. Ponce Wong, N. Varghese, S. Wagner, and B. Morrison, "Bridging the gap between in vivo and in vitro research: Reproducing in vitro the mechanical and electrical environment of cells in vivo," *Frontiers in cellular neuroscience,* vol. 12, 2018, doi: 10.3389/conf.fncel.2018.38.00069.
[55] T. F. S. Inc. "Cell culture basics handbook." Thermo Fisher Inc. https://www.thermofisher.com/content/dam/LifeTech/Documents/PDFs/PG1563-PJT1267-COL31122-Gibco-Cell-Culture-Basics-Handbook-Global-FLR.pdf (accessed 25.10.2021).
[56] C. N. Lannan, J. R. Winton, and J. L. Fryer, "Fish Cell Lines: Establishment and Characterization of Nine Cell Lines from Salmonids," *In Vitro,* vol. 20, no. 9, pp. 671-676, 1984, doi: 10.1007/BF02618871.
[57] B. L. Schiøtz *et al.*, "Enhanced transfection of cell lines from Atlantic salmon through nucoleofection and antibiotic selection," *BMC Res Notes,* vol. 4, no. 1, pp. 136-136, 2011, doi: 10.1186/1756-0500-4-136.
[58] M. KGaA. "Cell dissociation protocol with trypsin." Merck KGaA. https://www.sigmaaldrich.com/NO/en/technical-documents/protocol/cell-culture-and-cell-culture-analysis/mammalian-cell-culture/cell-dissociation-with-trypsin (accessed 13.09.2021)).
[59] S.-A. C. LLC, *Fundamental techniques in cell culture*, 3rd ed.: Sigma-Aldrich Co.LLC, 2016, p. 82. [Online]. Available: https://www.sigmaaldrich.com/deepweb/assets/sigmaaldrich/marketing/global/documents/425/663/fundamental-techniques-in-cell-culture.pdf.
[60] T. F. Scientific. "Introduction to transfection." Thermo Fisher Scientific. https://www.thermofisher.com/no/en/home/references/gibco-cell-culture-basics/transfection-basics/introduction-to-transfection.html (accessed 06.11.2021).
[61] Lonza. "Transfection methods for cell culture." Lonza. https://bioscience.lonza.com/lonza_bs/NO/en/transfection?_bt=545476411435&_bk=&_bm=b&_bn=g&_bg=128799661402&gclid=Cj0KCQjwrJOMBhCZARIsAGEd4VFiXBoUz7rgi-KeC_GFAGDzMyH7dXF6gLFMHtXm62nsemo9NmJZFBMaAiwvEALw_wcB (accessed 06.11.2021).
[62] T. F. Scientific. "Types of transfection." Thermo Fisher Scientific. https://www.thermofisher.com/no/en/home/references/gibco-cell-culture-basics/transfection-basics/types-of-transfection.html (accessed 06.11.2021).
[63] K. R. Dean, V. H. S. Oliveira, C. Wolff, T. Moldal, and M. D. Jansen, "Description of ISAV-HPRΔ-positive salmon farms in Norway in 2020," *J Fish Dis,* vol. 45, no. 1, pp. 225-229, 2022, doi: 10.1111/jfd.13538.
[64] T. F. S. Inc. "Thermo Scientific Pierce Immunofluorescence Handbook." https://static.fishersci.eu/content/dam/fishersci/en_EU/lifescience/doctechnical/proteomics/TS_Pierce_Immunofluorescence-Handbook.pdf (accessed 23.11.2021).
[65] B. Alberts *et al.*, "Visualizing cells," in *Molecular biology of the cell*, 6th ed. New York: W. W. Norton & Company, 2015, ch. 9, pp. 529-564.

[66] J. Flint, V. R. Racaniello, G. F. Rall, T. Hatziioannou, and A. M. Skalka, "The Infectious Cycle," in *Principles of virology*, vol. 1, A. Press Ed., 5th ed. Hoboken, NJ: John & Wiley Sons Inc, 2020, ch. 2, pp. 26-60.
[67] I. Bio-Rad Laboratories. "Flow cytometry." Bio-Rad Laboratories, Inc. https://www.bio-rad-antibodies.com/flow-cytometry.html (accessed 24.11.2021).
[68] J. Willey, K. Sandman, and D. Wood, "Methods in Microbial Ecology," in *Prescott's Microbiology*. New York: McGraw-Hill Education, 2020, pp. 646-657.
[69] R. R. Jahan-Tigh, C. Ryan, G. Obermoser, and K. Schwarzenberger, "Flow Cytometry," *Journal of Investigative Dermatology,* vol. 132, no. 10, pp. 1-6, 2012, doi: 10.1038/jid.2012.282.
[70] J. L. Tymoczko, J. M. Berg, and L. Stryer, "Immunological Techniques Are Used To Purify and Characterize Proteins," in *Biochemistry: a short course*, 3rd ed. New York: W. H. Freeman and Company, 2015, ch. 5.3, sec. 2, pp. 78-85.
[71] J. Willey, K. Sandman, and D. Wood, "Immune Responses Can Be Exploited to Detect Infections," in *Prescott's Microbiology*, 11th ed. New York: McGraw-Hill Education, 2020, ch. 37.3, pp. 816-822.
[72] I. Bio-Rad Laboratories. "ELISA Basics Guide." Bio-Rad Laboratories, Inc. https://www.bio-rad-antibodies.com/static/Lit-pdfs/Brochures1/elisa-basics-guide.pdf (accessed 07.12.2021).
[73] E. V. Lourenço and M.-C. Roque-Barreira, "Immunoenzymatic Quantitative Analysis of Antigens Expressed on the Cell Surface (Cell-ELISA)," *Methods Mol Biol,* vol. 588, pp. 301-309, 2009, doi: 10.1007/978-1-59745-324-0_29.
[74] K. Falk, E. Namork, and B. H. Dannevig, "Characterization and applications of a monoclonal antibody against infectious salmon anaemia virus," *Dis Aquat Organ,* vol. 34, no. 2, pp. 77-85, 1998, doi: 10.3354/dao034077.
[75] A. Müller *et al.*, "Structural and functional analysis of the hemagglutinin-esterase of infectious salmon anaemia virus," *Virus Res,* vol. 151, no. 2, pp. 131-141, 2010, doi: 10.1016/j.virusres.2010.03.020.
[76] K. Falk, V. Aspehaug, R. Vlasak, and C. Endresen, "Identification and Characterization of Viral Structural Proteins of Infectious Salmon Anemia Virus," *J Virol,* vol. 78, no. 6, pp. 3063-3071, 2004, doi: 10.1128/JVI.78.6.3063-3071.2004.
[77] K. Falk, E. Namork, E. Rimstad, S. Mjaaland, and B. H. Dannevig, "Characterization of infectious salmon anemia virus, an orthomyxo-like virus isolated from Atlantic salmon (Salmo salar L.)," *J Virol,* vol. 71, no. 12, pp. 9016-9023, 1997, doi: 10.1128/JVI.71.12.9016-9023.1997.
[78] M. Kristiansen, M. K. Froystad, A. L. Rishovd, and T. Gjoen, "Characterization of the receptor-destroying enzyme activity from infectious salmon anaemia virus," *J Gen Virol,* vol. 83, no. 11, pp. 2693-2697, 2002, doi: 10.1099/0022-1317-83-11-2693.
[79] R. Vlasak, M. Krystal, M. Nacht, and P. Palese, "The influenza c virus glycoprotein (HE) exhibits receptor-binding (hemagglutinin) and receptor-destroying (esterase) activities," *Virology,* vol. 160, no. 2, pp. 419-425, 1987, doi: 10.1016/0042-6822(87)90013-4.
[80] D. Hoekstra, T. De Boer, K. Klappe, and J. Wilschut, "Fluorescence method for measuring the kinetics of fusion between biological membranes," *Biochemistry,* vol. 23, no. 24, pp. 5675-5681, 1984, doi: 10.1021/bi00319a002.
[81] S. Bagai and R. A. Lamb, "Quantitative measurement of paramyxovirus fusion: differences in requirements of glycoproteins between simian virus 5 and human parainfluenza virus 3 or Newcastle disease virus," *J Virol,* vol. 69, no. 11, pp. 6712-6719, 1995, doi: 10.1128/JVI.69.11.6712-6719.1995.
[82] T. F. Scientific. "Lipid-Mixing Assays of Membrane Fusion—Note 13.1." Thermo Fisher Scientific. https://www.thermofisher.com/no/en/home/references/molecular-probes-the-handbook/technical-notes-and-product-highlights/lipid-mixing-assays-of-membrane-fusion.html (accessed 21.12.2021).

[83] A. Technologies. "How Normalizing Biological Data Works." LabX Media Group, Wilmington, DE, USA. https://www.labmanager.com/how-it-works/how-normalizing-biological-data-works-1969 (accessed 25.04.2022).
[84] L. L. Slocombe and I. G. Colditz, "A rapid colorimetric assay for measuring low concentrations of haemoglobin in large numbers of bovine plasma samples," *Food and agricultural immunology,* vol. 22, no. 2, pp. 135-143, 2011, doi: 10.1080/09540105.2010.549209.
[85] S. Sapkota, "Transfection optimization and gene editing method establishment for fish cells," Master's thesis, Faculty of Biosciences, Norwegian University of Life Sciences, 2021.
[86] H. M. Byun *et al.*, "Erythrocyte ghost-mediated gene delivery for prolonged and blood-targeted expression," *Gene Ther,* vol. 11, no. 5, pp. 492-496, 2004, doi: 10.1038/sj.gt.3302180.
[87] D. Ditlecadet, C. Gautreau, L. Boston, R. Liston, E. Johnsen, and N. Gagné, "First report of successful isolation of a HPR0-like variant of the infectious salmon anaemia virus (ISAV) using cell culture," *J Fish Dis,* vol. 45, no. 3, pp. 479-483, 2022, doi: 10.1111/jfd.13556.

Appendix 1

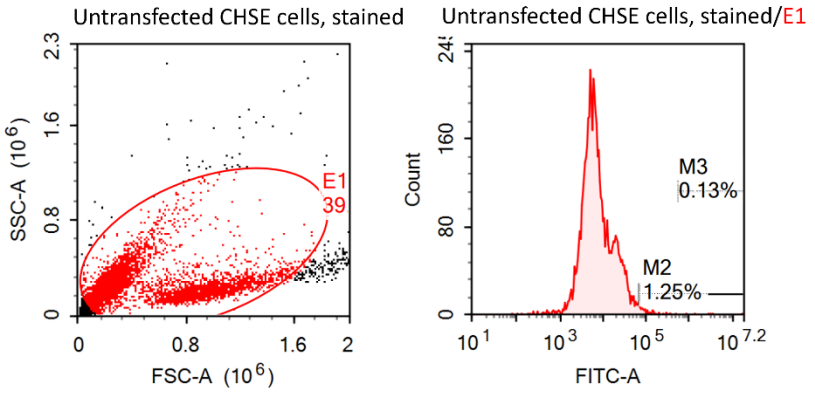

Sample Statistics of untransfected CHSE cells, stained

Gate	Count	% Parent	X	Y	Median X	Median Y
All	13 425					
E1	5 352	39.87 %	FSC-A	SSC-A	305 016	221 456
M2	67	1.25 %	FITC-A	Count	99 417	
M3	7	0.13 %	FITC-A	Count	3 159 120	

Figure 36. Flow cytometry results for negative control (non-transfected cells).

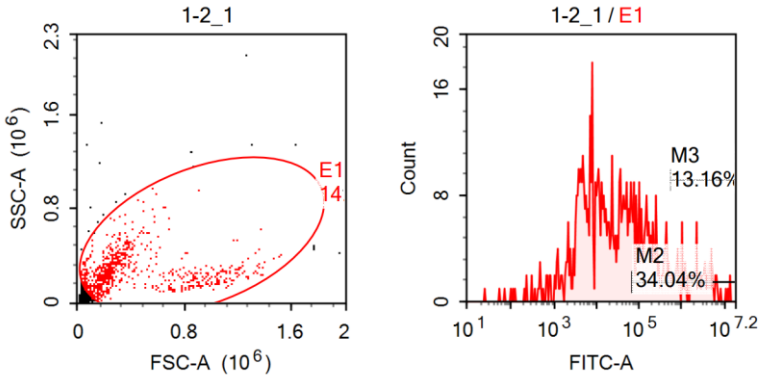

Sample Statistics of 1-2_1

Gate	Count	% Parent	X	Y	Median X	Median Y
All	5 120					
E1	752	14.69 %	FSC-A	SSC-A	248 090	241 791
M2	256	34.04 %	FITC-A	Count	276 558	
M3	99	13.16 %	FITC-A	Count	2 292 582	

Figure 37. Flow cytometry results for HPR0 shows 34 % transfection efficiency when 10^5 CHSE cells were transfected with 1.6 µg plasmid DNA.

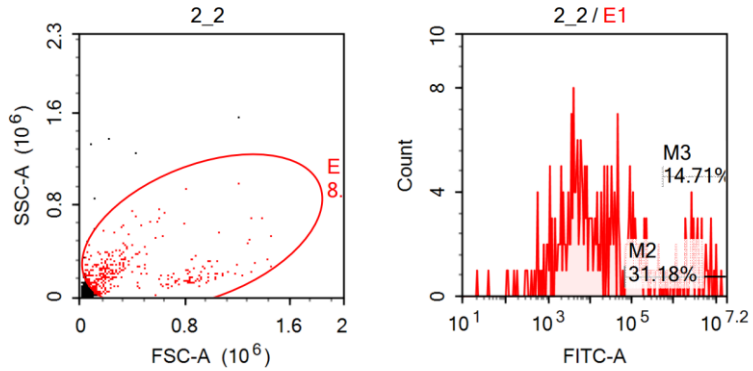

Sample Statistics of 2_2

Gate	Count	% Parent	X	Y	Median X	Median Y
All	4 063					
E1	340	8.37 %	FSC-A	SSC-A	217 097	191 126
M2	106	31.18 %	FITC-A	Count	431 858	
M3	50	14.71 %	FITC-A	Count	3 213 143	

Figure 38. Flow cytometry results for HPR-del shows 31 % transfection efficiency when 10^5 CHSE cells were transfected with 1.6 µg plasmid DNA.

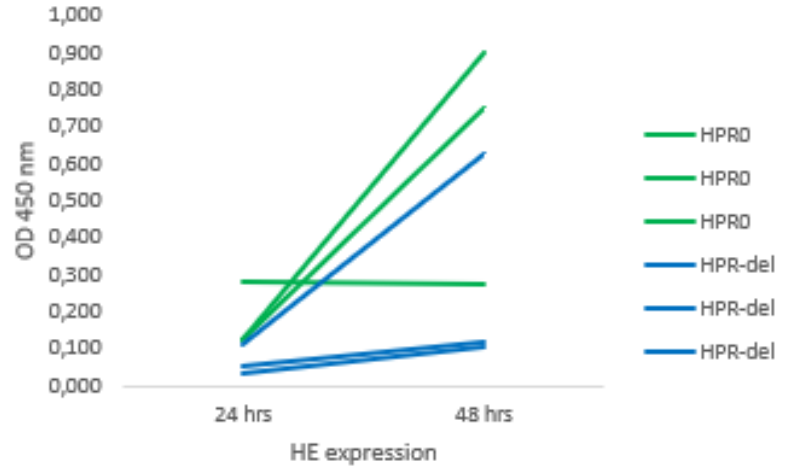

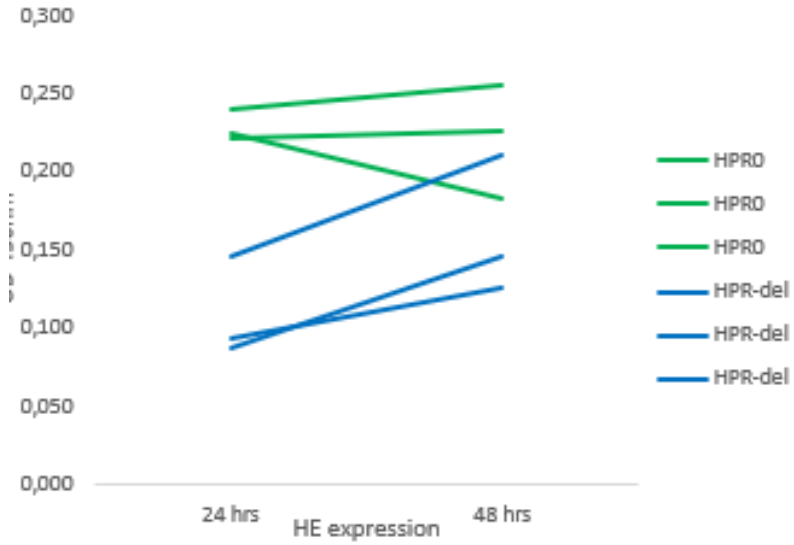

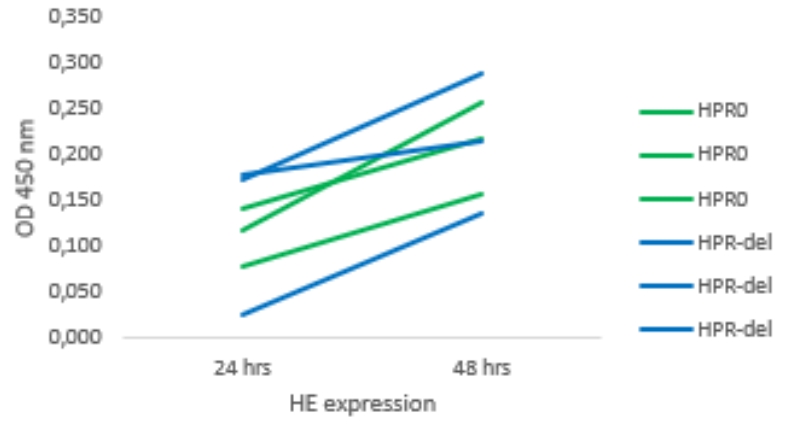

Figure 39. Graphs from three cELISA experiments. Results show that the overall HE expression is higher 48 hours post transfection.

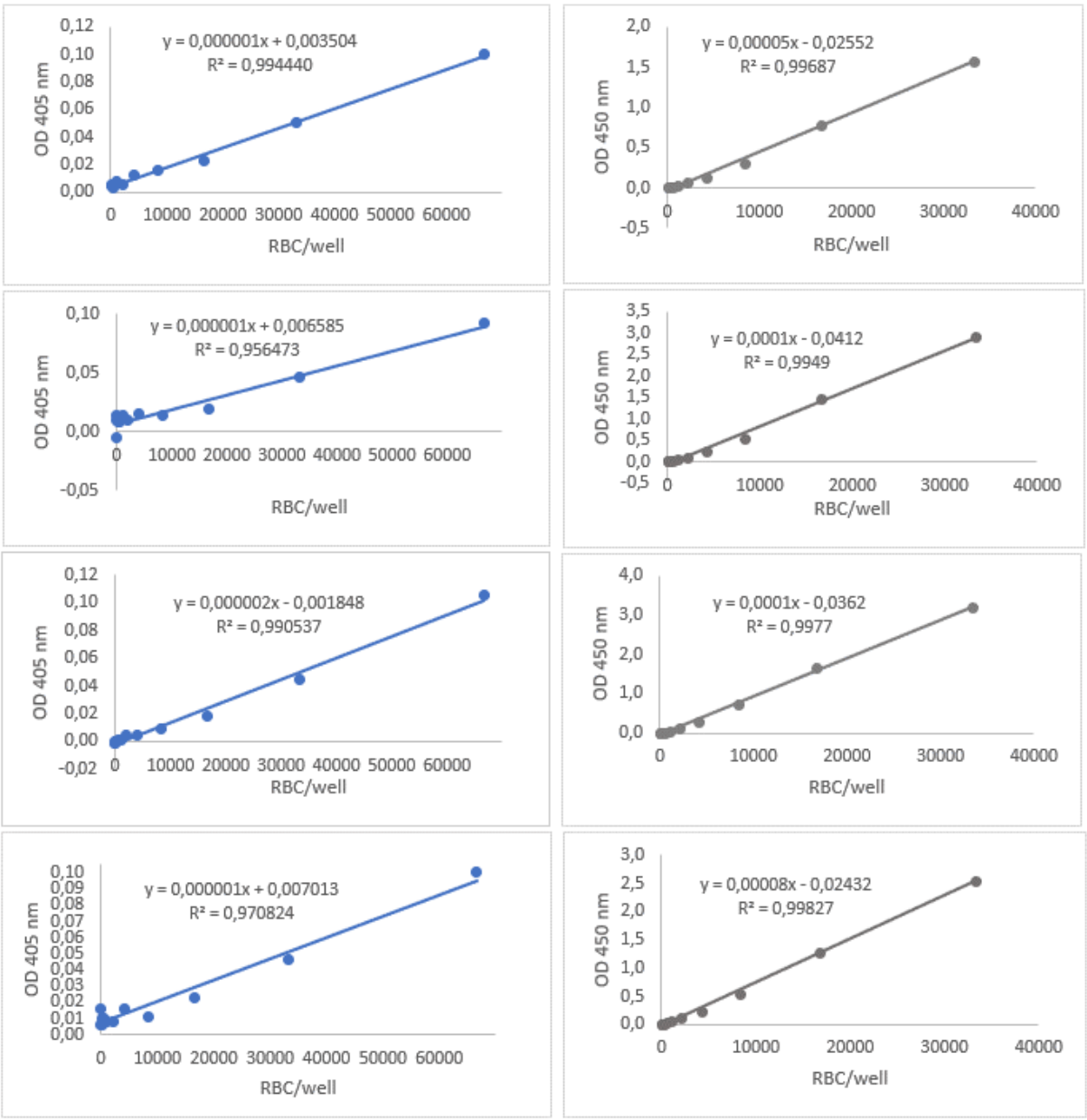

Figure 40. Standard curves from haemadsorption assays. The OD values are plotted as a function of the number of RBCs per well. Curves to the left (haemoglobin) in blue are not as linear as curves from haemadsorption (TMB-pseudoperoxidase) in gray to the right.

Table 5. Haemadsorption data (OD) raw data.

HPR0	HPR-del
1,1192	0,3262
1,1762	0,3062
1,1202	0,3952
0,7954	0,3824
0,5834	0,6064
0,8934	0,4474
1,8512	1,7932
2,3102	1,2892
1,8662	1,2182
0,2646	0,2146
0,2426	0,2776
0,1696	0,1476

Table 6. HE-expression (OD) raw data.

HPR0	HPR-del
0,158	0,289
0,218	0,215
0,257	0,137
0,182	0,210
0,255	0,125
0,226	0,146
0,231	0,143
0,171	0,147
0,224	0,108
0,278	0,104
0,751	0,116
0,900	0,629

Table 7. Haemadsorption data normalised to HE-expression.

HPR0	HPR-del
1,67	0,74
1,11	1,29
0,66	1,08
10,17	8,54
9,06	10,31
8,25	8,34
3,47	2,71
3,44	4,16
4,01	4,19
4,03	3,14
1,57	2,64
1,24	0,63

Table 8. Ratio haemadsorption data (OD-values) relative to HE expression (cELISA data), normalised to the mean of HPR0 to adjust for variations between experiments.

HPR0	HPR-del
1,46	0,65
0,97	1,12
0,57	0,94
1,11	0,93
0,99	1,13
0,90	0,91
0,95	0,74
0,95	1,14
1,10	1,15
1,77	1,38
0,69	1,16
0,55	0,28

Table 9. Background noise (OD values) from negative controls (non-transfected cells) in the esterase activity assays.

No.of cells plated	25000	12500	6250	3125
	0,59	0,29	0,21	0,2
	0,57	0,39	0,24	0,25
	0,49	0,33	0,23	0,23
	0,59	0,2	0,21	0,1
	0,67	0,31	0,22	0,13
	0,58	0,29	0,2	0,13
	0,45	0,23	0,12	0,06
	0,43	0,22	0,11	0,06
	0,42	0,21	0,13	0,06
	0,45	0,21	0,13	0,09
	0,43	0,2	0,13	0,08
	0,43	0,23	0,14	0,1

Table 10. Esterase activity (OD) raw data.

HPR0	HPR-del
0,26	0,24
0,33	0,30
0,27	0,19
0,49	0,44
0,54	0,29
0,52	0,33
0,73	0,32
0,58	0,27
0,70	0,29
0,49	0,28
0,37	0,28
0,57	0,28
0,69	0,26
0,72	0,25
0,62	0,32

Table 11. Esterase activity data plotted as a function of haemadsorption data.

HA (OD-BG)	HPR0	HPRdel
1,17	0,91	
1,08	1,15	
0,75	0,94	
0,95		0,84
1,23		1,05
0,65		0,66
1,10		
2,42		
0,85		
0,92	0,95	
1,15	1,04	
0,93	1,01	
0,89		0,84
0,64		0,56
0,61		0,63
0,54		
0,42		
0,79		
1,04	1,09	
0,83	0,87	
1,13	1,04	
0,43		0,48
0,30		0,40
0,37		0,44
0,54		
0,80		
0,86		
1,05	1,03	
0,77	0,78	
1,18	1,20	
0,51		0,59
0,80		0,59
0,59		0,59
0,73		
1,04		
1,16		
0,98	1,02	
1,03	1,06	
0,98	0,92	
0,29		0,39
0,27		0,37
0,35		0,48
0,67		
0,68		
0,67		

Table 12. Ratio of esterase activity to haemadsorption data, normalised to the mean HPR0 value to correct for variation between experiments.

HPR0	HPRdel
0,75	0,85
1,04	0,82
1,21	0,98
1,02	0,50
0,90	1,29
1,08	1,17
1,03	1,22
1,04	1,51
0,94	1,29
0,98	1,16
1,01	0,73
1,01	0,99
1,04	1,35
1,03	1,39
0,93	1,37

Haemagglutination assay for elution, experiment 1

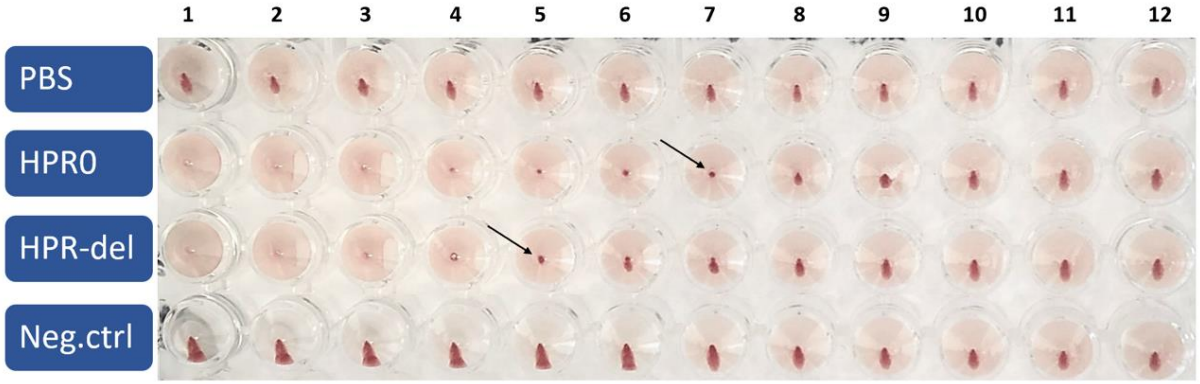

Figure 41. RBC suspension was added to a twofold serial dilution of membrane fractions of HE-transfected CHSE cells. After one hour incubation time with RBC suspension, the plate was tilted. For HPR0, well 7 slows down the running of RBC button and contains 1 HAU. The haemagglutination titer is 64 HAU/well. The haemagglutination titer is 16 HAU/well for HPR-del.

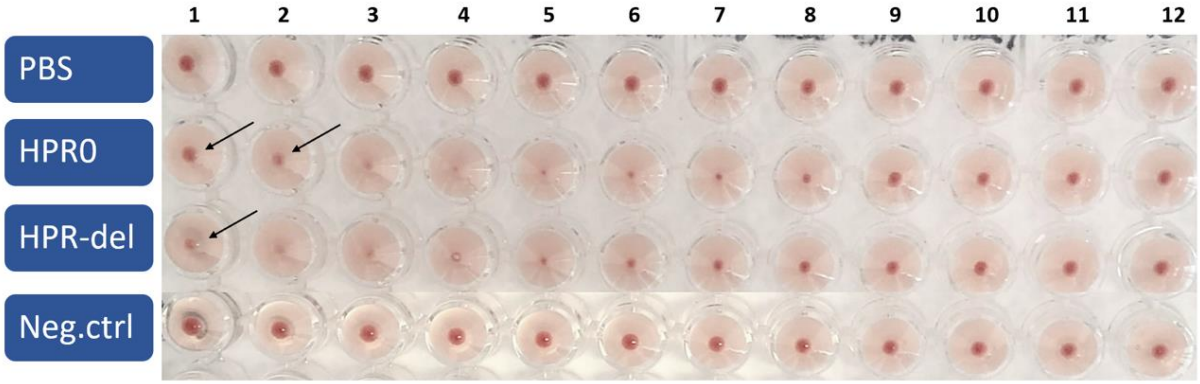

Figure 42. The plate was checked for elution after 21 hours. The reapperance of a RBC button in the first wells, and in well 2 for HPR0 have occurred. 32 HAU and 16 HAU is required for elution for HPR0 and HPR-del, respectively in this experiment.

Haemagglutination assay for elution, experiment 2

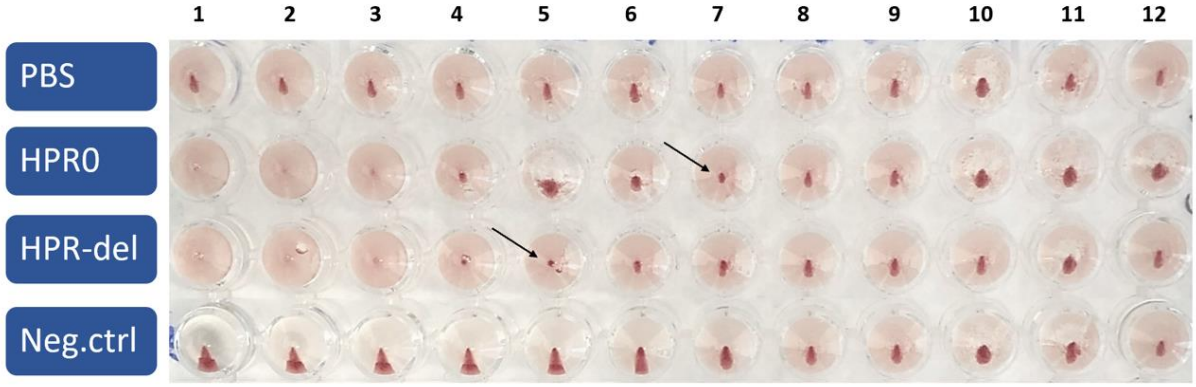

Figure 43. RBC suspension was added to a twofold serial dilution of membrane fractions of HE-transfected CHSE cells. After one hour incubation time with RBC suspension, the plate was tilted. For HPR0, well 7 slows down the running of RBC button and contains 1 HAU. The haemagglutination titer is 64 HAU/well. The haemagglutination titer is 16 HAU/well for HPR-del.

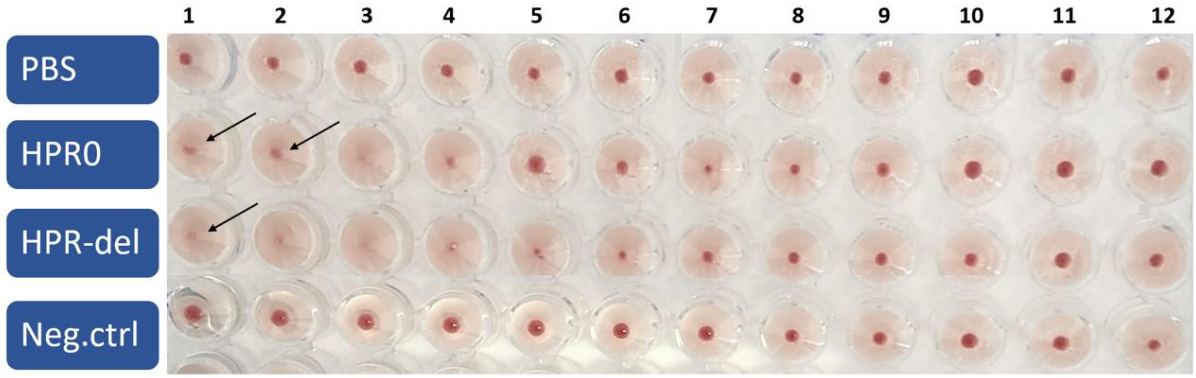

Figure 44. The plate was checked for elution after 21 hours. The reapperance of a RBC button in the first wells, and in well 2 for HPR0 have occurred. 32 HAU and 16 HAU is required for elution for HPR0 and HPR-del, respectively in this experiment.

Haemagglutination assay for elution, experiment 3

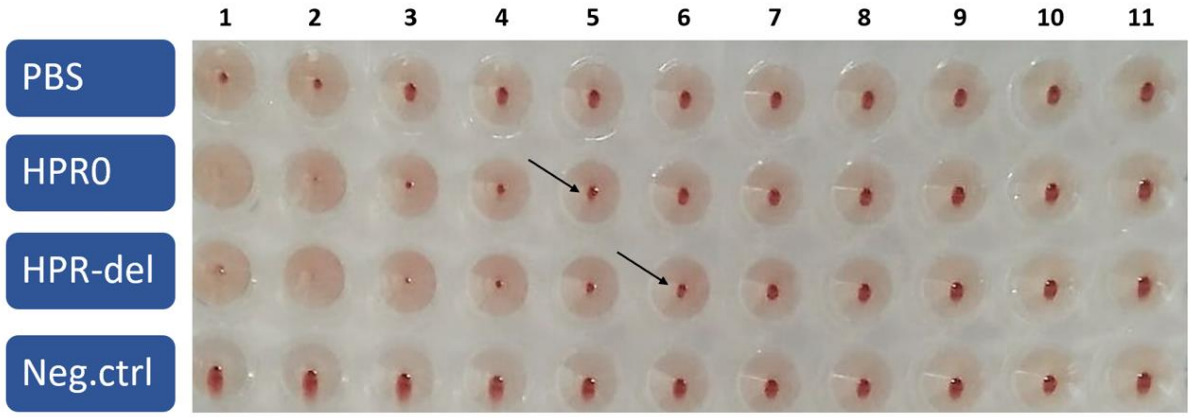

Figure 45. RBC suspension was added to a twofold serial dilution of membrane fractions of HE-transfected CHSE cells. After one hour incubation time with RBC suspension, the plate was tilted. For HPR0, well 5 slows down the running of RBC button and contains 1 HAU. The haemagglutination titer is 16 HAU/well. The haemagglutination titer is 32 HAU/well for HPR-del.

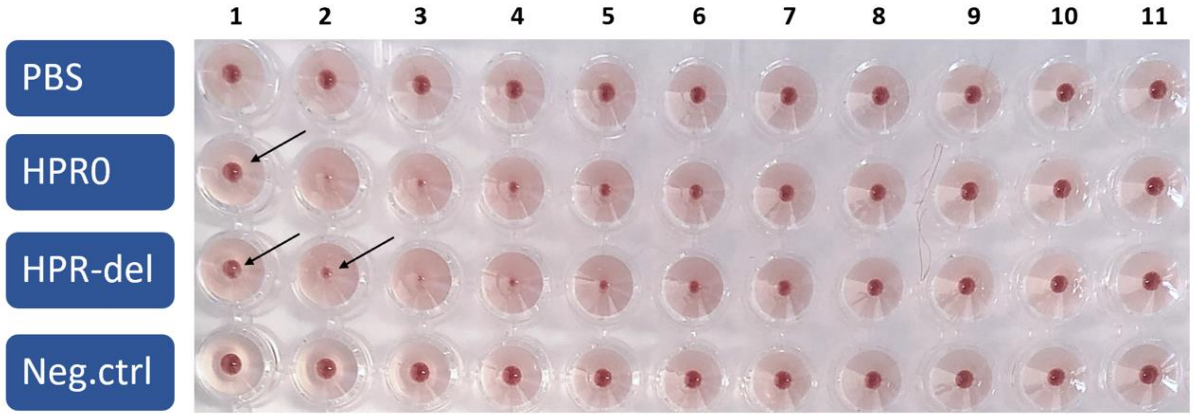

Figure 46. The plate was checked for elution after 20 hours. The reapperance of a RBC button in the first wells, and in well 2 for HPR-del have occurred. 16 HAU is required for elution for both HPR0 and HPR-del in this experiment.

Table 13. Overview of the haemagglutination titers and HAU required for elution from four experiments.

	Dilution	**HAU/well**	**HAU required for elution**
HPR0	1:32	16	16
HPR-del	1:64	32	16
HPR0	1:64	32	32
HPR-del	1:64	32	32
HPR0	1:128	64	32
HPR-del	1:32	16	16
HPR0	1:128	64	32
HPR-del	1:32	16	16

Appendix 2

Table 14. Fusion activation raw data (fusion positive cells).

HPR0-pilot	HPR0-1	HPR0-2	HPR0-3	HPR-del pilot	HPR-del 1	HPR-del 2	HPR-del 3
24	35	14	24	71	28	49	29
20	25	36	24	23	43	49	62
35	19	28	34	14	63	46	30
17	25	50	47	39	36	51	48
29	16	49	29	50	25	26	21
34	34	35	37	57	42	55	59
21	18	20	32	32	14	33	45
23	32	37	58	60	82	37	27
17	42	42	29	75	70	55	32
27	34	61	22	9	46	56	32
19	23	17	19	46	69	50	25
12	37	44	31	26	69	38	42
23	40	47	43	33	72	61	36
32	25	40	48	50	55	58	58
18	23	29	29	69	60	46	29
16	14	26	29	66	65	56	44
22	21	7	8	0	18	25	11
19	34	23	20	0	47	47	37
19	37	11	20	44	46	67	43
15	23	20	54	48	34	46	36
23				55			
7				54			
10				41			
15				35			
6				17			
11				58			
7				11			
40				44			
23				31			
11				48			

Table 15. Fusion activation as the ratio of fusion positive cells normalised to haemadsorption data.

HPR0-parallell 1	HPR0-parallell 2	HPR0-parallell 3	HPR-del-1	HPR-del-2	HPR-del-3
0,49	0,25	0,42	0,77	0,47	0,59
0,37	0,20	0,35	0,57	0,45	0,63
0,33	0,29	0,57	0,71	0,50	0,64
0,56	0,29	0,41	0,65	0,55	0,55
0,35	0,34	0,29	0,59	0,50	0,60
0,39	0,27	0,49	0,59	0,41	0,56
0,24	0,29	0,48	0,65	0,43	0,60
0,40	0,49	0,55	0,68	0,46	0,57
0,53	0,36	0,42	0,87	0,48	0,52
0,35	0,50	0,40	0,67	0,51	0,59
0,39	0,23	0,29	0,53	0,44	0,56
0,36	0,25	0,29	0,46	0,47	0,47
0,32	0,28	0,34	0,53	0,49	0,47
0,26	0,27	0,29	0,49	0,46	0,44
0,19	0,18	0,21	0,47	0,42	0,46
0,13	0,15	0,23	0,44	0,43	0,43
0,27	0,14	0,33	0,50	0,47	0,48
0,37	0,24	0,24	0,46	0,41	0,46
0,44	0,15	0,30	0,51	0,42	0,49
0,34	0,17	0,41	0,62	0,49	0,46

Table 16. Fusion activation as the ratio of fusion positive cells normalised to CHSE cells bound to RBCs. The first two columns are from the pilot run.

HPR-del pilot	HPR0-pilot	HPR0-1	HPR0-2	HPR0-3	HPRdel-1	HPRdel-2	HPRdel-3
0,78	0,53	0,44	0,30	0,43	0,64	0,61	0,60
0,45	0,48	0,33	0,24	0,35	0,47	0,58	0,64
0,34	0,53	0,29	0,35	0,58	0,58	0,65	0,65
0,59	0,3	0,50	0,34	0,42	0,54	0,71	0,56
0,76	0,6	0,31	0,40	0,30	0,49	0,65	0,62
0,74	0,5	0,35	0,32	0,49	0,49	0,53	0,57
0,84	0,51	0,21	0,35	0,49	0,54	0,56	0,62
0,53	0,34	0,36	0,59	0,56	0,56	0,60	0,59
0,82	0,25	0,47	0,43	0,43	0,71	0,62	0,53
0,38	0,79	0,31	0,60	0,41	0,55	0,66	0,60
0,57	0,28	0,51	0,37	0,41	0,66	0,61	0,71
0,32	0,2	0,47	0,40	0,40	0,57	0,64	0,60
0,44	0,3	0,42	0,44	0,48	0,66	0,67	0,60
0,82	0,59	0,34	0,43	0,41	0,62	0,63	0,56
0,8	0,55	0,25	0,29	0,30	0,59	0,58	0,59
0,83	0,33	0,17	0,24	0,32	0,56	0,58	0,55
NA	0,65	0,36	0,22	0,47	0,62	0,64	0,61
NA	0,31	0,49	0,38	0,34	0,58	0,57	0,59
0,83	0,28	0,58	0,24	0,42	0,64	0,58	0,62
0,86	0,25	0,44	0,27	0,57	0,77	0,67	0,59
0,8	0,32						
0,73	0,18						
0,69	0,17						
0,67	0,33						
0,94	0,38						
0,81	0,3						
0,41	0,44						
0,58	0,49						
0,53	0,51						
0,73	0,24						

Table 17. D'Agostino and Pearson normality test for fusion activation normalised to RBC-bound CHSE cells (data in Table 16).

	HPR-del pilot	**HPR0 pilot**	**HPR0-1**	**HPR0-2**	**HPR0-3**	**HPR-del 1**	**HPR-del 2**	**HPR-del 3**
K2	3,914	1,89	0,3745	3,446	0,3841	1,755	0,2576	8,19
P value	0,1413	0,3886	0,8292	0,1785	0,8253	0,4157	0,8792	0,0167
Passed normality test (alpha=0.05)?	Yes	Yes	Yes	Yes	Yes	Yes	Yes	No
P value summary	ns	ns	ns	ns	ns	ns	ns	*

Table 18. Mann Whitney U-test for fusion activation normalised to RBC-bound CHSE cells (data in Table 16).

P value	0,0286
Exact or approximate P value?	Exact
P value summary	*
Significantly different (P < 0.05)?	Yes
One- or two-tailed P value?	Two-tailed
Sum of ranks in column A,B	10 , 26
Mann-Whitney U	0

Appendix 3

Table 19. Summary of published fusion assay studies that compare ISAV HPR0 and HPR-del.

Ref.	Variant HPR0	Variant HPRdel	Findings	Comments
Fourrier et al. [2]	HE NWM10	HE NWM10 with induced deletions F Glesvaer/2/90 F Nevis 390/98	<u>Stimulated conditions: Treated with trypsin/low pH:</u> • HPR_{mut_del}[a] HE/F_{vir}[b] have higher fusion activity than HPR0 HE/F_{vir} • In combination with F Nevis, fusion activation was much higher than with F Glesvaer (due to several aa differences, rather than the HPR deletion (length and position)) • Induced deletions in the HPR region of the HE increased fusion activity to varying extents	Sequences from naturally occurring HPR0 HE, and HPR-del F was used, but they mutated the HPR0 HE region to synthesise HPR-del HE variants.
Fourrier et al. [3]	HE and F SK779/06	HE SK779/06 with induced deletions F SK779/06 with insertions and mutations	<u>Stimulated conditions: Treated with trypsin/low pH:</u> • HPR0 HE/F_{mut}[c] have increased fusion activity compared to HE HPR0/F_0[d] • HPR0 HE/ F_{mut} have higher fusion activity than HPR_{mut_del} HE/F_{mut} <u>Unstimulated conditions: no trypsin/low pH:</u> • HPR_{mut_del}HE/any F protein increased fusion activity <u>Comparison fusion activity under different conditions:</u> • Significantly higher fusion activity when treated with trypsin and low pH, but deletions in the HE HPR reduced activity.	Sequences from naturally occurring HE and F was used, but they induced mutations to synthesise HPR-del HE and F variants.
		HE and F Nevis 390/98	<u>Unstimulated conditions: no trypsin/low pH:</u> • Fusion activity was reduced when calcium ionophore A23187 was added to culture media (dose-dependantly), suggesting that the activating protease is calcium-dependent.	
Ojeda et al. [4]	HE and F GIM-19336	HE and F GIM-HPR3a	<u>Stimulated conditions: Treated with trypsin/low pH:</u> • HPR-del HE/F_{vir} have increased fusion activity compared to HPR0 HE/F_{vir}	Sequences from naturally occuring HE and F was used, but there are additional differences in the HE proteins outside the HPR region. The differences are very small and most likely insignificant. Note that they have not combined the homotypic HPR0 HE/F_0, but have rather combined HPR0 HE with $F_{vir.}$

a) HPR_{mut_del} - HPR0 mutated with deletion in the HPR. b) F_{vir} - F protein from virulent HPR-del variant. c) F_{mut} – HPR0 F protein with mutations. d) F_0 - HPR0 F protein

Appendix 4

A4.1 Preliminary experiments with bead-based protease activity assay

In this study, a bead-based protease activity assay was to be established to test the ability of different proteases to cleave target peptides based on the F protein of ISAV-HPR0 and HPR-del by using magnetic beads coupled to avidin (MagPlex®-Avidin). The target peptides are synthetically made, and includes the cleavage site, K_{276}, of the F protein, as well as the mutation site at position 266 that is characteristic for the transition from ISAV-HPR0 to HPR-del. This was initiated, but due to time constraints, this assay was put on hold, and will be pursued in the future.

A bead-based assay is a technique where multiple analytes can be assayed simultaneously in the same sample volume within the same run. Each set of beads is coated with a different capture or target molecule, a protein, or nucleic acid, thus multiple analytes can be simultaneously captured or treated in a single sample. Compared to an ELISA, each bead function as a different ELISA well, and up to 100 beads - i.e. up to 100 different analyses - can be combined in one sample. The beads used in this study are conjugated to avidin that will bind strongly to biotinylated target peptides. These peptides are conjugated to a FLAG-tag, which can be detected by an antibody-conjugated phycoerythrin (PE), a fluorophore. The principle behind is that if the sample contains proteases that facilitate cleavage of the target peptide, the FLAG-tag will be removed, the antibody will not bind, and PE will not be detected. If the sample lack proteases that can cleave the peptide, the antibody will bind and PE is detectable. Figure 47 is an illustration of the the MagPlex®-Avidin protease activity assay used in this study.

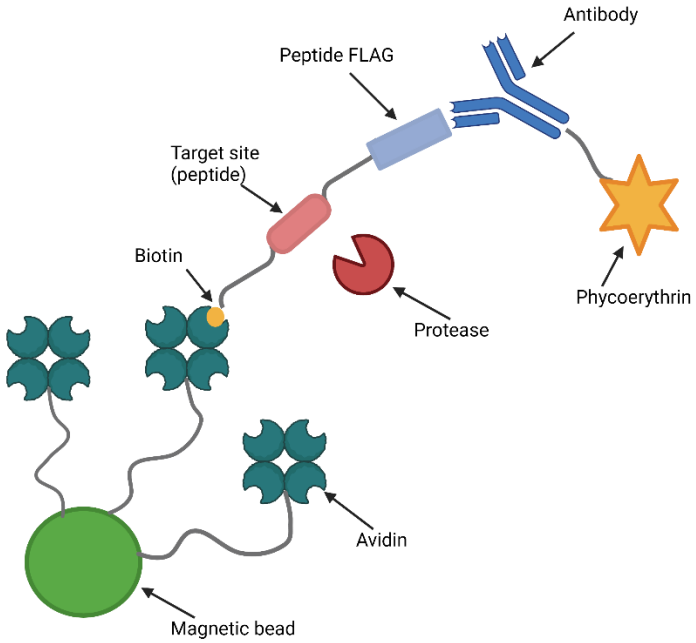

Figure 47. Illustration of the bead-based protease activity assay. Magnetic beads with different colours coupled to avidin will bind to different biotinylated peptides based on the F protein of ISAV-HPR0 and HPR-del. The peptides are coupled to a FLAG-tag, which is detected by an antibody conjugated with phycoerythrin. If the sample contains proteases that can cleave the peptide, there will be no detection of PE, but if the sample do not contain proteases that can cleave the peptide, the biotin/avidin-complex is intact and PE can be detected. *Created with BioRender.com.*

Procedure

The first step was to couple MagPlex®-Avidin beads #12 (Luminex Corporation, Austin, TX, USA) with biotinylated control-trypsin peptide and to perform a detection test to assess if the beads had been successfully coupled to the control-peptide. $6.25*10^5$ beads were transferred to a microcentrifuge tube and beads were pelleted by a magnetic separator. The supernatant was aspirated and the pelleted beads were resuspended in 250 µL PBS-TBN by vortex and sonication for 20 seconds. 5 µg biotinylated control-trypsin peptide (Thermo Fisher Scientific, Waltham, MA, USA) was added to the beads solution, mixed by vortex and incubated for 30 minutes on a tube rotator (VWR, Radnor, PA, USA) at room temperature. The tube with coupled beads was placed in a magnetic separator, the supernatant was aspirated, and the beads-pellet was resuspended in 500 µL PBS-TBN by vortex. Beads were washed once more with PBS-TBN and separated on a magnetic separator. The coupled beads were resuspended in 250 µL PBS-TBN by vortex and sonication for 20 seconds. 2500 beads was added to duplicate wells on a Bio-Plex Pro™ 96-well plate (Bio-Rad, Hercules, CA, USA) and washed three times with PBST on a Bio-Plex Pro™ magnetic plate washer (Bio-Rad). Uncoupled MagPlex®-Avidin #12 beads were plated as negative controls. PE-conjugated anti-FLAG monoclonal antibody was added in different dilutions (Abcam plc, Cambridge, UK): 1:200, 1:500, and 1:1000, respectively (50 µL/well), and incubated for 60 minutes on shaker at 750 rpm, at room temperature. The plate was washed with

PBST three times on the plate washer, and beads were resuspended in 100 µL sheath fluid (Bio-Rad). Beads were analysed on the Bio-Plex 200 System (Bio-Rad).

The second step was to add different trypsin concentrations to the coupled beads to assess if the control-trypsin peptides will get cleaved, and at which concentrations. The trypsin-activity assay was performed in two experiments:

1) Duplicate plates were used in the first experiment. Different incubation times were also tested: 5, 15, 30, and 60 minutes. 1000 coated beads were added to wells on a 96-well plate (Greiner). Uncoated beads were plated as negative controls. Additionally, no trypsin (only PBS) was added to wells as negative controls. Beads were treated with trypsin (Sigma-Aldrich, St.Louis, MO, USA) (100 nM, 10 nM, 1 nM, and only PBS, respectively), and trypsination was stopped by adding FBS after different incubation times (5, 15, and 30 minutes, respectively). Parallell wells on plates were transferred to the same Bio-plex Pro™ 96-well plate (Bio-Rad, Hercules, CA, USA), and the plate was washed 3 times with PBST on Bio-Plex Pro™ magnetic platewasher (Bio-Rad). 50 µL PE-conjugated anti-FLAG monoclonal antibody was added per well (1:500 in PBS-TBN) (Abcam plc, Cambridge, UK), and incubated for 60 minutes on shaker at 750 rpm, at room temperature. The plate was washed with PBST three times on the plate washer, and beads were resuspended in 100 µL sheath fluid (Bio-Rad. Trypsin-activation were analysed on the Bio-Plex 200 System (Bio-Rad).

2) A second trypsin activation assay was performed where higher concentrations of trypsin was tested, as well as longer incubation times. A new trypsin stock was made by dissolving trypsin in PBS rather than hydrochloric acid (HCl) and tested to evaluate if the trypsin inactivity in the previous experiment was pH related. Trypsin-EDTA in two concentrations was also tested. The EDTA is a chelating agent that binds metal ions. This was chosen to test if the beads somehow had positive ions that block or interfere with the trypsin activity.

Trypsin-activation was tested at 5, 15, 30, and 60 minutes, with the concentrations: 300 nM, 100 nM, 10 nM (Sigma-Aldrich, St.Louis, MO, USA), and no trypsin (only PBS) as negative control. For the Trypsin-EDTA (Lonza, Basel, Switzerland) , a 1:2, and 1:4 dilution was tested. 1000 coated beads were added to wells on a Bio-Plex Pro™ 96-well plate. Uncoated beads were also plated as negative controls. Beads were treated with trypsin at different time points, and trypsination was stopped by adding FBS. The plate was washed 3 times with PBST on Bio-Plex Pro™ magnetic platewasher (Bio-Rad, Hercules, CA, USA). 50 µL PE-conjugated anti-FLAG monoclonal antibody was added (1:500 in flow buffer) per well, and incubated for 60 minutes on shaker at 750 rpm, at room temperature. The plate was washed

with PBST three times on the plate washer, and beads were resuspended in 100 µL sheath fluid (Bio-Rad). Trypsin-activation was analysed on Bio-Plex 200 System (Bio-Rad).

MagPlex®-Avidin beads were successfully coupled to biotinylated control-trypsin peptides

MagPlex®-Avidin beads #12 were coupled with biotinylated control-trypsin peptide, and a detection test was performed using three different dilutions of PE-conjugated anti-FLAG antibody. The results revealed that the coupling was successful, and that all three antibody-PE concentrations emitted signals (Figure 48). The 1:500 dilution was chosen for subsequent assays.

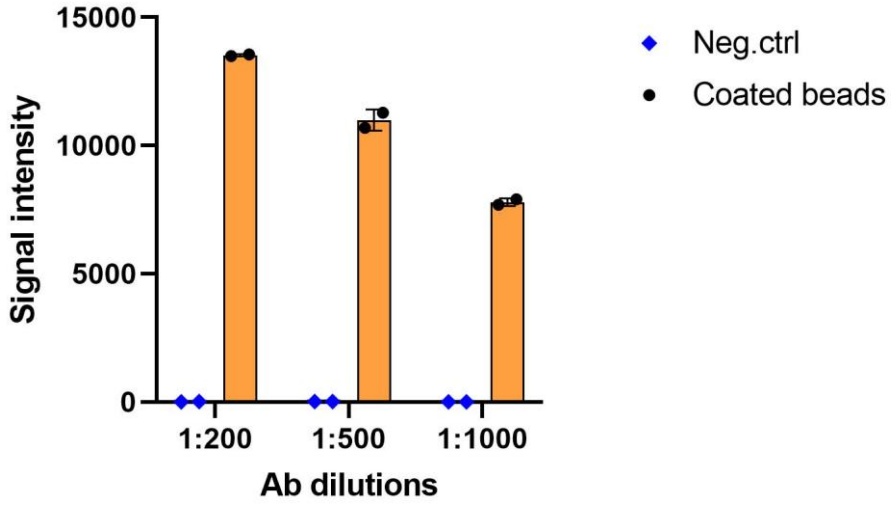

Figure 48. Results from the detection test. The beads were successfully coupled to the control-trypsin peptides. All dilutions of PE-conjugated anti-FLAG antibody work. Negative controls (uncoated beads) showed very little background. Each dot represents one replicate, and mean with standard deviation error bars are displayed.

Trypsin activity was not detected on the MagPlex®-Avidin beads coupled to control-trypsin peptide

Next step was to perform a trypsin activity assay where different concentrations of trypsin was used to find control conditions. Different incubation times were also tested. Data in Figure 49 are plotted from two parallells. Note that the 15 minute incubation time was tested in four parallells.

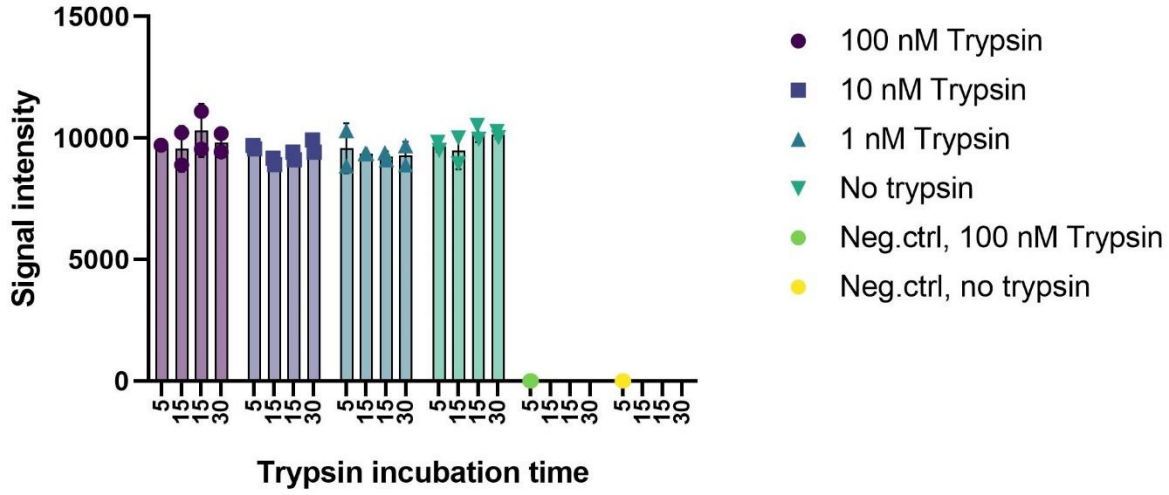

Figure 49. Results from the first trypsin activity assay. The different trypsin concentrations tested are listed in legends. No trypsin activity was detected. Negative controls (uncoated beads) showed very little background noise. The graph shows two replicates, and mean with standard deviation error bars.

The results from the first experiment did not show any trypsin activity. This could be explained by the trypsin concentration being too low or the incubation time being too short. Another explanation could be that the trypsin was not diluted enough to normalise the pH, and therefore was inactive, because the trypsin stock was dissolved in hydrochloric acid to keep inactive for storage. The pH optimum for trypsin activity is 7-9.

A second trypsin activation assay was performed where longer incubation times and higher concentrations of trypsin was tested using trypsin dissolved in PBS, as well as trypsin-EDTA (Figure 50).

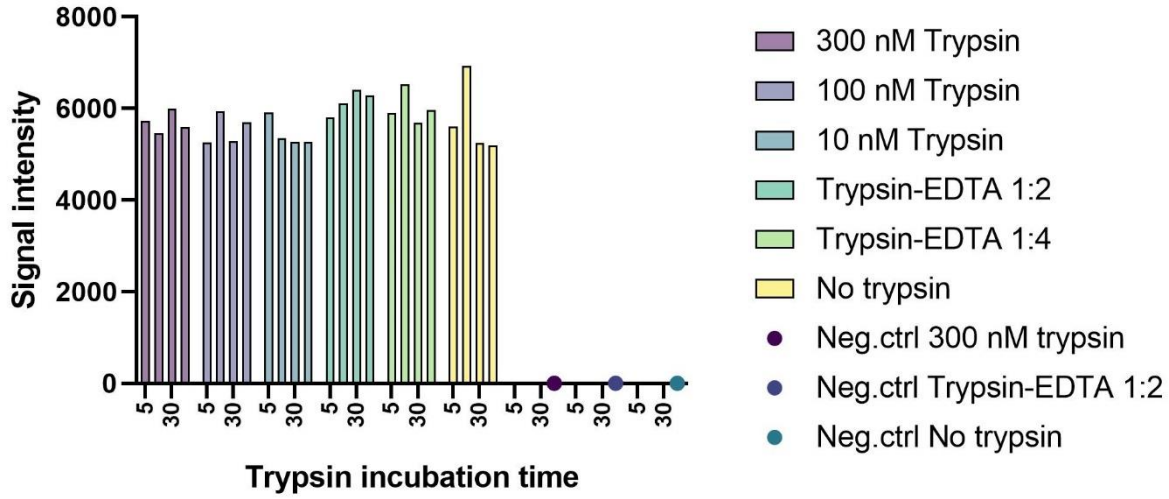

Figure 50. Results from the second trypsin activity test. Negative controls (uncoated beads) showed very little background noise. The different trypsin concentrations tested are listed in legends. No trypsin activity was detected.

Again, the results showed no trypsin activity. The signal intensities were lower than from the detection test, probably due to degradation of the coupled beads. This means that another factor prevented the cleavage. A possible explanation is that the FLAG-tag coupled to the control/trypsin peptide is located too close to the trypsin cleavage site and blocks the trypsin activity. This must be investigated further in future experiments before the assay can be applied to ISAV F proteins.

Norges miljø- og biovitenskapelige universitet
Noregs miljø- og biovitskapelege universitet
Norwegian University of Life Sciences

Postboks 5003
NO-1432 Ås
Norway